

DOE/ET-53088-344

IFSR #344

The Quasi-interchange Mode as a Mechanism
for Fast Sawtooth Crashes

FRANCOIS WELBROECK

Institute for Fusion Studies
The University of Texas at Austin
Austin, Texas 78712

October 1988

Abstract

It has been suggested that the recently observed fast sawtooth crashes are caused by a low-shear, pressure-driven ideal instability. This hypothesis is investigated, using asymptotic methods to solve the toroidal mode equations for a class of equilibria characterized by a low-shear central region in which $q-1$ is small, separated from the wall by a region with finite shear. A dispersion relation which differs significantly from previous results is obtained. The new instability displays no threshold with regard to the poloidal beta. An explicit expression for the growth rate is given for a model q profile. The linear growth rates are found to rise steeply near marginal stability but not sufficiently so as to account for the rapid onset of growth observed in the experiments. The nonlinear corrections to the mode growth are evaluated to lowest order in the amplitude, using a low-beta expansion of the reduced Magnetohydrodynamic equations. These equations are shown to be identical to the full Magnetohydrodynamic equations in the linear regime except for the neglect of parallel kinetic energy and the effects of compressibility. The calculation differs from previous bifurcation analyses by the inclusion of toroidal curvature effects including coupling to non-resonant harmonics. The nonlinear forces are found to be stabilizing for the profiles investigated. These forces lead to the appearance of stable bifurcated equilibria above marginal stability. In this respect our conclusions resemble those for the zero-beta, free-boundary kink. The amplitude of the bifurcated equilibria, however, is found to be much larger than that for the fixed-boundary, finite-shear kink.

The Quasi-Interchange Mode as a Mechanism for Fast Sawtooth Crashes

Francois Waelbroeck

It has been suggested that the recently observed fast sawtooth crashes are caused by a low-shear, pressure-driven ideal instability. This hypothesis is investigated, using asymptotic methods to solve the toroidal mode equations for a class of equilibria characterized by a low-shear central region in which $q-1$ is small, separated from the wall by a region with finite shear. A dispersion relation which differs significantly from previous results is obtained. The new instability displays no threshold with regard to the poloidal beta. An explicit expression for the growth rate is given for a model q profile. The linear growth rates are found to rise steeply near marginal stability but not sufficiently so as to account for the rapid onset of growth observed in the experiments. The nonlinear corrections to the mode growth are evaluated to lowest order in the amplitude, using a low-beta expansion of the reduced Magnetohydrodynamic equations. These equations are shown to be identical to the full Magnetohydrodynamic equations in the linear regime except for the neglect of parallel kinetic energy and the effects of compressibility. The calculation differs from previous bifurcation analyses by the inclusion of toroidal curvature effects including coupling to non-resonant harmonics. The nonlinear forces are found to be stabilizing for the profiles investigated. These forces lead to the appearance of stable bifurcated equilibria above marginal stability. In this respect our conclusions resemble those for the zero-beta, free-boundary kink. The amplitude of the bifurcated equilibria, however, is found to be much larger than that for the fixed-boundary, finite-shear kink.

**THE QUASI-INTERCHANGE MODE
AS A MECHANISM FOR FAST
SAWTOOTH CRASHES**

APPROVED BY
SUPERVISORY COMMITTEE:

U. Y. Tsydenin
Richard D. Hazeltine
James E. Main
Philip F. Merson
Clifford S. Gardner

To Susan

**THE QUASI-INTERCHANGE MODE
AS A MECHANISM FOR FAST
SAWTOOTH CRASHES**

by

FRANCOIS WELBROECK, B.Sc.

DISSERTATION

Presented to the Faculty of the Graduate School of

The University of Texas at Austin

in Partial Fulfillment

of the Requirements

for the Degree of

DOCTOR OF PHILOSOPHY

THE UNIVERSITY OF TEXAS AT AUSTIN

December, 1988

Acknowledgments

It has been a great privilege to work with and learn from Dr. Richard Hazeltine. I am extremely grateful to him for his constant support and encouragement. I am indebted to Dr. W. D. Drummond for support and guidance throughout my years at the University. I would like to thank him for his interest in my education.

I am grateful to Dr. Ahmet Aydemir for many instructive and stimulating discussions. I am also grateful to have had the opportunity to work with Dr. P. J. Morrison and Dr. K. W. Gentle. I am indebted to Dr. D. W. Ross for organizing the sawtooth discussion group and for bringing some important references to my attention. I would like to thank all the members of the sawtooth group for creating a stimulating forum for discussion and for providing many insightful comments. I benefited in particular from discussions with Dr. A. A. Ware and Dr. J. D. Meiss.

I am very grateful to Dr. W. H. Miner for patiently helping me to use TeX and MacDraw. This thesis could not have been completed without his assistance.

I would like to thank Mark Foster, Ed Synakowski and Dr. Steve McCool for allowing me to reproduce their soft X-Ray measurements in this thesis.

I have benefited from the hospitality of Austin Research Associates during most of the summers I spent in Austin. I am particularly grateful to Dr. Lee Sloan for spending a great deal of time helping me with a variety of

interesting problems.

My special thanks go to the Institute for Fusion Studies technical staff members for all the assistance they have given me. In particular, I thank Suzy Crumley and Laura Patterson for beautifully typesetting my papers, and Joyce Patton, Dawn East, Saralyn Stewart, and Carolyn Valentine for helping me in numerous ways throughout my employment at the Fusion Research Center and the Institute for Fusion Studies.

FRANCOIS WELBROECK

The University of Texas at Austin

December, 1988

Table of Contents

Acknowledgments	iv
Abstract	vi
Table of Contents	vii
List of Figures	viii
1. Introduction	1
1.1 Sawtooth Oscillations	1
1.2 Magnetohydrodynamic Instabilities	5
1.3 Historical Overview	8
2. Cylindrical Model	20
3. Toroidal Equilibrium	26
3.1 Flux Coordinates	26
3.2 Grad-Shafranov Equation	29
3.3 Calculation of the Metric Coefficients	32
4. Mode Equations	42
4.1 Introduction	42
4.2 Variational Formulation	43
4.3 Cylindrical Operator	49
4.4 Algebraic Minimizations	52

4.5	Minimization With Respect To Parallel Displacement	56
4.6	Final Minimizations	58
5.	Solution of the Mode Equations	64
5.1	Finite Shear Solution: The Toroidal Kink Mode	64
5.2	Low Shear Solution: The Quasi-Interchange Mode	70
6.	Nonlinear Growth	80
6.1	Introduction	80
6.2	Formulation	84
7.	Interchange-Reduced Equations	88
7.1	Simplification of the equations	88
7.2	Calculation of the average curvature	92
8.	Solution for Model Profiles	97
8.1	General Formulation	97
8.2	Constant current case	101
8.3	Gaussian rotational transform	102
9.	Resistive Interchange	107
9.1	Introduction	107
9.2	Stability	109
9.3	Nonlinear Growth	114
10.	Conclusion	116
	BIBLIOGRAPHY	119
	Vita	

List of Figures

- (i) Soft X-Ray signals from selected channels of the TEXT array showing typical sawtooth behavior (Courtesy of M. Foster, S. Mc Cool and the TEXT group)
- (ii) Soft X-Ray signals from TEXT showing time delay of the arrival of the sawtooth peak in the outer channels (Courtesy of M. Foster, S. Mc Cool and the TEXT group).
- (iii) Sawtooth crash displaying strong precursor oscillation (Courtesy of E. Synakowski, S. Mc Cool and the TEXT group).
- (iv) Flow pattern for the kink instability. The return flow occurs in a singular layer around $r = r_s$.
- (v) Flow pattern for the quasi-interchange instability.
- (vi) Topology of the hot inner core during a fully developed quasi interchange instability.
- (vii) Topology of the hot inner core during Kadomtsev reconnection.
- (viii) Evolution of the pressure profile during a quasi-interchange crash, from Ref. (31) (Courtesy of A. Y. Aydemir).
- (ix) Radial Eigendisplacement for a q-profile with $q' \sim 1$ at the rational surface $r = r_s$, where $q(r_s) = 1$.

- (x) Radial Eigendisplacement for a q -profile with a low shear central region such that $|q - 1| \sim \epsilon$.
- (xi) Flux Coordinate System
- (xii) Geometric solution of the dispersion relation
- (xiii) Supercritical (top) and subcritical (bottom) bifurcations of equilibrium.
Solid lines indicate stable equilibria, dashed lines unstable equilibria.
- (xiv) Effect of near-degenerescence on bifurcated equilibria.
- (xv) Evolution of Δ' with β_p for a low shear equilibrium

Chapter 1

Introduction

1.1 Sawtooth Oscillations

Ohmically heated toroidal magnetic confinement devices, or tokamaks, have long been known to sustain internal oscillations called sawtooth oscillations¹. Each sawtooth period consists of a slow rise or ramp phase followed by an abrupt fall (Fig.1). The ramp phase of the sawteeth results from the slow diffusive evolution of the plasma. After a period of time, typically on the order of ten to a hundred milliseconds, a rapid instability develops, resulting in the collapse of the central temperature and density. This process, called sawtooth crash or minor disruption, usually lasts between 50 and 100 microseconds. On the outside of the plasma, the sawtooth is inverted, displaying a slow decay and a fast rise (Figs.1 and 2). The temperature profile is observed to sharpen during the ramp phase, only to be leveled during the crash. The instability thus causes increased radial transport. Since the mixing region includes a large portion of the plasma core, sawteeth clearly have an important effect on the macroscopic confinement properties of tokamaks².

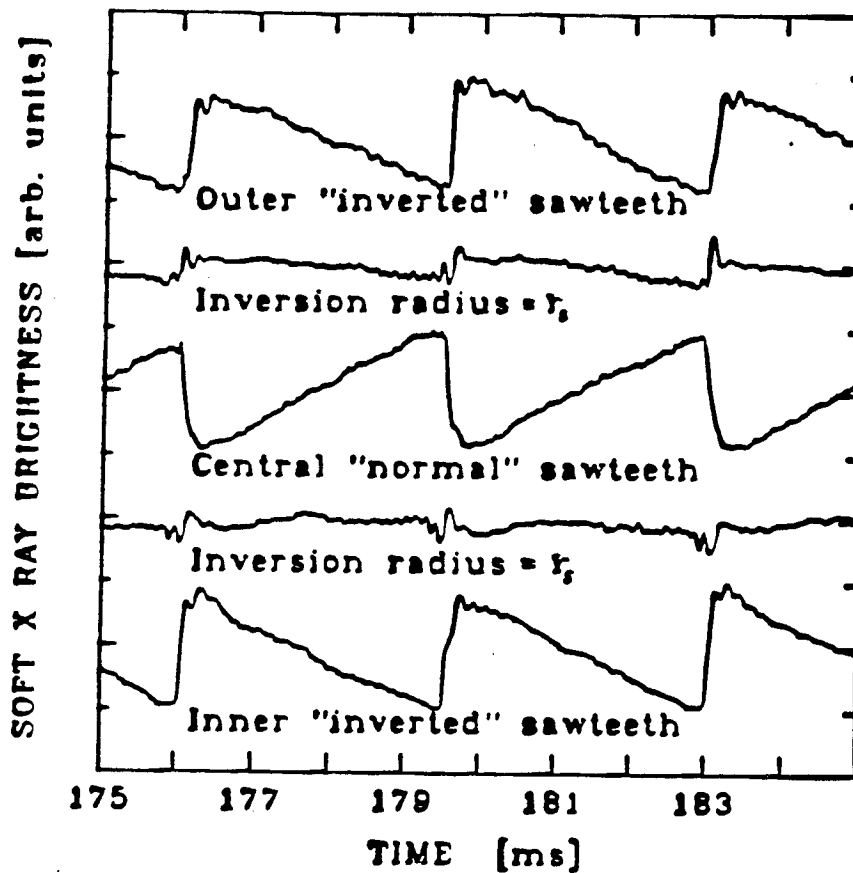


Fig.1: Soft X-Ray signals from selected channels of the TEXT array showing typical sawtooth behavior (Courtesy of M. Foster, S. Mc Cool and the TEXT group)

Recent experimental observations³⁻⁶ have forced a critical reevaluation of the widely accepted theoretical explanation of sawtooth oscillations, the Kadomtsev model⁷. An alternative model which accounts for most of the newly observed features has been suggested by Wesson^{8,9}. This new model is

the subject of this thesis. All these theories have in common that they rely on Magnetohydrodynamic instabilities to explain the sawtooth crash. Thus, we will begin by reviewing the most salient features of Magnetohydrodynamic instabilities before describing the history of sawtooth investigations leading to Wesson's suggestion.

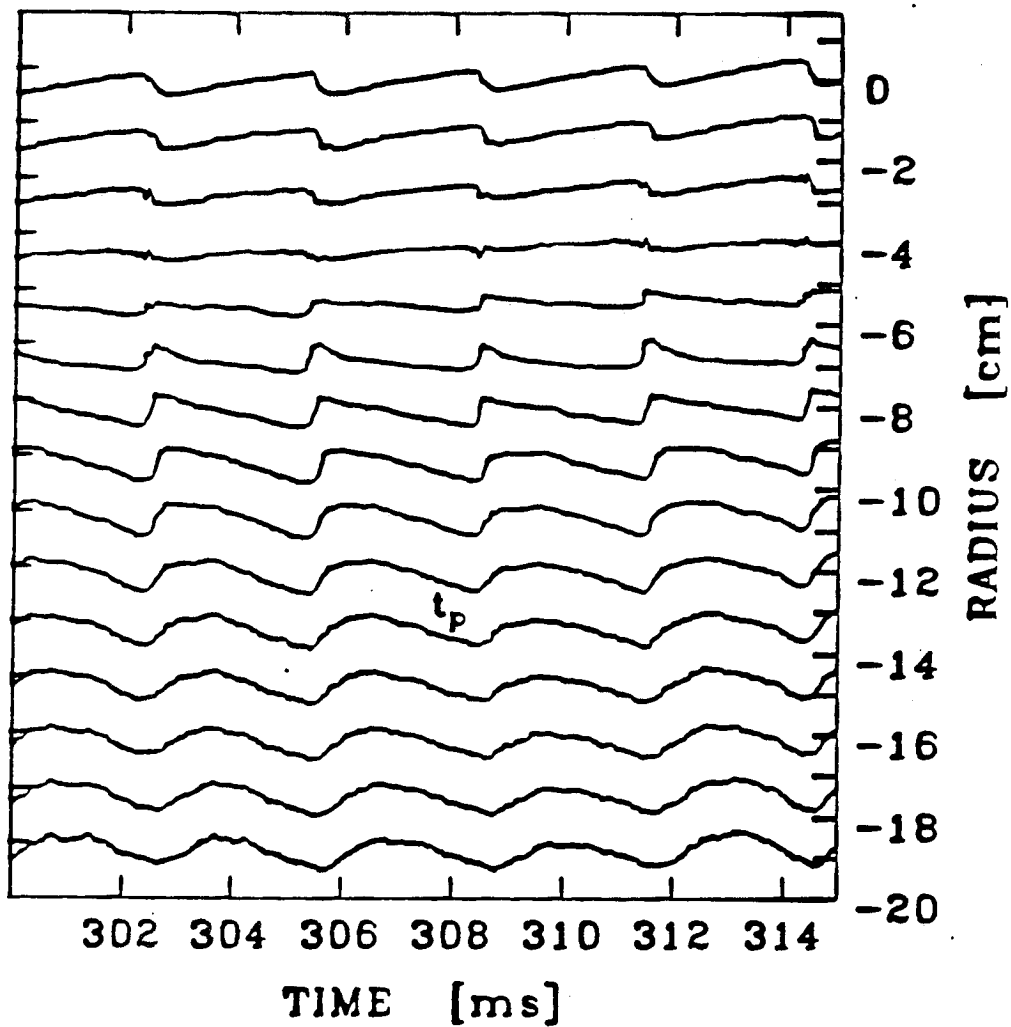


Fig.2: Soft X-Ray signals from TEXT showing time delay of the arrival of the sawtooth peak in the outer channels (Courtesy of M. Foster, S. McCool and the TEXT group).

1.2 Magnetohydrodynamic Instabilities

Most of the theoretical work devoted to the sawtooth oscillation has attempted to identify the instability responsible for the crash. The global, coherent nature of this instability has concentrated attention on magnetohydrodynamic (MHD) models. In these models, because of the disparity in the characteristic time scales for transport phenomena and Alfvénic dynamics, the plasma evolves through a continuous sequence of quasi-equilibrium states during the ramp phase of the sawtooth. The crash is then thought to occur as a result of the evolution of the plasma into an unstable equilibrium.

All MHD instabilities share certain characteristics resulting from constraints imposed by the nature of tokamak confinement¹⁰. These constraints result from the combined effects of the large toroidal magnetic field and from the presence within the plasma of large toroidal currents used for ohmic heating. The toroidal currents induce poloidal magnetic fields which, combined with the externally imposed toroidal field, give rise to helical field lines winding around closed, nested flux surfaces. These flux surfaces surround a closed field line, called the magnetic axis. Flux surfaces can be characterised by their magnetic winding number, called the safety factor. The safety factor may be defined heuristically as the limit of the ratio of toroidal to poloidal rotations as one follows a field line around the torus. For rounded current profiles the safety factor varies from surface to surface, giving rise to magnetic shear.

Certain flux surfaces, called rational surfaces, are of fundamental significance for stability. Their distinguishing feature is that the field lines which they contain close upon themselves after circling the torus a number of times. In a sheared magnetic field, these rational surfaces are densely embedded in the torus. Irrational surfaces, by contrast, are ergodically covered by the field

lines.

The importance of rational surfaces to stability is the result of a combination of two circumstances¹⁰. First, the strong toroidal magnetic field favors perturbations which vary slowly along the field lines, thereby minimizing the line bending. On the other hand, perturbations which are constant along field lines cannot vary on ergodic flux surfaces. Instabilities are thus always connected to the presence of one or more rational surfaces, in the vicinity of which the field lines may slip with respect to one another, or be interchanged, without the restoring action of field line bending^{11,12}.

These remarks can be made more precise by introducing a toroidal coordinate system (F, θ, φ) , where F is the poloidal flux through a ribbon bounded by the magnetic axis and a great circle, and θ and φ are respectively poloidal and toroidal angle coordinates on the flux surface. It is possible to choose these coordinates so that the magnetic field can be expressed as

$$\mathbf{B} = \nabla F \times \nabla(q\theta - \varphi) ,$$

where θ and φ increase by 2π as the flux surface is encircled once in the poloidal or toroidal directions, respectively. The field lines are then lines of constant $(q\theta - \varphi)$ in the flux surface, so that q is identified as the safety factor introduced above.

Using this coordinate system, perturbations can be expanded in Fourier series of the angles θ and φ .

$$u(r, \theta, \varphi) = \sum_{m,n} u_{m,n}(r) \exp[i(m\theta - n\varphi)] .$$

Because of the toroidal symmetry and approximate poloidal symmetry of tokamaks, unstable linear eigenmodes are usually dominated by a single harmonic,

with coefficient $u_{m,n}$. The variation of this harmonic within a flux surface can be characterised by its wave vector,

$$\mathbf{k} = m \nabla \theta - n \nabla \varphi .$$

The integers m and n are called respectively the poloidal and the toroidal mode numbers. The wave vector can then be decomposed into its component parallel to the equilibrium magnetic field,

$$k_{\parallel} = \mathbf{B}_0 \cdot \mathbf{k} / B_0 ,$$

and its perpendicular component,

$$\mathbf{k}_{\perp} = \mathbf{k} - k_{\parallel} \mathbf{B}_0 / B_0 .$$

From the above considerations we conclude that instabilities are characterised by small values of k_{\parallel} : specifically, $k_{\parallel}/k_{\perp} \ll 1$. In general, this requires the perturbation to be localised in the vicinity of the mode rational surface for which the helicity of the perturbation matches that of the magnetic field, $q = m/n$ ¹³⁻¹⁷. An apparent exception to this rule is the internal kink mode. The kink mode involves a global displacement of the plasma core, but its growth nonetheless remains critically dependent on processes occurring near its mode-rational surface.

The description of the kink mode is greatly simplified by relying on the large aspect-ratio property of tokamaks. The aspect ratio A of a torus is defined as the quotient of its major to its minor radius, $A = R_0/a$. The equations of motion can be expanded in powers of the inverse aspect-ratio $\epsilon = A^{-1}$. In the lowest order term in this expansion, toroidal curvature can be neglected, so that low toroidal mode-number perturbations have a behavior

similar to long wavelength perturbations in a cylindrical plasma¹⁸. It is found that $m \geq 2$ modes are stabilized by shear in plasmas with circular cross sections. The $m = n = 1$ kink mode, however, is only marginally stable at this order. Projected on the poloidal plane, it has the form of a rigid displacement of the plasma core inside the $q = 1$ rational surface.

The stability of the internal kink mode is determined by higher order terms in the inverse aspect-ratio expansion. These terms depend critically on toroidal geometry. Because of the difficulty of toroidal calculations, however, the cylindrical model is often relied on to make stability predictions.

1.3 Historical Overview

We now review the theoretical work leading to Wesson's model. We conclude this section by describing some of the more recent work stimulated by Wesson's suggestion and presenting the motivations for the present work.

Most theories of sawtooth instability rely on the $m = 1$ internal kink mode as the cause of the crash. In cylindrical geometry, this mode is unstable whenever the value of the safety-factor q falls below one inside the plasma. The following sawtooth mechanism then suggests itself: as the plasma is heated, the decrease in central conductivity results in a peaking of the current profile, leading to a decline in the central value of the safety factor.¹⁹ When the safety factor falls below one on axis, the $m = 1$ kink becomes unstable. The instability eventually results in the destruction of the confinement properties and subsequent flattening of the temperature and current profiles. After a reheating period, the process is repeated.

This possibility motivated the investigation of the nonlinear properties of the $m = 1$ kink by Rosenbluth, Dagazian, and Rutherford²⁰. In a 1973

article, these authors demonstrated the existence of low amplitude bifurcated equilibria. The presence of these equilibria results in rapid saturation in the growth of the kink mode. Thus, the predicted fluctuations would be too small to account for experimental observations. One must also conclude from these results that the flattening of the temperature profile cannot be explained on the basis of a kink-driven sawtooth crash.

The first explanation of sawtooth oscillations to gain widespread acceptance was advanced by Kadomtsev in 1975.⁷ Kadomtsev attributed the sawtooth crash to the resistive reconnection of the magnetic field in the vicinity of the $q = 1$ singular layer. Although resistive processes are normally very slow, magnetic reconnection can be considerably faster because of the singular current-sheets induced on rational surfaces by resonant ideal motion of the bulk of the plasma.^{21,22} The resulting instability, the tearing mode, is driven by the free energy made available by the motion outside the singular layer.¹⁹ Tearing mode growth, however, had been shown by Rutherford to slow down considerably in the nonlinear regime for $m \geq 2$ modes.²³ Kadomtsev argued heuristically that the opposite should be true for the $m = 1$ mode. He noted that as a result of resistivity, the current layer caused by the nonlinear evolution of the kink mode would dissipate, and the flux surfaces within the $q = 1$ singular layer would tear and reconnect with the outer flux surfaces. The magnetic pressure on the outside of the kink would thereby be reduced, while that inside would be increased, causing further growth.

The essential features of this model were later confirmed by Waddell et. al.²⁴ by using a numerical code to chart the evolution of the $m = 1$ kink-tearing mode. The mode was found to continue growing exponentially at approximately the linear rate well into the nonlinear regime, and to proceed

until complete reconnection of the flux inside the $q = 1$ surface had occurred. Detailed comparison of the predictions of the theory with experimental results were subsequently carried out by Jahns et. al,²⁵ and Callen and Jahns.²⁶

The first toroidal analysis of the ideal internal kink was completed by Bussac et. al²⁷ about the same time as Kadomtsev's paper. The surprising conclusion they reached was that the ideal kink was stable for sufficiently low pressure. Specifically, they found that the kink would be stable for $\beta_p < \beta_{pc}$, where the poloidal beta is defined by

$$\beta_p = \frac{\overline{P(r_1)} - P(r_1)}{(B_p^2/2)} .$$

Here $\overline{P(r_1)}$ is the volume-averaged pressure within the $q = 1$ rational surface $r = r_1$, and $(B_p^2/2)$ is the poloidal magnetic pressure. The value of the critical β_p needed for instability was found to depend on the current profile outside of the $q = 1$ surface, and particularly on the location of the $q = 2$ surface. This fact can be explained by the crucial role played by toroidal coupling of the $m = n = 1$ harmonic to an $m = 2, n = 1$ sideband. For a parabolic q-profile the critical β_p was estimated to be

$$\beta_{pc} = \left(\frac{13}{144} \right)^{1/2} .$$

In a subsequent paper²⁸ the same authors extended their analysis to include the effects of resistivity, and concluded that the $m = 1$ tearing mode would be unstable in toroidal geometry, with growth rates similar to those predicted by the cylindrical model. Toroidal coupling to the $m = 2$ tearing mode was found to be negligible for sheared equilibria, but it was remarked that this coupling could be expected to become important for low central shear. The conclusions of the toroidal analysis were thus consistent with Kadomtsev's

theory, and excluded further the possibility that the ideal kink was the cause of the minor disruption.

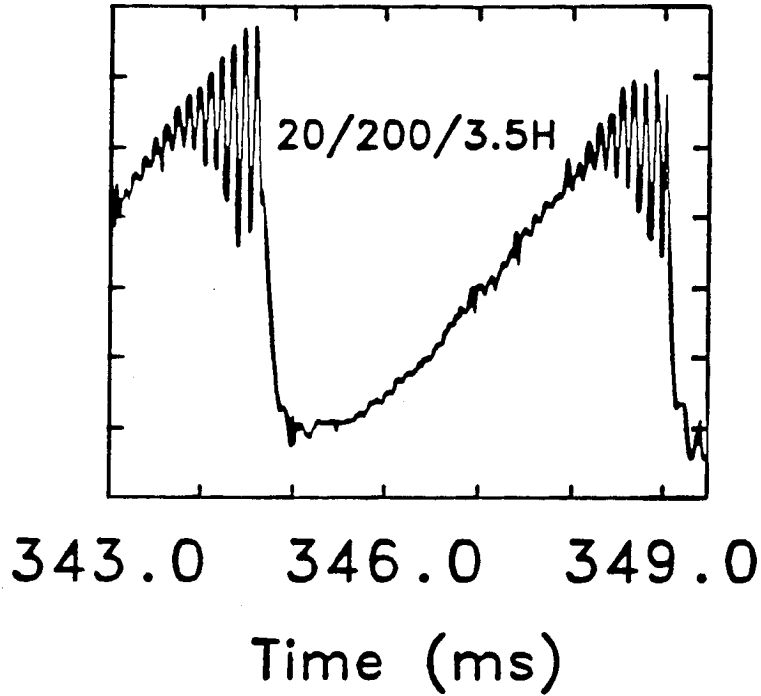


Fig.3: Sawtooth crash displaying strong precursor oscillation (Courtesy of E. Synakowski, S. Mc Cool and the TEXT group).

The appropriateness of the Kadomtsev reconnection model has now been seriously challenged by recent observations on the Joint European Tokamak (JET).⁴⁻⁶ Early results indicated that the sawtooth crashes were too rapid to be accounted for on the basis of resistive reconnection.⁴ Furthermore, estimates of the transport rate after a crash indicated that if the current profile were leveled by the minor disruptions, it would remain essentially constant during the sawtooth rise phase.⁸ Such current profiles would result in a uniform safety factor with $q \gtrsim 1$ within the plasma core. This prompted Wesson

to suggest an alternative mechanism for the crash, in which the disruption is caused by an ideal interchange-like instability.⁸ This instability will appear as the central value of q uniformly approaches one from above. For sufficiently low shear, Wesson argued, the equilibrium would not benefit from the stabilization found by Bussac et. al. The distinguishing characteristics of this mode would be first, a fast growth rate and second, a convective flow pattern easily distinguishable from the rigid shift displacement of kink-tearing mode theory. The reconnection would occur after the collapse, on a slower time scale. Wesson called this instability the quasi-interchange mode.

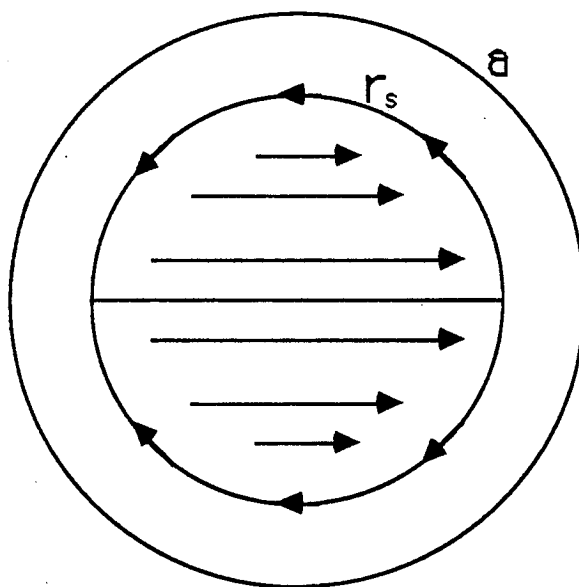


Fig. 4: Flow pattern for the kink instability. The return flow occurs in a singular layer around $r = r_s$.

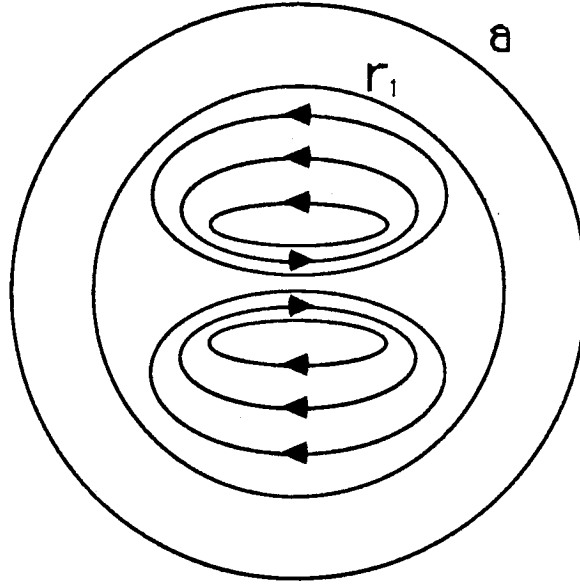
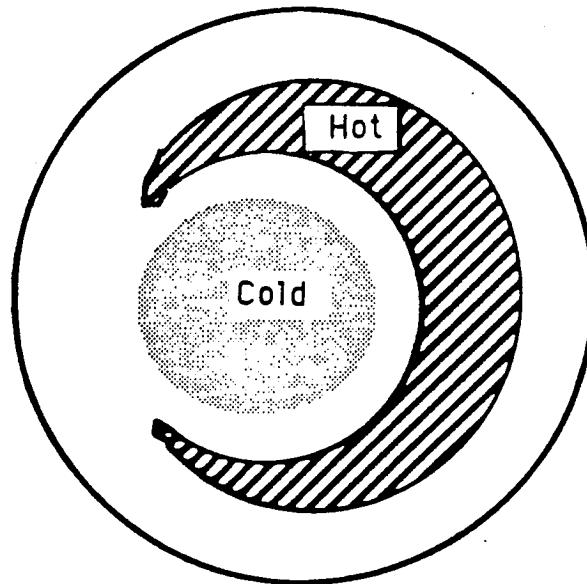


Fig.5: Flow pattern for the quasi-interchange instability.

Soon afterwards this conjecture was given vigorous support by new results on JET.^{5,6} The broad convective nature of the motion was confirmed and the formation of a cold plasma bubble at the center of the discharge was observed. The existence of decaying oscillations after the collapse was cited as evidence of delayed reconnection. In a second paper,⁹ Wesson et. al compared the experimental results to predictions made on the basis of two simple calculations. First, the marginal stability conditions were estimated from an extrapolation of the Bussac et. al analysis to the low shear regime^{9,29}. Second, nonlinear growth was simulated numerically for cylindrical geometry^{9,30}. Wesson concluded this investigation by drawing attention to the fundamental difficulty of explaining the occurrence of sawtooth crashes without precursor oscillations. This problem is particularly serious for some JET crashes where the growth rate reaches its maximum value in a fraction of the disruption time.

This fact is incompatible with the idea of a transport-triggered instability, given the extreme slowness of diffusive processes in tokamaks.



Quasi - Interchange

Fig.6: Topology of the hot inner core during a fully developed quasi interchange instability.

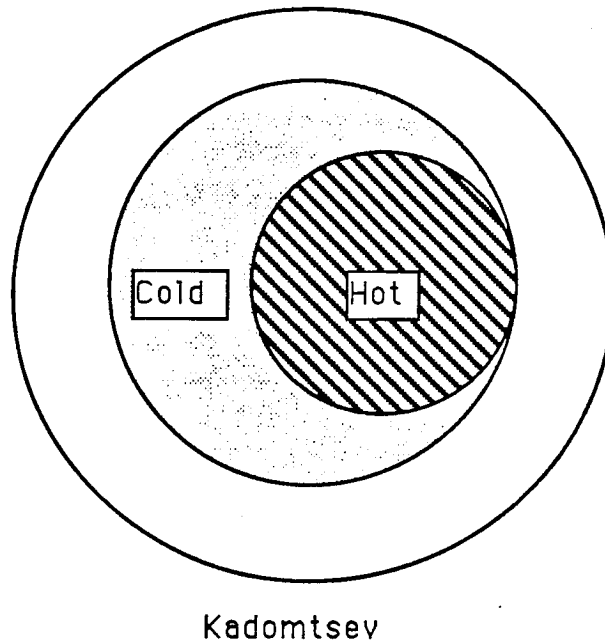
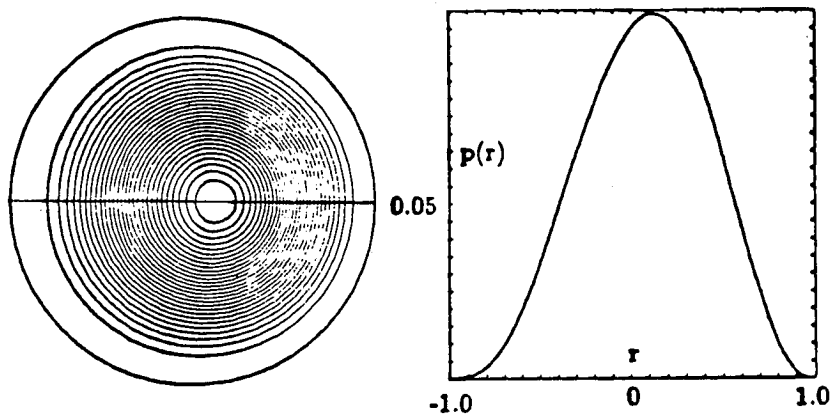
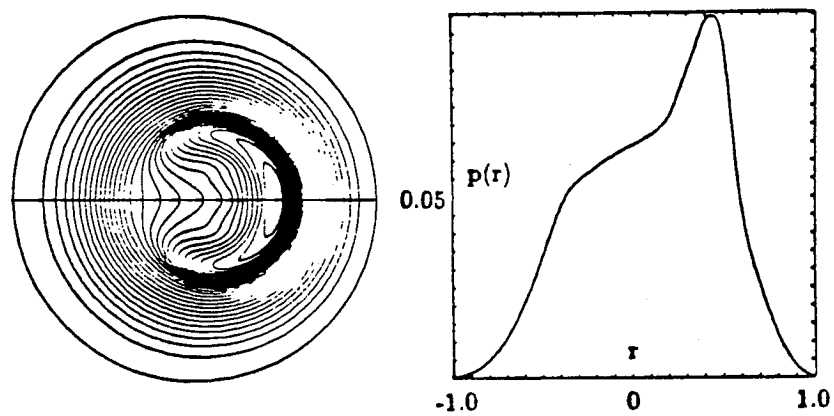
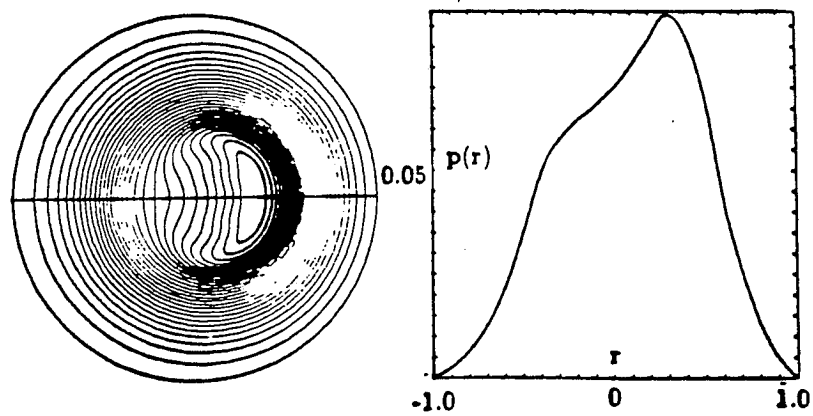


Fig.7: Topology of the hot inner core during Kadomtsev reconnection.

The quasi-interchange mode was subsequently investigated both with a Reduced Magnetohydrodynamic code and with a fully toroidal code by Aydemir.³¹ The essential features of the model were confirmed, and it was discovered that the instability would persist at arbitrarily low values of beta. Safety factor profiles with minima away from the magnetic axis were shown to have stability properties similar to those of profiles with uniformly small $q - 1$.

a) $t=0$ c) $t=617$ d) $t=1660$

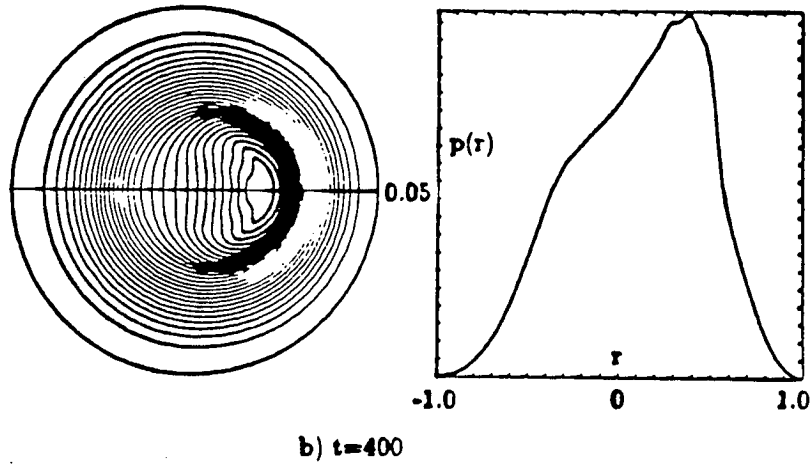


Fig.8: Evolution of the pressure profile during a quasi-interchange crash, from Ref. (31) (Courtesy of A. Y. Aydemir).

The present work was begun with the aim of extending the toroidal analysis of Bussac et. al to low shear configurations. Interest in the problem of the onset of growth then motivated a bifurcation calculation based on the Reduced MHD equations of Strauss³². As this work was being completed new current-measurement techniques have produced evidence supporting the claim that the safety factor is in fact significantly below unity in the center of the plasma, and is essentially unaffected by sawtooth oscillations.^{33,34} These observations are clearly inconsistent with every model of sawtooth instability suggested to date, including the quasi-interchange model.

It should be noted that throughout this thesis, as in most of the ideal MHD stability literature, the analysis has been limited to a very restricted class of motions. First, the equilibrium state is assumed to be static, or flow-free. Furthermore, only trajectories passing through the equilibrium configuration are considered. The state of the plasma can then be completely described

by the fluid displacement and velocity fields in the Lagrangian representation. The apparent inability of this conventional analysis to account for the sawtooth phenomenon may be due to its failure to consider more general perturbations. Recent work in this area has resulted in some rigorous derivations of stability criteria based on the Lyapunov method.^{35,36} This method consists of constructing a constant of the motion with a local extremum at the equilibrium. The construction of such constants of the motion for MHD systems was made possible by the discovery of new classes of conserved functionals, called Casimirs, which appear in the hamiltonian formulation of field theories with constraints such as MHD.³⁷⁻³⁹ New instability mechanisms have been suggested based on this hamiltonian theory, and it is possible that such a mechanism is responsible for the sawtooth crash.

This thesis is organized as follows. In chapter 2 we review the analysis for both kink and interchange modes in the simple context of cylindrical geometry. The equilibrium properties of tokamaks with circular cross-section are then described in chapter 3, where the metric of the flux coordinate system is calculated to second order in the inverse aspect ratio. In Chapter 4 the general mode equations are derived variationally from the linearized energy for perturbations of a static plasma equilibrium, the so-called δW principle.⁴⁰ After reviewing the solution to these equations in the case of finite shear, we describe in chapter 5 the solution to the low shear equation. As a result of fundamental differences in the nature of low shear instabilities as compared to the kink mode, a new solution scheme had to be used. In chapter 6 we describe the motivation for the non-linear analysis and discuss the underlying assumptions. The nonlinear equations are then simplified in chapter 7 with the help of the low shear ordering. The resulting, "interchange-reduced" equations are then solved in chapter 8. In chapter 9 we consider the effect of resistivity on

the quasi-interchange mode and show that this mode is in fact related to the $m=2$ tearing mode. We conclude in chapter 10 with a discussion of the results.

Chapter 2

Cylindrical Model

The difference between the kink instability for a sheared equilibrium and the corresponding quasi-interchange instability of low shear equilibria can be illustrated by the cylindrical tokamak model. The potential energy per unit length of a perturbation with poloidal mode number m and toroidal wavelength $k_z = n/R_0$ can be expanded for large wavelengths ($\epsilon = k_z a \ll 1$) as^{18,20}

$$\delta W = \delta W_0 + \epsilon^2 \delta W_2 + O(\epsilon^4), \quad (2.1)$$

$$\delta W_0 = \pi \int r dr \frac{(\vec{k} \cdot \vec{B})^2}{m^2} \left\{ r^2 \left(\frac{d\xi}{dr} \right)^2 + (m^2 - 1) \xi^2 \right\}, \quad (2.2)$$

where

$$(\vec{k} \cdot \vec{B}) = k_z B_z (m\mu - 1), \quad \mu = \frac{B_\theta}{k_z r B_z} = \frac{1}{nq}. \quad (2.3)$$

The lowest order term in the expansion, δW_0 , is non-negative, reflecting the stabilizing effect of field-line bending. Instability requires $(m\mu - 1) \sim \epsilon$ somewhere within the plasma. For sheared equilibria, such that $r \frac{d\mu}{dr} \sim 1$, this can only occur in a singular layer of width $\delta \sim \epsilon/\mu'$ (Fig. 9). The $m = 1$ mode is then constrained by the line-bending term to take the form of a rigid displacement, with the return flow taking place in the singular layer. This is the conventional $m = 1$ kink instability.²⁰ The $m \neq 1$ modes are strongly stabilized.

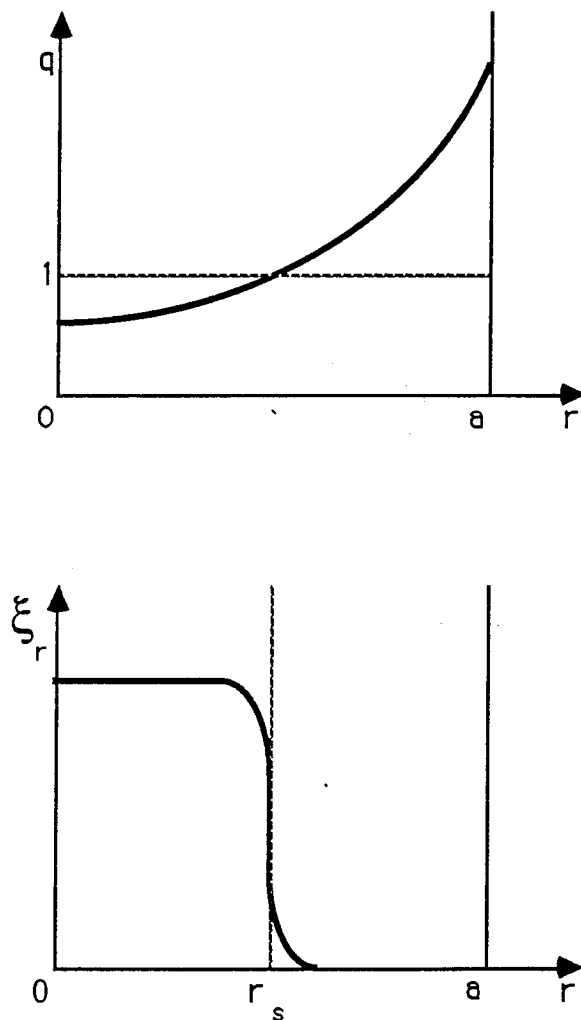


Fig.9: Radial Eigendisplacement for a q -profile with $q' \sim 1$ at the rational surface $r = r_s$, where $q(r_s) = 1$.

As the shear is reduced, however, the layer width grows until it eventually includes the entire core (Fig. 10). In the resulting low-shear $|m\mu - 1| \ll 1$ region the line bending energy is of the same order as the ϵ^2 -order pressure-

gradient driving term. The “quasi-interchange” instabilities associated with such equilibria will thus have continuous eigen-displacements distinct from the rigid displacement characteristic of the kink mode. The $m \neq 1$ modes are no longer strongly stabilized but the $m = 1$ mode will always be the first to reach criticality.⁴¹

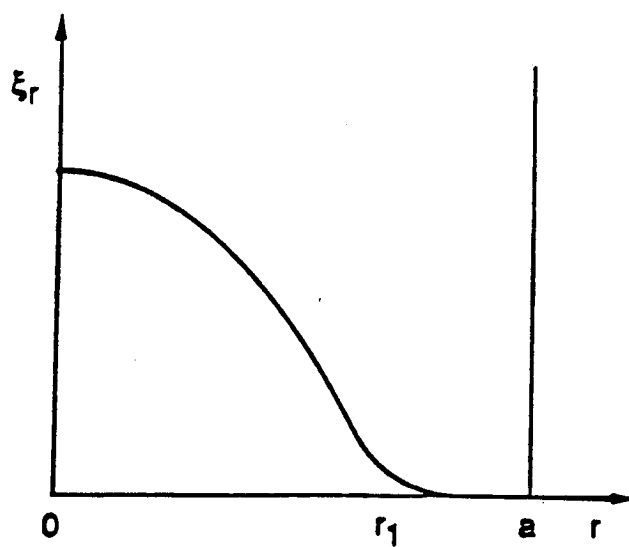
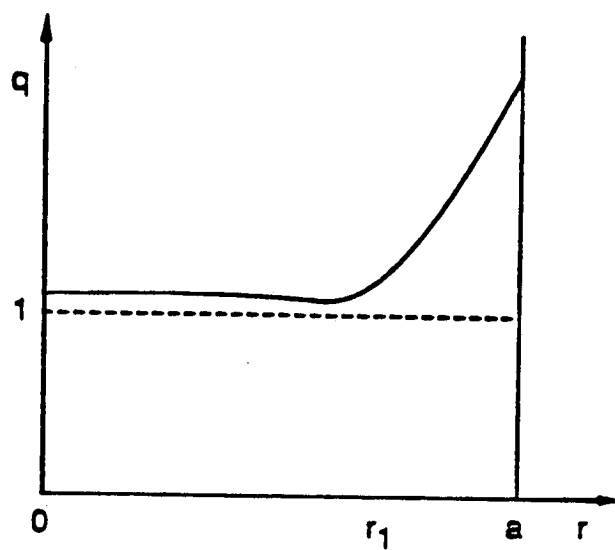


Fig.10: Radial Eigendisplacement for a q -profile with a low shear central region such that $|q - 1| \sim \epsilon$.

The cylindrical mode equation can be solved in the case of a parabolic pressure profile ($p = p_0 \cdot [1 - (r/a)^2]$) and a constant q profile ($q = q_0$).⁴² Assuming $\epsilon \ll 1$, $\beta = \frac{p_0}{B_0^2} \sim \epsilon^2$, $\mu_0 = 1/nq_0$ such that $|m\mu_0 - 1| \ll 1$, one finds that

$$\xi_r(r) = \frac{1}{r} J_m(\kappa r/a) \quad (2.4)$$

$$\kappa^2 = 4 \frac{k_z^2 a^2}{m^2} \frac{\beta_p + (m\mu_0 - 1)}{\hat{\gamma}^2 + (m\mu_0 - 1)^2}, \quad (2.5)$$

where J_m is the m th order Bessel function, $\hat{\gamma}$ is the normalized growth rate

$$\hat{\gamma} = \gamma \tau_A, \quad \tau_A = (k_z v_A)^{-1},$$

and $\beta_p = \frac{p_0}{B_{\theta a}^2}$, $B_{\theta a} = B_\theta(a)$ where a is the wall radius. The growth rate is determined by imposing appropriate boundary conditions. We consider two cases:

- (i) q is constant throughout the plasma. The boundary condition is then $\xi(a) = 0$.
- (ii) The constant q region is separated from the wall by a sheared region. In the sheared region the mode equation can be written

$$\frac{d}{dr} \left\{ (m\mu - 1)^2 r^3 \frac{d\xi}{dr} \right\} - (m^2 - 1) (m\mu - 1)^2 r \xi = O(\epsilon^2). \quad (2.6)$$

The displacement must satisfy $\xi(a) = 0$ and must remain of order one as $(m\mu - 1) \rightarrow \epsilon$ in the low shear region. It is generally not possible to satisfy both conditions simultaneously in the lowest order due to the singularity in the mode equation for $m\mu - 1 = 0$. We therefore conclude that $\xi(r) \sim \epsilon^2$ in the sheared region. Assuming that the transition between the constant- q region and the sheared region is sharp, we may then

deduce the growth rate by imposing the boundary condition $\xi(r_1) = 0$, where r_1 is the transition radius.

The growth rate for both of these cases can be written

$$\hat{\gamma}^2 = \frac{4k_z^2 \tilde{r}^2}{j_{m,n_r}^2 m^2} [\beta_p + (m\mu_0 - 1)] - (m\mu_0 - 1)^2, \quad (2.7)$$

where $\tilde{r} = a$ in Case (i) and $\tilde{r} = r_1$ in Case (ii). Here j_{m,n_r} is the n_r th radial node of the Bessel function $J_m(r)$.

$$J_m(j_{m,n_r}) = 0, \quad j_{1,1} = 3.83.$$

We emphasize that these results are for a compressible plasma.⁴² The various terms can be identified as the pressure-gradient driving term, a parallel current driving term, and the stabilizing line-bending term. We can distinguish two possible orderings for β_p and $(m\mu_0 - 1)$;

- (i) For $(m\mu_0 - 1) \sim \epsilon$ the current driving term in the bracket can be neglected. The growth rate will be of order ϵ , as distinguished from the kink mode growth rate which is of order ϵ^2 .
- (ii) For $(m\mu_0 - 1) \sim \epsilon^2$ there will be a stabilizing contribution from the parallel current term for $q_0 > m/n$. As we will see, the sign of this term is reversed in toroidal geometry.

Chapter 3

Toroidal Equilibrium

3.1 Flux Coordinates

We assume that the equilibrium is adequately described by continuously nested flux-surfaces. Cylindrical coordinates (R, ζ, Z) are introduced with the Z axis lying along the axis of symmetry of the torus (Fig.11). Toroidal symmetry is then simply expressed by $\partial/\partial\zeta = 0$. The magnetic field can be separated into its components in the toroidal direction, \mathbf{B}_t , and in the poloidal plane, \mathbf{B}_p :

$$\mathbf{B} = \mathbf{B}_p + \mathbf{B}_t .$$

In terms of the Magnetic vector Potential these are

$$\mathbf{B}_t = \nabla \times \mathbf{A}_\perp ,$$

$$\mathbf{B}_p = \nabla A_\zeta \times \nabla \zeta .$$

Applying Stokes' Theorem to a ribbon bounded by the magnetic axis and a major circle, one concludes that A_ζ is simply $1/2\pi$ times the poloidal flux F . Clearly magnetic surfaces are surfaces of constant F . From the equilibrium condition,

$$\nabla P = \mathbf{J} \times \mathbf{B} , \tag{3.1}$$

we see that $\mathbf{B} \cdot \nabla P = 0$. For sheared magnetic fields, this implies that $P = P(F)$. The equilibrium equation then requires that \mathbf{J} lie in the flux surfaces. Applying

Stokes' theorem to the current flux through the surface defined above yields

$$2\pi R B_t = \int_S d\mathbf{S} \cdot \mathbf{J} .$$

Since $\mathbf{J} \cdot \nabla F = 0$ the right hand side integral must be a flux function. The toroidal field may thus be written

$$\mathbf{B}_t = -T(F)\nabla\zeta , \quad (3.2)$$

where use has been made of $|\nabla\zeta|^2 = R^{-2}$. Note that $T(F)$ is $-1/2\pi$ times the poloidal current flux.

The eigenmode equations are most conveniently expressed in a flux coordinate system for which the magnetic field lines are straight . Let this coordinate system be (F, θ, φ) where θ is a poloidal angle variable oriented similarly to its cylindrical analog and $\varphi = -\zeta$ is chosen so as to preserve the right-handedness of the system (Fig.7).

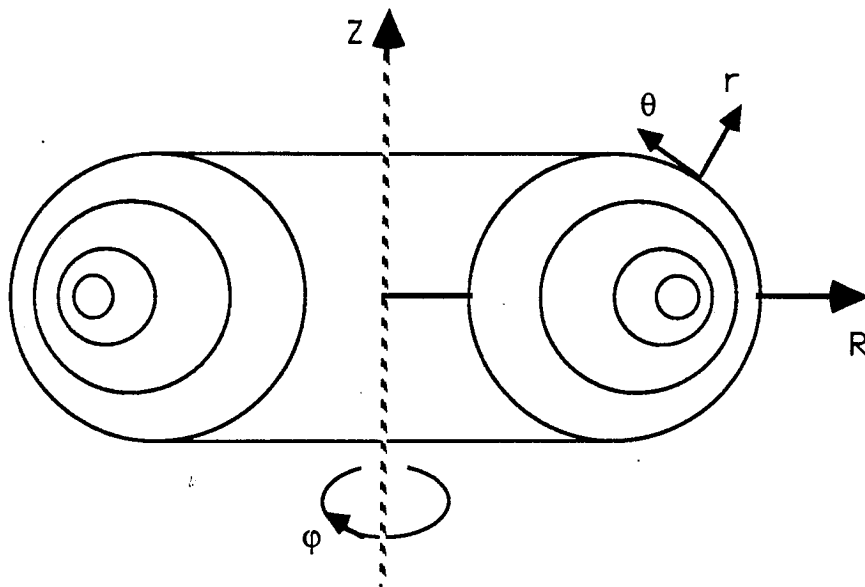


Fig.11: Flux Coordinate System

The angle θ is determined by requiring that the magnetic field take the form

$$\mathbf{B} = q(F) \nabla F \times \nabla \theta - \nabla F \times \nabla \varphi. \quad (3.3)$$

Multiplying both sides of this equation by $\nabla \varphi$, this is seen to imply

$$(\nabla F \times \nabla \theta) \cdot \nabla \varphi = \frac{T}{q R^2}. \quad (3.4)$$

The angle θ is then determined by multiplying Eq.(3.3) by $\nabla \theta$ and using Eq.(3.4). After integration we find

$$\theta = \frac{T}{q} \int \frac{dl}{|\mathbf{B}_p| R^2},$$

where the integral is to be carried out along the cross section of the flux surface F in the poloidal plane. A formula for the safety factor q is now obtained by requiring θ to have period 2π :

$$q(F) = \frac{T(F)}{2\pi} \oint \frac{dl}{|\mathbf{B}_p| R^2}. \quad (3.5)$$

To facilitate comparison with the cylindrical limit it is helpful to replace the poloidal flux coordinate F by a minor radius coordinate r defined by²⁷

$$r^2 = 2R_0 \int_0^F dF \left(\frac{q}{T} \right), \quad (3.6)$$

where R_0 is the major radius of the Magnetic axis. The jacobian for the system is then

$$\begin{aligned} \sqrt{g} &= [(\nabla r \times \nabla \theta) \cdot \nabla \varphi]^{-1} \\ &= \frac{R^2 r}{R_0}. \end{aligned} \quad (3.7)$$

3.2 Grad-Shafranov Equation

We now examine the consequences of the equilibrium condition, Eq.(3.1). To do this we must calculate the current \mathbf{J} . This is most easily accomplished by introducing tensor notation. Covariant basis vectors are defined for a general coordinate system (ξ_1, ξ_2, ξ_3) by

$$\mathbf{e}^i = \nabla \xi_i \text{ for } i = 1, 2, 3 .$$

The contravariant basis is given by

$$\mathbf{e}_i = \epsilon_{ijk} \sqrt{g} (\mathbf{e}^j \times \mathbf{e}^k) ,$$

where ϵ^{ijk} is the usual Kronecker symbol:

$$\epsilon^{ijk} = \epsilon_{ijk} = \begin{cases} 1 & \text{if } (ijk) \text{ is an even permutation of } (1, 2, 3) \\ -1 & \text{if } (ijk) \text{ is an odd permutation of } (1, 2, 3) \\ 0 & \text{otherwise} \end{cases} .$$

The covariant components of a vector \mathbf{A} are then given by

$$A_i = \mathbf{A} \cdot \mathbf{e}_i ,$$

and the contravariant components by

$$A^i = \mathbf{A} \cdot \mathbf{e}^i .$$

Note that the basis vectors satisfy

$$\mathbf{e}_i \cdot \mathbf{e}^j = \delta_i^j ,$$

where

$$\delta_i^j = \begin{cases} 1 & \text{if } i = j \\ 0 & \text{if } i \neq j \end{cases} .$$

Thus, $\mathbf{A} \cdot \mathbf{B}$ is given by

$$\mathbf{A} \cdot \mathbf{B} = A^i B_i = A_i B^i ,$$

where the summation over repeated indices convention has been adopted. The vector product

$$\mathbf{W} = \mathbf{A} \times \mathbf{B}$$

has contravariant components

$$W^i = g^{-1/2} \epsilon^{ijk} A_j B_k$$

and covariant components

$$W_i = g^{1/2} \epsilon_{ijk} A^j B^k .$$

The contravariant components of \mathbf{B} are thus simply given by

$$B^r = 0 ,$$

$$B^\theta = \frac{T}{qR^2} ,$$

$$B^\varphi = \frac{T}{R^2} .$$

The covariant components of the magnetic field are more complicated. They are given by

$$B_r = -\sqrt{g} R^{-2} \frac{dF}{dr} (\nabla r \cdot \nabla \theta) ,$$

$$B_\theta = \sqrt{g} R^{-2} \frac{dF}{dr} (\nabla r \cdot \nabla r) ,$$

$$B_\varphi = T .$$

The equilibrium current is now written in terms of its contravariant components as

$$\mathbf{J} = \sqrt{g} \left(J^r \nabla \theta \times \nabla \varphi + J^\theta \nabla \varphi \times \nabla r + J^\varphi \nabla r \times \nabla \theta \right) .$$

These components can be calculated by applying the $\nabla \times$ operator to the covariant expression of \mathbf{B} ,

$$\mathbf{B} = B_r \nabla r + B_\theta \nabla \theta + B_\varphi \nabla \varphi ,$$

and using the identities

$$\nabla \times (f\mathbf{V}) = \nabla f \times \mathbf{V} + f \nabla \times \mathbf{V} ,$$

$$\nabla \times (\nabla f) = 0 .$$

One finds

$$J^r = g^{-1/2} \left(\frac{\partial B_\varphi}{\partial \theta} - \frac{\partial B_\theta}{\partial \varphi} \right) ,$$

$$J^\theta = g^{-1/2} \left(\frac{\partial B_r}{\partial \varphi} - \frac{\partial B_\varphi}{\partial r} \right) ,$$

$$J^\varphi = g^{-1/2} \left(\frac{\partial B_\theta}{\partial r} - \frac{\partial B_r}{\partial \theta} \right) .$$

Substituting the expressions found above for the covariant components of \mathbf{B} yields

$$J^r = 0 ,$$

$$J^\theta = -\frac{T}{qR^2} \frac{dT}{dF} ,$$

$$\begin{aligned} J^\varphi &= \frac{1}{\sqrt{g}} \left\{ \frac{\partial}{\partial r} \left(\sqrt{g} R^{-2} \frac{dF}{dr} \nabla r \cdot \nabla r \right) + \frac{\partial}{\partial \theta} \left(\sqrt{g} R^{-2} \frac{dF}{dr} \nabla r \cdot \nabla \theta \right) \right\} \\ &= \nabla \cdot (R^{-2} \nabla F) . \end{aligned}$$

We now return to the equilibrium equation. Its only nontrivial component is along the covariant basis vector $\mathbf{e}_r = \nabla r$:

$$\frac{dP}{dr} = \sqrt{g} (J^\theta B^\varphi - J^\varphi B^\theta) ,$$

or

$$\frac{dP}{dF} = (qJ^\theta - J^\varphi) .$$

Substituting the contravariant components of J found above yields the Grad-Shafranov equation

$$\begin{aligned} \Delta^* F &\equiv R^2 \nabla (R^{-2} \nabla F) \\ &= - \left(T \frac{dT}{dF} + R^2 \frac{dP}{dF} \right) . \end{aligned} \quad (3.8)$$

Note that the Grad Shafranov equation depends on the geometry of the flux surfaces through the metric coefficients $(\nabla r \cdot \nabla \theta)$ and $|\nabla r|^2$. These coefficients also appear in the energy principle. They are evaluated in the next section.

3.3 Calculation of the Metric Coefficients

We now consider the solution of the Grad-Shafranov equation in the large aspect ratio limit. We will show that when the plasma is bounded by a perfectly conducting casing of circular cross section, the flux surfaces are circular to first order in the inverse aspect ratio. The center of these flux surfaces is continuously shifted towards the outside of the torus as one approaches the magnetic axis. The resulting equilibria are referred to as Shafranov shifted-circle equilibria. In modern tokamaks the highly conducting casing is replaced by the equivalent image currents flowing in external coils. Of course this equivalence only holds with regards to equilibrium: The stability of the plasma will generally depend on the precise form of the boundary conditions, unless the motion is localized within the plasma. This is the case during the early stages of the sawtooth crash.

The derivation of the properties of Shafranov equilibria is usually done by postulating the shifted-circle geometry at the outset and solving for the shift

function $\Delta(r)$ so as to satisfy the equilibrium equation. We will instead refrain from making any ad hoc assumptions about the geometry and derive all the results constructively. This makes the extension of the calculation to second order more transparent. It also shows clearly how the circularity assumption can be relaxed. A similar equilibrium analysis has been given by Greene et. al⁴³.

Following Shafranov and Yurchenko⁴⁴, a toroidal coordinate system (ρ, ω, φ) is introduced by

$$\begin{aligned} R &= R_c + \rho \cos \omega, \\ Z &= \rho \sin \omega, \end{aligned} \tag{3.9}$$

where R_c is the major radius of the center of the vacuum vessel. The coordinates ρ and ω are related to the true flux coordinates r and θ by

$$\begin{aligned} \rho &= \rho(r, \theta) \\ \omega &= \omega(r, \theta). \end{aligned}$$

To lowest order this is the identity transformation, $\rho = r$ and $\omega = \theta$. At this order the Grad-Shafranov equation reduces to the cylindrical equilibrium equation:

$$\frac{1}{r} \frac{dF}{dr} \frac{d}{dr} \left(r \frac{dF}{dr} \right) = - \left(T \frac{dT}{dr} + R_0^2 \frac{dP}{dr} \right). \tag{3.10}$$

This equation can be used to determine either one of the three variables F , T , or P from the other two. Note that

$$q(r) = \frac{rT}{R_0 \frac{dF}{dr}}, \tag{3.11}$$

so that $q \sim 1$ implies

$$\frac{1}{T} \frac{dF}{dr} = O\left(\frac{r}{R_0}\right).$$

The “low-beta” ordering results when all the terms in the equilibrium equation, Eq.(3.10), are taken to be of similar magnitude. Thus,

$$\frac{1}{T} \frac{dT}{dr} = O\left(\frac{r}{R_0}\right)^2 ,$$

and

$$\frac{R_0^2}{T^2} = O\left(\frac{r}{R_0}\right)^2 .$$

The first order corrections to the flux coordinate transformation can be presented as Fourier series in ω :

$$\begin{aligned} \rho &= r + \sum_{l=0}^{\infty} a_l(r) \cos l\theta , \\ \omega &= \theta + \sum_{l=1}^{\infty} b_l(r) \sin l\theta , \end{aligned} \tag{3.12}$$

where we have assumed symmetry about the equatorial plane.

The metric is calculated in terms of these coefficients in the following way: using Eq. (3.12) in Eq. (3.9) and taking the gradient of R and Z yields a linear relation between the covariant basis vectors of the two coordinate systems (R, Z) and (r, θ) .

$$\begin{pmatrix} \nabla R \\ \nabla Z \end{pmatrix} = M \cdot \begin{pmatrix} \nabla r \\ \nabla \theta \end{pmatrix} , \tag{3.13}$$

where the matrix M is given by

$$M = \begin{pmatrix} \frac{\partial R}{\partial r} & \frac{\partial R}{\partial \theta} \\ \frac{\partial Z}{\partial r} & \frac{\partial Z}{\partial \theta} \end{pmatrix} . \tag{3.14}$$

The matrix M is now decomposed into a product of two matrices representing the transformations from the coordinate system (R, Z) to (ρ, ω) and from (ρ, ω) to (r, θ) .

$$M = O \cdot N ,$$

where

$$O = \begin{pmatrix} \cos \omega & -\sin \omega \\ \sin \omega & \cos \omega \end{pmatrix} \quad (3.15)$$

is an orthogonal matrix:

$$O^t = O^{-1},$$

$$\det(O) = 1.$$

The matrix N is given by

$$N = \begin{pmatrix} \frac{\partial \rho}{\partial r} & \frac{\partial \rho}{\partial \theta} \\ \rho \frac{\partial \omega}{\partial r} & \rho \frac{\partial \omega}{\partial \theta} \end{pmatrix}. \quad (3.16)$$

Thus, $\det(M) = \det(N)$ and $M^{-1} = N^{-1} \cdot O^t$. To invert the matrix M note that its determinant is the jacobian of the poloidal coordinate transformation. It is related to the jacobian of the full flux coordinate system, given in Eq. (3.7), by

$$\begin{aligned} J\left(\frac{R, Z}{r, \theta}\right) &= J\left(\frac{R, \zeta, Z}{r, \theta, \varphi}\right) \\ &= J\left(\frac{R, \zeta, Z}{X, Y, Z}\right) J\left(\frac{X, Y, Z}{r, \theta, \varphi}\right) \\ &= \frac{Rr}{R_0}. \end{aligned} \quad (3.17)$$

This relation can be used to solve for the b_l in terms of the a_l by calculating $\det(M) = \det(N)$ explicitly and setting it equal to the expression above. Note that to lowest order the magnetic axis is located in the center of the conducting vessel, $(R_0 - R_c)/R_0 = O(a/R_0)^2$. Thus

$$\frac{rR}{R_0} = r + \frac{r^2}{R_0} \cos \theta + O(a/R_0)^2$$

We find

$$b_1 = \frac{r}{R_0} - \left(\frac{da_1}{dr} + \frac{1}{r}a_1 \right), \quad (3.18)$$

$$b_l = - \left(\frac{da_l}{dr} + \frac{1}{r}a_l \right), \text{ for } l \neq 1. \quad (3.19)$$

The inverse of N is now

$$N^{-1} = \frac{R_0}{Rr} \begin{pmatrix} \rho \frac{\partial \omega}{\partial \theta} & -\frac{\partial \rho}{\partial \theta} \\ -\rho \frac{\partial \omega}{\partial r} & \frac{\partial \rho}{\partial r} \end{pmatrix}. \quad (3.20)$$

The metric coefficients,

$$g_{ij} = \mathbf{e}_i \cdot \mathbf{e}_j,$$

are then readily derived, given $|\nabla R|^2 = |\nabla Z|^2 = 1$ and $\nabla R \cdot \nabla Z = 0$:

$$\begin{aligned} G &= \begin{pmatrix} \nabla r \\ \nabla \theta \end{pmatrix} \otimes \begin{pmatrix} \nabla r & \nabla \theta \end{pmatrix} \\ &= N^{-1} \cdot O^{-1} \cdot \begin{pmatrix} \nabla R \\ \nabla Z \end{pmatrix} \otimes \begin{pmatrix} \nabla R & \nabla Z \end{pmatrix} \cdot O^{-1^t} \cdot N^{-1^t} \\ &= N^{-1} \cdot O^{-1} \cdot I \cdot O^{-1^t} \cdot N^{-1^t} \\ &= N^{-1} \cdot N^{-1^t}. \end{aligned} \quad (3.21)$$

The corrections to the metric coefficients are clearly linear functions of the b_l and their first derivatives, but more importantly there is a one to one correspondence between Fourier harmonics of the coordinate transformation between (ρ, ω) and (r, θ) and the harmonics of the metric coefficients. It is to bring forward this correspondence that we decomposed the matrix M into the product of O and N . Consider now the first order Grad-Shafranov equation:

$$\frac{1}{r} \frac{\partial}{\partial r} \left(r \frac{dF}{dr} g_{rr}^{(1)} \right) + \frac{\partial}{\partial \theta} \left(\frac{dF}{dr} g_{r\theta}^{(1)} \right) = -2R_0 r \cos \theta \left(\frac{dP}{dF} \right).$$

After Fourier decomposition this becomes a set of second order differential equations for the coefficients a_l . These equations are all homogeneous except for $l = 1$. If the conducting wall is strictly circular the boundary conditions are that $a_l = 0$ at $r = 0$ as well as at the wall ($r = a$). The general solution is thus $a_l = 0$, for all $l \neq 1$. To see that this implies circularity of the flux surfaces we replace ρ and ω in Eq. (3.9), keeping only lowest order terms and dropping the indices:

$$R - R_c = r \cos \theta + a - (a + rb) \sin^2 \theta + O(a/R_0)^2 ,$$

$$Z = r \sin \theta + (a + rb) \sin \theta \cos \theta + O(a/R_0)^2 .$$

In terms of the angle ω_0 defined by

$$\omega_0 = \theta + \frac{1}{r} (a + rb) \sin \theta ,$$

this is

$$R - R_c = r \cos \omega_0 - a + O(a/R_0)^2 , \quad (3.22)$$

$$Z = r \sin \omega_0 + O(a/R_0)^2 . \quad (3.23)$$

Eqs. (3.22) and (3.23) are easily recognized as the equations for a circle of radius r and center $R_c + a$. Since the conducting shell is only fictitious it is conventional to write Eq. (3.22) in terms of the major radius of the magnetic axis R_0 . The distance between the center of the flux surface r and the magnetic axis is then denoted by Δ :

$$\begin{aligned} R - R_0 &= r \cos \omega_0 - \Delta + O(\varepsilon)^2 , \\ Z &= r \sin \omega_0 + O(\varepsilon)^2 , \end{aligned} \quad (3.24)$$

The shift $\Delta(r)$ is related to a_1 and the magnetic axis shift $\Delta_t = R_0 - R_c$ by:

$$\Delta = \Delta_t - a_1$$

Note that the metric may easily be generalized to the case of a slightly shaped conducting wall by including additional harmonics in the flux coordinate transformation, with coefficients determined by solving the above equation with boundary condition $a_l = \text{cst}$. One may thus consider the effect of small ellipticity or triangularity by including $l = 2$ and $l = 3$ harmonics, respectively.

In order to derive the lowest order mode equations, it is necessary to calculate the metric to second order in the inverse aspect ratio. Fortunately, for reasons that will become clear in the next chapter, only the $l = 0$ harmonic is needed at second order. The calculation goes essentially as sketched above except for the addition of a second order term $c(r)$ in the flux coordinate transformation:

$$\begin{aligned}\rho &= r + a(r) \cos \theta + c(r) , \\ \omega &= \theta + b(r) \sin \theta .\end{aligned}\tag{3.25}$$

This term is determined by setting the jacobian equal to rR/R_0 . Introducing the notation $k = 1/R_0$ one finds that to second order accuracy,

$$krR = r + kr^2 \cos \theta + \frac{1}{2}kr(a - rb - 2\Delta_t)$$

and

$$\det N = r + ((ra)' + rb) \cos \theta + \left(rc + \frac{1}{4}a^2 + \frac{1}{2}rab \right)' ,$$

where the primes denote differentiation with respect to r . We repeat for emphasis that only the $l = 0$ harmonic of the second order term is retained in this

and the following formulas. Setting these equal, we recover Eq. (3.18) and an equation determining c in terms of a :

$$rc = \frac{1}{4}a^2 + \frac{1}{2}raa' - \frac{1}{8}k^2r^4 - \frac{1}{2}kr^2\Delta_t. \quad (3.26)$$

we find for N

$$N = \begin{pmatrix} 1 + a' \cos \theta + c' & -a \sin \theta \\ rb' \sin \theta & r + (a + rb) \cos \theta + c + \frac{1}{2}ab \end{pmatrix}. \quad (3.27)$$

Its inverse is given by

$$\begin{aligned} N^{-1} &= \frac{1}{r}H \\ &= \frac{1}{r} \begin{pmatrix} h_{11} & h_{12} \\ h_{21} & h_{22} \end{pmatrix}, \end{aligned} \quad (3.28)$$

where

$$\begin{aligned} h_{11} &= r + (a + rb - kr^2) \cos \theta - \frac{1}{2}kr(a + rb) + c \\ &\quad + \frac{1}{2}ab + \frac{1}{2}k^2r^3 - \frac{1}{2}kr(a - rb - 2\Delta_t), \\ h_{12} &= a \sin \theta, \\ h_{21} &= -rb' \sin \theta, \\ h_{22} &= 1 + (a' - kr) \cos \theta + c' - \frac{1}{2}kra' \\ &\quad + \frac{1}{2}k^2r^2 - \frac{1}{2}k(a - rb - 2\Delta_t) \end{aligned}$$

Eliminating b and c with Eqs. (3.16) and (3.24), respectively, this becomes:

$$\begin{aligned} h_{11} &= r - ra' \cos \theta - \frac{1}{2}kra - \frac{a^2}{4r} + \frac{3}{8}k^2r^3 + \frac{1}{2}kr\Delta_t, \\ h_{12} &= a \sin \theta, \end{aligned}$$

$$\begin{aligned}
h_{21} &= -\left(kr - ra'' - a' + \frac{a}{r}\right) \sin \theta, \\
h_{22} &= 1 + (a - kr) \cos \theta + \frac{1}{2r}aa' - \frac{1}{4r^2}a^2 + \frac{1}{2}a'^2 \\
&\quad + \frac{1}{2}aa'' - kra' - ka + \frac{1}{2}k\Delta_t + \frac{5}{8}k^2r^2.
\end{aligned}$$

The metric is now given by $(1/r^2)HH^t$:

$$\begin{aligned}
(\nabla r)^2 &= 1 - 2a' \cos \theta + \frac{1}{2}(a')^2 - ka + \frac{3}{4}k^2r^2 + k\Delta, \\
(r\nabla\theta \cdot \nabla r) &= (ra'' + ra' - kr) \sin \theta, \\
(r\nabla\theta)^2 &= 1 + 2(a' - kr) \cos \theta + \frac{1}{2}r^2(a'')^2 + 2(a')^2 + ra'a'' \\
&\quad - 4kra' - ka + k\Delta_t + \frac{9}{4}k^2r^2 - kr^2a'',
\end{aligned}$$

or in terms of the shift from the magnetic axis $\Delta(r)$:

$$(\nabla r)^2 = 1 + 2\Delta' \cos \theta + \frac{1}{2}(\Delta')^2 + k\Delta + \frac{3}{4}k^2r^2, \quad (3.29)$$

$$(r\nabla\theta \cdot \nabla r) = -(r\Delta'' + r\Delta' - kr) \sin \theta, \quad (3.30)$$

$$\begin{aligned}
(r\nabla\theta)^2 &= 1 - 2(\Delta' + kr) \cos \theta + \frac{1}{2}r^2(\Delta'')^2 + 2(\Delta')^2 \\
&\quad + r\Delta'\Delta'' + 4kr\Delta' + k\Delta + k\Delta_t + \frac{9}{4}k^2r^2 + kr^2\Delta''. \quad (3.31)
\end{aligned}$$

The shift Δ can now be calculated from the Grad-Shafranov equation by substituting the above metric coefficients. Note that these are only needed to first order in the equilibrium equation.

$$\frac{r^2}{q^2}\Delta'' + 3\frac{r}{q^2}\Delta' + 2\frac{r^2}{q}\left(\frac{1}{q}\right)'\Delta' - \frac{r^2}{q^2} = -2r\frac{R_0^3}{T^2}P'$$

This equation can be integrated, giving

$$\frac{d\Delta(r)}{dr} = \frac{r}{R_0} \cdot \left(\beta_p(r) + \frac{1}{2}l_i(r)\right), \quad (3.32)$$

where

$$\beta_p(r) = -\frac{2R_0^2 q^2}{B_0^2 r^4} \int_0^r \hat{r}^2 \frac{dp(\hat{r})}{d\hat{r}} d\hat{r}, \quad (3.33)$$

$$l_i(r) = \frac{2q^2}{r^4} \int_0^r \frac{\hat{r}^3}{q^2(\hat{r})} d\hat{r}. \quad (3.34)$$

The quantity B_0 is the toroidal magnetic field on axis:

$$B_0 = \frac{T_0}{R_0}.$$

This completes the calculation of the metric. These results will be used in the next chapter to derive explicit linear eigenmode equations for a Shafranov equilibrium with arbitrary shear. Note that the magnitude of the shear has no qualitative effect on the *equilibrium*: It is only for *stability* considerations that low shear requires particular attention.

Chapter 4

Mode Equations

4.1 Introduction

The cylindrical analysis owes its simplicity to its high degree of symmetry, which allows the reduction of the linearized stability problem to a second order ordinary differential equation similar to the Sturm-Liouville equation. In toroidal geometry the poloidal symmetry is lost. Toroidal symmetry can still be invoked to reduce the problem to a system of two partial differential equations in the two variables r, θ ⁴⁵. In order to study this system analytically one must use approximate methods. The methods which can be applied fall under two categories:

- (i) WKB techniques, based on the assumption of large toroidal mode number. This approach provides information on the behavior of the discrete spectrum near its accumulation points⁴⁶⁻⁴⁸. Eigenmodes found by this method are referred to as Mercier or Ballooning modes according to their degree of localization. The ballooning representation was discovered almost simultaneously by several authors⁴⁹⁻⁵¹. Note that the applicability of WKB techniques to the analysis of modes which vary slowly along the magnetic field lines is not clear. The proof that perturbations can in fact be constructed which simultaneously satisfy the conflicting requirements of periodicity, small parallel and large perpendicular wavenumber, and

that the WKB expansion can be carried out to all orders, has been given by Dewar and Glasser⁵².

- (ii) Large aspect ratio asymptotic expansions: For large aspect ratio tori, the geometry of the equilibrium becomes locally similar to that of a cylinder. The eigenmode equations thus have approximate poloidal symmetry and the poloidal harmonics are decoupled at lowest order. The problem can thus be reduced to a set of coupled ordinary differential equations for the various harmonics. Note that although the curvature is only weakly perturbed by large aspect-ratio toroidal corrections, the stability properties are strongly affected. In fact, the eigenvalues and eigenmodes for the toroidal problem are generally quite different from those of the equivalent cylindrical problem, the only exception being for free-boundary modes¹⁸.

We will restrict attention to equilibria such that the Mercier criterion is satisfied, i.e. such that high- n modes are stable, and adopt the second approach.

4.2 Variational Formulation

In this section we expand the energy principle⁴⁰, modified by the inclusion of the kinetic energy, in powers of the inverse aspect ratio. The eigenmode equations are then derived by variation of the linearized energy with respect to the displacement ξ . It is shown that for the Shafranov geometry introduced above the problem reduces to a system of two coupled second order differential equations for the $m = nq$ and $m = nq + 1$ poloidal harmonics of the radial components of the displacement. We will refrain from making any assumptions as to the magnitude of the shear. This will enable us to obtain

general equations containing the finite shear equations of Bussac et al. as a limiting case. We will then discuss the various low shear orderings and solve the mode equation for $n=1$ and for the more realistic ordering $r q' \sim (q - 1) \sim \epsilon$. Similar derivations have been carried out by Zakharov⁵³ in flux coordinates but for finite shear only, and by Crew and Ramos⁵⁴ for general shear but in Shafranov coordinates.

The total energy of the perturbed plasma is given by

$$\delta E = \delta W + \delta K ,$$

where δW is the potential energy and δK the kinetic energy of the perturbation, given respectively by

$$\begin{aligned} \delta W &= \frac{1}{2} \int d\tau \left\{ |\mathbf{Q}|^2 + \mathbf{J} \cdot (\boldsymbol{\xi} \times \mathbf{Q}^*) + \Gamma P |\boldsymbol{\nabla} \cdot \boldsymbol{\xi}|^2 + (\boldsymbol{\xi}^* \cdot \boldsymbol{\nabla} P) (\boldsymbol{\nabla} \cdot \boldsymbol{\xi}) \right\} , \\ \delta K &= \gamma^2 \int d\tau \rho |\boldsymbol{\xi}|^2 , \end{aligned} \quad (4.1)$$

where

$$\mathbf{Q} = \boldsymbol{\nabla} \times (\boldsymbol{\xi} \times \mathbf{B}) , \quad (4.2)$$

and Γ is the ratio of specific heats. The magnetic differential operator and the volume element in flux coordinates are given by

$$\mathbf{B} \cdot \boldsymbol{\nabla} = \frac{T}{R^2} \left(\frac{1}{q} \frac{\partial}{\partial \theta} + \frac{\partial}{\partial \varphi} \right) , \quad d\tau = \frac{R^2}{R_0} r dr d\theta d\varphi. \quad (4.3)$$

The fluid displacement $\boldsymbol{\xi}$ is decomposed as follows:

$$\boldsymbol{\xi} = \boldsymbol{\xi}_p + \xi_{\parallel} \mathbf{B}/B$$

such that

$$\boldsymbol{\xi}_p \cdot \boldsymbol{\nabla} \varphi = 0 .$$

The poloidal components of the displacement are defined by

$$\xi_r = (T/T_0) \xi_p \cdot \nabla r ,$$

$$\xi_\theta = (T/T_0) \xi_p \cdot r \nabla \theta .$$

The poloidal displacement is given in terms of these components by

$$\xi_p = \frac{T_0}{T} (\xi_r \mathbf{e}_r + \xi_\theta \mathbf{e}_\theta) .$$

Note that ξ_r, ξ_θ are not the covariant components. As a first step to calculating the perturbed magnetic field \mathbf{Q} we calculate the vector product

$$\xi \times \mathbf{B} = \frac{T_0}{R_0} \left(\xi_\theta \nabla r - r \xi_r \nabla \theta + \frac{r}{q} \xi_r \nabla \varphi \right) .$$

Taking the curl of this expression, we find the contravariant components of \mathbf{Q}

$$\begin{aligned} Q^r &= \frac{T_0}{R^2} \left(\frac{1}{q} \frac{\partial}{\partial \theta} + \frac{\partial}{\partial \varphi} \right) \xi_r , \\ Q^\theta &= -\frac{T_0}{R^2} \left[\frac{1}{r} \frac{\partial}{\partial r} \left(\frac{r \xi_r}{q} \right) - \frac{1}{r} \frac{\partial \xi_\theta}{\partial \varphi} \right] , \\ Q^\varphi &= -\frac{T_0}{R^2} \left[\frac{1}{r} \frac{\partial}{\partial r} (r \xi_r) + \frac{1}{r} \frac{\partial \xi_\theta}{\partial \theta} \right] . \end{aligned} \tag{4.4}$$

The second term in the potential energy integral is now given by

$$\begin{aligned} \mathbf{J} \cdot (\xi \times \mathbf{Q}^*) &= \sqrt{g} \epsilon_{ijk} J^i \xi^j Q^{k*} , \\ &= \sqrt{g} \frac{dP}{dF} (-\xi^r Q^{\theta*} + \xi^\theta Q^{r*}) \\ &\quad + \sqrt{g} \frac{T}{R^2} \frac{dT}{dF} \left\{ \xi^r \left(\frac{1}{q} Q^{\varphi*} - Q^{\theta*} \right) + \xi^\theta Q^{r*} \right\} , \\ &= \frac{T_0^2}{R^2} \left\{ \frac{1}{R_0} \frac{dT}{dF} \left[r |\xi_r|^2 \frac{d}{dr} \left(\frac{1}{q} \right) + \xi_\theta^* \left(\frac{\partial \xi_r}{\partial \varphi} + \frac{1}{q} \frac{\partial \xi_r}{\partial \theta} \right) \right. \right. \end{aligned}$$

$$\begin{aligned}
& + \xi_\theta \left(\frac{\partial \xi_r^*}{\partial \varphi} + \frac{1}{q} \frac{\partial \xi_r^*}{\partial \theta} \right) \Bigg] \\
& + \frac{1}{R_0} \frac{dP}{dF} \left[\frac{R^2}{T} \left(\frac{\partial}{\partial r} \left(\frac{r \xi_r^*}{q} \right) - \frac{\partial \xi_\theta^*}{\partial \varphi} \right) \xi_r \right. \\
& \left. + \frac{R^2}{T} \xi_\theta \left(\frac{\partial \xi_r^*}{\partial \varphi} + \frac{1}{q} \frac{\partial \xi_r^*}{\partial \theta} \right) \right] \Bigg\} .
\end{aligned}$$

The last term is

$$(\xi^* \cdot \nabla P) \nabla \cdot \xi = \frac{T_0^2}{R^2} \left\{ \frac{1}{R_0} \frac{dP}{dF} \left[\frac{\xi_r^*}{q} \frac{\partial}{\partial r} \left(\frac{r R^2}{T} \xi_r \right) + \xi_r^* \frac{\partial}{\partial \theta} \left(\frac{R^2}{q T} \xi_\theta \right) \right] \right\} . \quad (4.5)$$

The total energy of the perturbation can now be written

$$E = \delta W_a + \delta W_b + \delta W_d + \hat{\gamma}^2 N \quad (4.6)$$

where

$$N = \frac{n^2 B_0^2}{2 R_0} \int \hat{\rho} |\xi|^2 \left(\frac{R}{R_0} \right)^2 r dr d\theta d\varphi, \quad \hat{\rho} = \frac{\rho}{\rho_0} \quad (4.7)$$

$$\delta W_d = \frac{1}{2} \int \Gamma p \left| \nabla \cdot \xi_p + \mathbf{B} \cdot \nabla \left(\frac{\xi_{\parallel}}{B} \right) \right|^2 \frac{R^2}{R_0} r dr d\theta d\varphi \quad (4.8)$$

$$\delta W_a = \frac{1}{2} B_0^2 R_0 \int r dr d\theta d\varphi \left| \frac{1}{r} \frac{\partial (r \xi_r)}{\partial r} + \frac{1}{r} \frac{\partial \xi_\theta}{\partial \theta} \right|^2 \quad (4.9)$$

$$\begin{aligned}
\delta W_b = & \frac{1}{2} \frac{B_0^2}{R_0} \int r dr d\theta d\varphi \left\{ \left| r \nabla \theta \left(\frac{\partial \xi_r}{\partial \varphi} + \frac{1}{q} \frac{\partial \xi_r}{\partial \theta} \right) + \nabla r \left(\frac{\partial}{\partial r} \left(\frac{r \xi_r}{q} \right) - \frac{\partial \xi_\theta}{\partial \varphi} \right) \right|^2 \right. \\
& + R_0 \frac{dT}{dF} \left[|\xi_r|^2 r \frac{d}{dr} \left(\frac{1}{q} \right) + \xi_\theta \left(\frac{\partial}{\partial \varphi} + \frac{1}{q} \frac{\partial}{\partial \theta} \right) \xi_r^* + \xi_\theta^* \left(\frac{\partial}{\partial \varphi} + \frac{1}{q} \frac{\partial}{\partial \theta} \right) \xi_r \right] \\
& \left. + R_0 \frac{dP}{dF} \left[\frac{1}{r} \frac{\partial}{\partial r} \left(\frac{R^2 |\xi_r|^2 r^2}{q T} \right) + \frac{R^2}{T} \left(\xi_\theta \frac{\partial \xi_r^*}{\partial \varphi} + \xi_\theta^* \frac{\partial \xi_r}{\partial \varphi} \right) \right] \right\} . \quad (4.10)
\end{aligned}$$

Here $B_0 = T_0/R_0$ and $\hat{\gamma}$ is defined as in Ch. 2: $\hat{\gamma} = \gamma \tau_A$.

The large aspect-ratio expansion of the energy can be obtained by straightforward expansion of the coefficients in these expressions. We define ϵ by $\epsilon = na/R_0$ so that the cylindrical model may be recovered by taking the limit $n \rightarrow \infty$, $\epsilon \rightarrow k_z a$. After rescaling $r : r/a \rightarrow r$ we rewrite the metric in terms of the normalized shift δ defined by $\delta = R_0 \Delta/a^2$ and in terms of the subsidiary ble

$$\alpha = \frac{d\delta}{dr},$$

so as to make the scalings with the small parameter ϵ/n explicit. Thus these new variables are given by

$$\frac{d\delta(r)}{dr} \equiv \alpha(r) = \left(\beta_p(r) + \frac{1}{2} l_i(r) \right) \cdot r \quad (4.11)$$

The metric is given in terms of these normalised variables by

$$(\bar{\nabla} r)^2 = 1 - 2 \left(\frac{\epsilon}{n} \right) \alpha \cos \theta + \left(\frac{\epsilon}{n} \right)^2 \left[\frac{1}{2} \alpha^2 + \frac{3}{4} r^2 + \delta \right], \quad (4.12)$$

$$\begin{aligned} (r \bar{\nabla} \theta)^2 &= 1 + 2 \left(\frac{\epsilon}{n} \right) (\alpha + r) \cos \theta \\ &+ \left(\frac{\epsilon}{n} \right)^2 \left[2\alpha^2 + 4r\alpha + \frac{9}{4} r^2 + \frac{1}{2} r^2 \alpha'^2 \right. \\ &\quad \left. + r\alpha' \alpha + r^2 \alpha' + \delta \right] \end{aligned} \quad (4.13)$$

$$(r \bar{\nabla} \theta \cdot \bar{\nabla} r) = \left(\frac{\epsilon}{n} \right) [r\alpha' + \alpha + r] \sin \theta. \quad (4.14)$$

The energy can now be expanded in a power series of ϵ

$$E = \epsilon^{-2} \delta W_a + \delta W_0 + \hat{\gamma}^2 N_0 + \frac{\epsilon}{n} \delta W_{1T} + \epsilon^2 \left(\delta W_{2C} + \frac{1}{n^2} \delta W_{2T} \right). \quad (4.15)$$

The linearized equations of motion can be obtained variationally from the Lagrangian. After substituting the assumed exponential time dependence of the

eigenmode, the eigenmode equations are given by minimizing the energy given in Eq. (4.6). The energy is a symmetric bilinear form with respect to the norm N :

$$E(\xi, \eta) = E(\eta, \xi) .$$

Note that the decomposition of the energy introduced in Eq. (4.6) preserves the symmetry property of E for each of its terms. It is often useful to think of the energy in terms of the inner product defined in terms of the norm N , and a symmetric operator F :

$$\begin{aligned} N(\xi, \eta) &= \langle \xi, \eta \rangle , \\ \delta W(\xi, \eta) &= \langle \xi, F\eta \rangle = \langle F\xi, \eta \rangle \end{aligned} \quad (4.16)$$

This force operator F is often improperly described as self-adjoint. In fact the correct mathematical definition of self-adjointness requires the domains of an operator and its adjoint to be identical. Demonstration of self-adjointness thus involves rather complicated functional-analytic considerations. This is *not* a mathematical fine point: self-adjointness has real physical consequences, such as completeness of the eigenfunction decomposition. This has bearing on such important questions as the sufficiency of the energy principle for magnetohydrodynamic stability. In fact it is unlikely that a self-adjoint extension of the force operator can be found for a toroidal plasma. Fortunately a demonstration of the sufficiency of the energy principle which does not rely on the completeness of the eigenfunction decomposition has been given by Laval et. al⁵⁵.

We proceed by substituting the expansion

$$\xi = \sum_{k=0}^{\infty} \sum_m \epsilon^k \xi_m^{(k)}(r) \exp \{i(m\theta - n\varphi)\} \quad (4.17)$$

into (4.6) and minimize order by order. Note that the symmetry of F implies that only even-order minimizations will be necessary. For arbitrary ξ , i.e. before any minimizations have been carried out, the relative ordering of the various terms in the energy principle is as follows:

$$\delta W_a \sim \epsilon^{-2}, \quad \delta W_b \sim \delta W_d \sim N \sim \epsilon^0.$$

The lowest order minimization involves a perfect square. The minimum value $\delta W_a = 0$ is reached for

$$\frac{\partial(r\xi_r^{(0)})}{\partial r} + \frac{\partial\xi_\theta^{(0)}}{\partial \theta} = 0. \quad (4.18)$$

Note that this is precisely the leading order term in δW_d , so that δW_d will be of order ϵ^2 for displacements which satisfy Eq. (4.18). The physical interpretation of this result is that slow plasma dynamics must be area preserving in the poloidal plane in order to avoid the large restoring forces associated with toroidal magnetic field compression.

4.3 Cylindrical Operator

The next order minimizations involve terms of order ϵ^0 . At this order the forces acting on the perturbation do not include the effects of toroidicity. The force operator which results from variation of the energy functional is thus identical to the cylindrical force operator. This operator is of considerable importance: it plays a central role in ideal as well as resistive stability; in the calculation of nonlinear corrections to mode growth; and in the study of the effects of noncircularity of the plasma cross-section. We shall derive its form variationally, for general m and n .

In addition to the work done by the cylinder-like forces on the lowest order perturbation $\xi^{(0)}$, the ϵ^0 -order terms include terms representing the

compressional energy associated with the order ϵ and ϵ^2 corrections to the eigenmode. These terms can be written symbolically

$$2\delta W^{(-2)}(\xi^{(0)}, \xi^{(2)}) + \delta W^{(-2)}(\xi^{(1)}, \xi^{(1)}) + \delta W^{(0)}(\xi^{(0)}, \xi^{(0)}) .$$

One of the terms at this order, $\delta W_a(\xi^{(0)}, \xi^{(2)})$ is clearly zero whenever $\xi^{(0)}$ satisfies the incompressibility property, Eq. (4.18). The remaining terms are formally functionals of $\xi_r^{(0)}, \xi_\theta^{(0)}, \xi_r^{(1)}$ and $\xi_\theta^{(1)}$. However the minimization condition found above implies that $\xi_r^{(0)}$ and $\xi_\theta^{(0)}$ are not independent. Thus $\xi_\theta^{(0)}$ should be eliminated in favor of $\xi_r^{(0)}$ before minimizing. The first order displacements $\xi_r^{(1)}, \xi_\theta^{(1)}$ appear only in δW_a and minimization with respect to these terms is thus achieved for

$$\frac{\partial(r\xi_{rm}^{(1)})}{\partial r} + \frac{\partial\xi_{\theta m}^{(1)}}{\partial \theta} = 0 \quad \forall m . \quad (4.19)$$

The only remaining nonzero terms in $E^{(0)}$ are now δW_b and N . After elimination of $\xi_\theta^{(0)}$, δW_b becomes:

$$\begin{aligned} \delta W_b = & \frac{n^2 B_0^2}{2R_0} \int r dr \left\{ \left[(m\mu - 1)^2 \xi_{r1}^{(0)2} + \left((m\mu - 1) \frac{1}{m} \frac{d(r\xi_{r1}^{(0)})}{dr} + r\xi_{r1}^{(0)} \frac{d\mu}{dr} \right)^2 \right] \right. \\ & \left. + \left(\frac{R_0}{n} \frac{dT}{dF} + \frac{R_0^3}{nT_0} \frac{dP}{dF} \right) \left[r\xi_{r1}^{(0)2} \frac{d\mu}{dr} - 2 \left(\frac{1}{m} - \mu \right) \xi_{r1}^{(0)} \frac{d(r\xi_{r1}^{(0)})}{dr} \right] \right\} \end{aligned}$$

where $\mu = \frac{1}{nq}$. The Zeroth order Grad-Shafranov equation, Eq. (3.10),

$$\begin{aligned} T_0 \frac{dT}{dF} + R_0^2 \frac{dP}{dF} &= -\frac{1}{r} \frac{d}{dr} \left(r \frac{dF}{dr} \right) \\ &= -\frac{T_0}{R_0} \left[\frac{2}{q} + r \frac{d}{dr} \left(\frac{1}{q} \right) \right] \end{aligned} \quad (4.20)$$

can be used to simplify δW_b . One finds

$$\delta W_b = \quad (4.21)$$

$$\frac{n^2 B_0^2}{2m^2 R_0} \int dr \left\{ \left[(m^2 - 1)(m\mu - 1)^2 + 2(1 - m^2 \mu^2) - 2m^2 r \mu \frac{d\mu}{dr} \right] r \xi_{r1}^{(0)2} \right. \\ \left. + (1 - m^2 \mu^2) r^2 \frac{d(\xi_{r1}^{(0)2})}{dr} + (m\mu - 1)^2 r^3 \left(\frac{d\xi_{r1}^{(0)}}{dr} \right)^2 \right\}$$

after integration by parts this becomes

$$\delta W_b = \frac{n^2 T_0^2}{m^2 R_0^3} \int dr \left\{ (m^2 - 1)(m\mu - 1)^2 r \xi_{r1}^{(0)2} \right. \\ \left. + (m\mu - 1)^2 r^3 \left(\frac{d\xi_{r1}^{(0)}}{dr} \right)^2 \right\} \quad (4.22)$$

We introduce an inner product defined by

$$\langle \xi, \eta \rangle = \frac{n^2 B_0^2}{2R_0} \int dr (\xi_r^* \cdot \eta_r) . \quad (4.23)$$

The bilinear form $\delta W^{(0)}$ can be written with this inner product in terms of a symmetric operator L_m as

$$\delta W^{(0)}(\xi, \eta) = \langle \xi, L_m \eta \rangle = \langle L_m \xi, \eta \rangle . \quad (4.24)$$

The operator L_m is easily found by integration by parts of Eq. (4.22).

$$L_m \xi = \frac{d}{dr} \left[\left(\mu - \frac{1}{m} \right)^2 r^3 \frac{d\xi}{dr} \right] - (m^2 - 1) \left(\mu - \frac{1}{m} \right)^2 r \xi . \quad (4.25)$$

The operator L_m is the cylindrical force-operator discussed at the beginning of this section. It has a regular singular point at the origin with characteristic exponents $m-1$ and $-m-1$, and at the mode rational surfaces, where $m\mu = 1$, with characteristic exponents 0 and 1. For $m=1$, it can readily be inverted by simple quadratures, but inverting it for $m \neq 1$ can only be done for certain special current profiles. An important case is that of constant current profiles, for which μ is constant, so that L_m is then an Euler operator: that is, it is

homogeneous in r . It can then also be inverted by simple quadratures. A more complicated but still important case is that of the power-law current profile for which L_m is a hypergeometric operator.

The identity of the energy expansions for cylindrical and toroidal geometries up to this order justifies the use of the cylindrical model to draw conclusions as to the nature of the possible instabilities. In particular the conclusion that the unstable modes are characterized by rigid shift displacements for sheared equilibria and cellular convection flows within low shear regions is also valid in toroidal geometry. However, at this order the appropriate displacements are only marginally stable: stability is ultimately determined by the ϵ^2 -term in the energy expansion. This implies that $\hat{\gamma}$ is at most of order ϵ . This observation justifies delaying consideration of the kinetic energy terms until the order ϵ^2 minimizations are undertaken.

In this chapter we are primarily interested in comparing the finite shear analysis of Bussac et. al to the low shear case. Since finite shear equilibria are always stable to $m \neq 1$ perturbations we will henceforth restrict attention to the $m = 1$ case. The results of the minimizations carried out so far are summarized by:

$$\frac{d}{dr} \left(r \xi_{rm}^{(k)} \right) + im \xi_{\theta m}^{(k)} = 0, \quad k = 0, 1, \forall m \quad (4.26)$$

and

$$\delta W_0 = \frac{n^2 B_0^2}{2R_0} \int r dr (\mu - 1)^2 \left(r \frac{d\xi_{r1}^{(0)}}{dr} \right)^2, \quad (4.27)$$

4.4 Algebraic Minimizations

We now consider the order ϵ^2 terms in the energy. After eliminating $\xi_{\theta 1}^{(0)}$, $\xi_{\theta 2}^{(1)}$, and $\xi_{r0}^{(1)}$ with Eq. (4.18), the ϵ^2 -order term can be expressed as a

functional of $\xi_{r1}^{(0)}$, $\xi_{\theta 0}^{(1)}$, $\xi_{r2}^{(1)}$, $\xi_{\theta 1}^{(2)}$, $\xi_{||0}^{(0)}$, and $\xi_{||2}^{(0)}$. All of these variables except $\xi_{r1}^{(0)}$ and $\xi_{r2}^{(1)}$ can be eliminated through algebraic minimizations. By this it is meant that the energy can be minimized with respect to these variables without solving a differential equation. This occurs when a variable η appears in the energy functional in the form

$$\begin{aligned} E &= \int dr \left(a\eta^2 + \eta B[\xi] + \xi B[\eta] \right) , \\ &= \langle \eta, a\eta \rangle + \langle \eta, B\xi \rangle + \langle \xi, B\eta \rangle , \end{aligned}$$

where a is a simple multiplicative coefficient and B is a linear differential operator. The energy is then minimized by

$$\eta = -\frac{1}{a}B[\xi] ,$$

and the minimum value is

$$E = - \int dr \left(\frac{1}{a} |B[\xi]|^2 \right) .$$

We now carry out the three algebraic minimizations in turn. The minimization with respect to $\xi^{(2)}$ is the simplest, being identical to that in the cylindrical case. The relevant terms are

$$\delta W^{(-2)}(\xi^{(2)}, \xi^{(2)}) + 2\delta W^{(0)}(\xi^{(2)}, \xi^{(0)}) .$$

We define the second-order perpendicular-divergence term χ by

$$\chi = - \left(\frac{d(r\xi_{r1}^{(2)})}{dr} + i\xi_{\theta 1}^{(2)} \right) ,$$

so that

$$\begin{aligned} \delta W^{(-2)}(\xi^{(2)}, \xi^{(2)}) &= \epsilon^2 \delta W_a(\xi^{(2)}, \xi^{(2)}) \\ &= \frac{n^2 B_0^2}{2R_0} \int dr \left| \frac{\chi}{r} \right|^2 \end{aligned}$$

The term linear in $\xi^{(2)}$ can be separated into a χ term and a $\xi_{r1}^{(2)}$ term as follows

$$\delta W^{(0)}(\xi^{(2)}, \xi^{(0)}) = \langle \chi, B\xi_{r1}^{(0)} \rangle + \langle \xi_{r1}^{(2)}, L^{(0)}\xi_{r1}^{(0)} \rangle$$

where B and L are linear differential operators. If χ is taken to be zero the second term in this equation should clearly reduce to the same bilinear form which was found above for the order ϵ^0 energy. The operator $L^{(0)}$ must therefore be the zeroth order cylindrical operator. This implies that

$$L^{(0)}\xi_{r1}^{(0)} = 0 ,$$

so that only terms in χ appear in the energy at this order. The operator B is then found most expediently by setting $\xi_{r1}^{(2)*} = 0$ and $\xi_{\theta 1}^{(2)*} = i\chi^*$ in δW_b . The actual value of $\xi_{r1}^{(2)*}$ is of course determined by higher order minimizations. One finds for B

$$\begin{aligned} B[\xi_{r1}^{(0)}] &= \left[\frac{d}{dr}(r\mu\xi_{r1}^{(0)}) - \frac{d}{dr}(r\xi_{r1}^{(0)}) \right] \\ &+ \frac{R_0}{n} \frac{dT}{dF} [-(\mu-1)\xi_{r1}^{(0)}] + \frac{R_0^3}{nT} \frac{dP}{dF} \xi_{r1}^{(0)} \end{aligned}$$

The minimization yields

$$\chi = -r^2 \left\{ \frac{d}{dr} [(\mu-1)r\xi_{r1}^{(0)}] + \frac{1}{r} \frac{d}{dr}(r^2\mu)(\mu-1)\xi_{r1}^{(0)} + \frac{\mu R_0^3}{nT} \frac{dP}{dF} \xi_{r1}^{(0)} \right\} ,$$

where the equilibrium equation has been used to eliminate the term dT/dF .

The minimum energy attained for this value of χ is

$$\begin{aligned} [\delta W^{(-2)}(\xi^{(2)}, \xi^{(2)}) + 2\delta W^{(0)}(\xi^{(2)}, \xi^{(0)})]_{min} \\ = -\frac{n^2 B_0^2}{2R_0} \int dr r^2 \left\{ [((\mu-1)r\xi_{r1}^{(0)})' \right. \\ \left. + \frac{1}{r}(r^2\mu)'(\mu-1)\xi_{r1}^{(0)}] \right. \\ \left. + \frac{\mu R_0^3}{nT} \frac{dP}{dF} \xi_{r1}^{(0)} \right\}^2 \end{aligned}$$

We next minimize with respect to $\xi_{\theta 0}^{(1)}$, that is, the first order poloidal component of the $m = 0$ harmonic. Note that first order incompressibility implies that the $m = 0$ harmonic of the radial displacement, $\xi_{r 0}^{(1)}$ is zero.

Before proceeding with the minimizations we introduce the following compact notation for the various terms in the metric coefficients:

$$\begin{aligned} (\nabla r)^2 &= 1 + 2 \left(\frac{\epsilon}{n} \right) a \cos \theta + \left(\frac{\epsilon}{n} \right)^2 f \\ (r \nabla \theta)^2 &= 1 + 2 \left(\frac{\epsilon}{n} \right) b \cos \theta + \left(\frac{\epsilon}{n} \right)^2 g \\ (r \nabla \theta \cdot \nabla r) &= \left(\frac{\epsilon}{n} \right) c \sin \theta \end{aligned}$$

We write

$$\eta = i n \xi_{\theta 0}^{(1)}$$

This variable appears quadratically in δW_b ,

$$\delta W_0(\eta, \eta) = \frac{1}{2} \frac{B_0^2}{R_0} \int r dr |\eta|^2, \quad (4.28)$$

and linearly in the term

$$\begin{aligned} \delta W_{1T}(\xi, \eta) &= \frac{B_0^2}{2R_0} \int r dr \left\{ -\frac{c}{2}(\mu - 1)\xi + \frac{a}{2}[(r\mu\xi)' - (r\xi)'] \right. \\ &\quad \left. - \frac{R_0^3}{nT} \frac{dP}{dF} r \xi \right\} \eta^* \end{aligned}$$

The minimum is thus attained for

$$\eta = -\frac{a}{2}((\mu - 1)(r\xi)' - \frac{a}{2}\mu' r \xi + \frac{c}{2}(\mu - 1)\xi + \frac{R_0^3}{nT} \frac{dP}{dF} r \xi \quad (4.29)$$

Recall that the first order equilibrium Grad-Shafranov equation implies that

$$\frac{R_0^3}{nT} \frac{dP}{dF} = -\frac{1}{2}(\mu\alpha' + (3\mu + 2r\mu')\frac{\alpha}{r} - \mu) \quad (4.30)$$

so that, replacing a and b by their value, η is given by

$$\eta = \alpha(\mu - 1)r\xi' + [\mu r - \frac{1}{2}(r\alpha' + 3\alpha + r)]\xi \quad (4.31)$$

and the minimum is

$$\delta W_0(\eta, \eta) = \frac{1}{2} \frac{B_0^2}{R_0} \int r dr \left| \alpha(\mu - 1)r\xi' + [\mu r - \frac{1}{2}(r\alpha' + 3\alpha + r)]\xi \right|^2, \quad (4.32)$$

4.5 Minimization With Respect To Parallel Displacement

We now consider the minimization of the parallel displacement term $\xi_{||}$. The divergence which appears in δW_d can be expanded as follows:

$$\begin{aligned} \nabla \cdot \xi &= \nabla \cdot \xi_p + \mathbf{B} \cdot \nabla \left(\frac{\xi_{||}}{B} \right) \\ &= 2\xi_p \cdot \nabla R/R - \xi_p \cdot \nabla T/T \\ &\quad + i\epsilon \sum_m (m\mu - 1)\xi_{||} + \frac{R^2}{T} \nabla \cdot \left(\frac{T}{R^2} \xi_p \right). \end{aligned}$$

The last term is of order ϵ^2 by virtue of previous minimizations. The second term, involving the logarithmic gradient of T , is clearly also of order ϵ^2 . The remaining terms are all of order ϵ :

$$\nabla \cdot \xi = 2\xi_p \cdot \nabla R/R + i\epsilon \sum_m (m\mu - 1)\xi_{||} + O(\epsilon^2),$$

so that δW_d is

$$\delta W_d = \frac{n^2 B_0^2}{2R_0} \int r dr d\theta \Gamma \beta \left| \frac{2}{n} \xi_p \cdot \nabla R + i \sum_m (m\mu - 1)\xi_{||} \right|^2,$$

where the toroidal β has been introduced

$$\beta = \frac{P}{B_0^2}.$$

The term $\xi_{||}$ also appears in the kinetic energy,

$$\hat{\gamma}^2 N = \frac{n^2 B_0^2}{2R_0} \int r dr d\theta \hat{\rho} \hat{\gamma}^2 \left[\sum_m |\xi_{||}|^2 + |\xi_{p1}^{(0)}|^2 \right] .$$

The term $\xi_p \cdot \nabla R$ is given explicitly by

$$2\xi_p \cdot \nabla R = \left(-\xi_{r1}^{(0)} + (r\xi_{r1}^{(0)})' \right) e^{2i\theta - in\varphi} + \left(\xi_{r1}^{(0)} + (r\xi_{r1}^{(0)})' \right) e^{-in\varphi} .$$

The term to be minimized can be written symbolically as

$$|if\xi_{||} + g|^2 + h^2|i\xi_{||}|^2 ,$$

where

$$f = (m\mu - 1) ,$$

$$g = \frac{2}{n} \xi_p \cdot \nabla R ,$$

$$h^2 = \frac{\hat{\rho} \hat{\gamma}^2}{\Gamma \beta} .$$

The minimum is reached for

$$\begin{aligned} i\xi_{||} &= -\frac{fg}{f^2 + h^2} \\ &= -\begin{cases} \frac{1}{n} \frac{\Gamma \beta}{\hat{\rho} \hat{\gamma}^2 + \Gamma \beta} \left(\xi_{r1}^{(0)} + (r\xi_{r1}^{(0)})' \right) & , \text{ for } m = 0 \\ \frac{1}{n} \frac{\Gamma \beta (1 - 2\mu)}{\hat{\rho} \hat{\gamma}^2 + \Gamma \beta (1 - 2\mu)^2} \left(-\xi_{r1}^{(0)} + (r\xi_{r1}^{(0)})' \right) & , \text{ for } m = 2 \end{cases} . \end{aligned}$$

The minimum value associated with these terms is

$$\begin{aligned} \delta W_d + \hat{\gamma}^2 N_{||} &= \frac{n^2 B_0^2}{2R_0} \int r dr \Gamma \beta \left(if\xi_{||min} + g \right)^2 + h^2 (\xi_{||min})^2 \\ &= \frac{n^2 B_0^2}{2R_0} \int r dr \Gamma \beta \frac{g^2 h^2}{f^2 + h^2} \\ &= \frac{B_0^2}{2R_0} \int r dr \frac{\Gamma \beta \hat{\rho} \hat{\gamma}^2}{\hat{\rho} \hat{\gamma}^2 + \Gamma \beta} \left(\xi_{r1}^{(0)} + (r\xi_{r1}^{(0)})' \right)^2 \\ &\quad + \frac{\Gamma \beta \hat{\rho} \hat{\gamma}^2}{\hat{\rho} \hat{\gamma}^2 + \Gamma \beta (1 - 2\mu)^2} \left(\xi_{r1}^{(0)} - (r\xi_{r1}^{(0)})' \right)^2 . \end{aligned}$$

We will see in the following sections that the kinetic energy term only plays a role in the resonant region, where $\mu - 1 = O(\epsilon)$. This is the case both for low shear and finite shear systems. This allows us to replace μ by one in the above expression:

$$\delta W_d + \hat{\gamma}^2 N_{\parallel} = \frac{B_0^2}{2R_0} \int r dr \hat{\rho} \hat{\gamma}^2 \frac{2\Gamma\beta}{\hat{\rho}\hat{\gamma}^2 + \Gamma\beta} \left((\xi_{r1}^{(0)})^2 + (r(\xi_{r1}^{(0)})')^2 \right) .$$

This term may be added to the kinetic energy of the perpendicular motion,

$$\hat{\gamma}^2 N_{\perp} = \frac{n^2 B_0^2}{2R_0} \int r dr \hat{\rho} \hat{\gamma}^2 \left((\xi_{r1}^{(0)})^2 + ((r\xi_{r1}^{(0)})')^2 \right) ,$$

to obtain the total kinetic energy, extremized over parallel compressional motion,

$$\delta W_d + \hat{\gamma}^2 N = \frac{n^2 B_0^2}{2R_0} \int r dr \hat{\rho} \hat{\gamma}^2, \left(\frac{\hat{\rho}\hat{\gamma}^2 + (1 + 2/n^2)\Gamma\beta}{\hat{\rho}\hat{\gamma}^2 + \Gamma\beta} \right) \left((\xi_{r1}^{(0)})^2 + ((r\xi_{r1}^{(0)})')^2 \right) .$$

Note that we have not made any assumption of incompressibility. It is customary when solving the mode equations to assume that mode growth is slow compared to sound wave propagation, so that $\hat{\gamma}^2/\Gamma\beta \ll 1$. This ordering applies, of course, close to marginal stability, but has more general validity. The kinetic energy term is then

$$\delta W_d + \hat{\gamma}^2 N = \left(1 + \frac{2}{n^2} \right) \hat{\gamma}^2 \frac{n^2 B_0^2}{2R_0} \int r dr \hat{\rho} \left((\xi_{r1}^{(0)})^2 + ((r\xi_{r1}^{(0)})')^2 \right) . \quad (4.33)$$

4.6 Final Minimizations

We now approach the minimization with respect to terms which cannot be eliminated algebraically. We first consider $\xi_{r2}^{(1)}$. This term appears in

the second order energy expansion in the following form:

$$\delta W^{(0)}(\xi_{r2}^{(1)}, \xi_{r2}^{(1)}) + \delta W_T^{(1)}(\xi_{r2}^{(1)}, \xi_{r1}^{(0)}) ,$$

where the term quadratic in $\xi_{r2}^{(1)}$ is of course simply

$$\delta W^{(0)}(\xi_{r2}^{(1)}, \xi_{r2}^{(1)}) = \langle \xi_{r2}^{(1)}, L_2[\xi_{r2}^{(1)}] \rangle .$$

To calculate the coupling energy $\delta W_T^{(1)}(\xi_{r2}^{(1)}, \xi_{r1}^{(0)})$ the following relations are used

$$\xi_{\theta 2}^{(1)} = \frac{i}{2} \frac{d}{dr} (r \xi_{r2}^{(1)}) ,$$

$$\frac{\partial \xi_{\theta 2}^{(1)}}{\partial \varphi} = \frac{1}{2} \frac{d}{dr} (r \xi_{r2}^{(1)}) .$$

The coupling energy $\delta W_T^{(1)}(\xi_{r2}^{(1)}, \xi_{r1}^{(0)})$ is given by

$$\begin{aligned} \delta W_T^{(1)}(\xi_{r2}^{(1)}, \xi_{r1}^{(0)}) = & \frac{n^2 B_0^2}{2R_0} \int dr \quad 2rb(\mu - 1)(\mu - 1/2) \xi_{r1}^{(0)} \xi_{r2}^{(1)} \\ & + (rc/2)(\mu - 1) \xi_{r1}^{(0)} [(\mu - 1/2)r \xi_{r2}^{(1)}]' \\ & - rc(\mu - 1/2) [(\mu - 1)r \xi_{r1}^{(0)}]' \xi_{r2}^{(1)} \\ & + ra[(\mu - 1)r \xi_{r1}^{(0)}]' [(\mu - 1/2)r \xi_{r2}^{(1)}]' \\ & p \{ \xi_{r1}^{(0)} [r^3(\mu - 1/2) \xi_{r2}^{(1)}]' \\ & + r^3(\mu - 1)(\xi_{r1}^{(0)})' \xi_{r2}^{(1)} \} \end{aligned}$$

where p is defined by

$$p = \frac{\mu}{2} \left[a' + \left(\frac{3}{r} + 2 \frac{\mu}{\mu'} \right) - 1 \right] . \quad (4.34)$$

Note that the term proportional to dT/dF does not contribute to the coupling integral. Define the operator $C^{(1)}$ by

$$\delta W_T^{(1)}(\xi_{r1}^{(0)}, \xi_{r2}^{(1)}) = \langle \xi_{r1}^{(0)}, C^{(1)}[\xi_{r2}^{(1)}] \rangle . \quad (4.35)$$

Note that $C^{(1)}$ is not a symmetric operator. Its adjoint is found by integrating by parts,

$$\langle \xi_{r1}^{(0)}, C^{(1)}[\xi_{r2}^{(1)}] \rangle = \langle C^{(1)\dagger}[\xi_{r1}^{(0)}], \xi_{r2}^{(1)} \rangle . \quad (4.36)$$

One finds

$$\begin{aligned} C^{(1)\dagger} = & 2rb(\mu - 1)(\mu - 1/2)\xi_{r1}^{(0)} - [(rc/2)(\mu - 1)\xi_{r1}^{(0)}]'(\mu - 1/2)r \\ & - rc(\mu - 1/2)[(\mu - 1)r\xi_{r1}^{(0)}]' - \{ra[(\mu - 1)r\xi_{r1}^{(0)}]'\}'(\mu - 1/2)r \\ & - (p\xi_{r1}^{(0)})'r^3(\mu - 1/2) + r^3p(\mu - 1)(\xi_{r1}^{(0)})' . \end{aligned}$$

After substitution of a, b, c and p by their value in terms of α this becomes

$$\begin{aligned} C^{(1)\dagger} = & (\mu - 1)(\mu - 1/2)\alpha r^3(\xi_{r1}^{(0)})'' \\ & + [2(\mu - 1/2)\mu'\alpha - (1/2)(\mu - 1/2)(\mu - 1)(\alpha' - 3\alpha/r + 3) \\ & - (\mu/4)(\alpha' + (3/r + 2\mu'/\mu)\alpha - 1)]r^3(\xi_{r1}^{(0)})' \\ & - [(\mu - 1/2)^2(r^2\alpha'' + 3r\alpha' - 3\alpha)r + (\mu - 1/2)\mu'(2r\alpha' + r)r^2]\xi_{r1}^{(0)} . \end{aligned}$$

The minimization with respect to $\xi_{r1}^{(0)}$ is accomplished in a similar fashion. However, it involves a plethora of terms, of which only a few actually play a role in the final equations. For this reason we omit the details of the algebra and simply list the results, along with a summary of the minimizations performed until now. The results are:

$$-in\xi_{\theta 0}^{(1)} = \alpha(\mu - 1)r\frac{d\xi_{r1}^{(0)}}{dr} - \left\{\frac{1}{2}(r\alpha' + 3\alpha + r) - r\mu\right\}\xi_{r1}^{(0)} \quad (4.37)$$

$$\begin{aligned}
-i\xi_{\theta 1}^{(2)} &= -r^2 \frac{d}{dr} [(\mu - 1)r\xi_{r1}^{(0)}] - r(r^2\mu)'(\mu - 1)\xi_{r1}^{(0)} \\
&\quad + \frac{1}{2}\mu^2 \left[r\alpha' + \left(3 + 2r\frac{\mu'}{\mu} \right) \alpha - r \right] r\xi_{r1}^{(0)} \quad (4.38)
\end{aligned}$$

$$-in\xi_{||0}^{(0)} = \frac{\Gamma\beta}{\hat{\rho}\hat{\gamma}^2 + \Gamma\beta} \left\{ \xi_{r1}^{(0)} + \frac{d}{dr} (r\xi_{r1}^{(0)}) \right\} \quad (4.39)$$

$$-in\xi_{||2}^{(0)} = \frac{\Gamma\beta(2\mu - 1)}{\hat{\rho}\hat{\gamma}^2 + \Gamma\beta(2\mu - 1)^2} \left\{ \xi_{r1}^{(0)} - \frac{d}{dr} (r\xi_{r1}^{(0)}) \right\}, \quad (4.40)$$

where $\beta = p/B_0^2$. Minimization with respect to the remaining two variables finally yields the two coupled second order differential equations.⁵⁴

$$[\epsilon^{-2}(L_1 + T) - G_1^{(2)}] \xi_{r1}^{(0)} = C^{(1)} \xi_{r2}^{(1)} \quad (4.41)$$

$$L_2 \xi_{r2}^{(1)} = C^{(1)\dagger} \xi_{r1}^{(0)}. \quad (4.42)$$

Here the operators L_m are the line-bending operators, T is the kinetic energy operator, $C^{(1)}$ is the toroidal coupling operator, and G_1 is the driving term containing the cylindrical coefficient g_1 as well as toroidal corrections. $C^{(1)\dagger}$ is the operator adjoint to $C^{(1)}$, defined by

$$\int_0^1 dr f(r) C^{(1)} [g(r)] = \int_0^1 dr g(r) C^{(1)\dagger} [f(r)]. \quad (4.43)$$

Explicitly,

$$L_m \xi = \frac{d}{dr} \left\{ \left(\mu - \frac{1}{m} \right)^2 r^3 \frac{d\xi}{dr} \right\} - (m^2 - 1) \left(\mu - \frac{1}{m} \right)^2 r \xi. \quad (4.44)$$

The general expression for C^\dagger is

$$\begin{aligned}
nC^\dagger \xi_1 &= \left(\mu - \frac{1}{2} \right) \alpha r^3 \frac{d}{dr} \left\{ (\mu - 1) \frac{d\xi_1}{dr} \right\} + \left\{ (\mu - 1) r \mu' \alpha \right. \\
&\quad \left. - \frac{1}{2} \left(\mu - \frac{1}{2} \right) (\mu - 1) (r\alpha' - 3\alpha + 3r) - \frac{1}{4} \mu (r\alpha' + 3\alpha - r) \right\} r^2 \frac{d\xi_1}{dr}
\end{aligned}$$

$$- \left\{ \left[\left(\mu - \frac{1}{2} \right)^2 r^3 \left(\alpha + \frac{r}{2} \right)' \right]' - 3r \left(\mu - \frac{1}{2} \right)^2 \left(\alpha + \frac{r}{2} \right) \right\} \xi_1, \quad (4.45)$$

where we note that the coefficient of ξ_1 is simply $-L_2(\alpha + r/2)$. For $q - 1 \sim \epsilon$, the kinetic energy operator can be written

$$T\xi_1 = \frac{d}{dr} \left\{ \hat{\rho} \hat{\gamma}^2 \zeta r^3 \frac{d\xi_1}{dr} \right\} + \hat{\gamma}^2 r^2 \frac{d}{dr} (\hat{\rho} \zeta) \xi_1, \quad (4.46)$$

where

$$\zeta = \frac{\hat{\rho} \hat{\gamma}^2 + (1 + 2n^{-2}) \Gamma \beta}{\hat{\rho} \hat{\gamma}^2 + \Gamma \beta}.$$

When $\hat{\gamma}^2 \ll \Gamma \beta$, $\hat{\rho} = 1$, this expression reduces to

$$T\xi_1 = \frac{d}{dr} \left\{ \left(1 + \frac{2}{n^2} \right) \hat{\gamma}^2 r^3 \frac{d\xi_1}{dr} \right\}. \quad (4.47)$$

The operator G can be written

$$G = \left(1 - \frac{1}{n^2} \right) G_C + \frac{1}{n^2} G_T, \quad (4.48)$$

$$\begin{aligned} G_C \xi_1 &= \frac{d}{dr} \left\{ (\mu - 1)^2 r^5 \frac{d\xi_1}{dr} \right\} - \left\{ (\mu^2 r^4 \beta_p)' + (\mu - 1)(\mu + 3)r^3 \right\} \xi_1 \\ &+ \left\{ \frac{r}{2} (\mu - 1)^2 (\mu^2 r^4 (\beta_p - 1))' \right\} \xi_1, \end{aligned} \quad (4.49)$$

where the last (total derivative) coefficient of ξ_1 arises from our definition of $\xi_r = (T/T_0) \xi \cdot \nabla r$;

$$\begin{aligned} G_T \xi_1 &= \frac{d}{dr} \left\{ (\mu - 1)^2 r^3 \frac{d\xi_1}{dr} \right\} + \left\{ \left(\mu - \frac{1}{2} \right)^2 r \left[r^2 \left(\alpha + \frac{r}{2} \right)' + 3 \left(\alpha + \frac{r}{2} \right)^2 \right] \right. \\ &+ \left. (\mu^2 - 1) \frac{r^3}{2} + \frac{3}{4} (r^2 \alpha^2 - r^3 \alpha)' \right\} \xi_1 \\ &+ \left\{ \frac{d}{dr} [(\mu - 1)^2 r^2 v + (\mu^2 - 1) r^2 w] \right\} \xi_1, \end{aligned} \quad (4.50)$$

where

$$\begin{aligned} u &= \frac{\alpha^2}{2} + \frac{1}{4}r^2 - \delta \\ v &= \frac{1}{4} [3r\alpha\alpha' + 3\alpha^2 + 5r\alpha + 3r^2] + \frac{1}{2r} [\mu^2 r^4 (\beta_p - 1)]' \\ w &= \frac{1}{4} [r\alpha\alpha' + 3\alpha^2 - r\alpha]. \end{aligned}$$

Three asymptotic cases can now be distinguished, according to the ordering of $q - 1$ and $r \frac{dq}{dr}$:

- (i) $r \frac{dq}{dr} \sim q - 1 \sim 1$ except in a singular layer of width ϵ^2 where $q - 1 \sim \epsilon^2$. This “finite shear” case was treated by Bussac et al.²⁷ for monotone q profiles and recently extended to more complicated profiles by Hastie et al.⁵⁶ The operators in Eqs. (4.44)-(4.50) have been written in such a way that one can easily recover these results.
- (ii) $r \frac{dq}{dr} \sim q - 1 \sim \epsilon$. In this “low shear” ordering we recover the equations of Ware and Haas.⁵⁷ The instability is pressure-driven, including the $j_{||}$ contribution arising from the nonzero divergence of j_{\perp} (Pfirsch-Schlüter current).⁵⁸
- (iii) $r \frac{dq}{dr} \sim q - 1 \sim \epsilon^2$, $\beta_p \sim \epsilon$. For this “very low shear” ordering there appears an additional driving term due to the divergenceless part of $j_{||}$.⁵⁸

The *free boundary* stability problem for the “low shear” and “very low shear” cases was studied by Frieman et al.,⁵⁹ who corrected a small error in the coefficient of the current driving term reported in Ref. 58. Their analysis was restricted to constant q profiles. We present the first complete *fixed boundary* stability analysis of the “low shear” case for general q profiles.

Chapter 5

Solution of the Mode Equations

5.1 Finite Shear Solution: The Toroidal Kink Mode

In this section we rederive the result of Bussac et. al. The most important aspect of this result is the conclusion that there exists a critical value of β_p below which the $m = 1$ kink instability, and therefore all global ideal modes, are stable. As discussed previously, the presence of shear stabilizes all perturbations except the $m = 1$ kink, for which the lowest order perpendicular eigen-displacement must take the form of a rigid shift of the plasma inside the $q = 1$ surface. This condition can be expressed as

$$\xi_{r1}^{(0)} = \begin{cases} \xi_0 & , \text{ for } r < r_s \\ 0 & , \text{ for } r > r_s \end{cases} \quad (5.1)$$

where r_s denotes the radial position of the singular surface where $q = 1$. The singularity at the rational surface is resolved by inertia. We first consider the solution of the sideband equation, Eq. (4.42). Substituting the expression given above for the main mode harmonic, this equation takes the form

$$\begin{aligned} & [(\mu - 1/2)^2 r^3 \xi_2']' - 3(\mu - 1/2)^2 r \xi_2 = \\ & - \left\{ \left[\left(\mu - \frac{1}{2} \right)^2 r^3 \left(\alpha + \frac{r}{2} \right)' \right]' \right. \\ & \quad \left. - 3r \left(\mu - \frac{1}{2} \right)^2 \left(\alpha + \frac{r}{2} \right) \right\} \xi_0 \end{aligned}$$

inside the singular surface. Outside of the singular surface the equation is homogeneous. Note that the right hand side has been written in such a way as to make explicit a particular solution to this equation:

$$\xi_{2\text{part}}(r) = -(\alpha + r/2) . \quad (5.2)$$

The general solution is given by the sum of this particular solution and of a solution of the homogeneous equation chosen so as to satisfy the boundary conditions as well as the jump conditions at the rational surface. The boundary conditions are $\xi_2 = 0$ at the origin and either $\xi_2 = 0$ at the wall $r = a$, if there is no $q = 2$ rational surface within the plasma, or ξ_2 must be taken to be the small solution at the $q = 2$ surface,

$$\xi_2'(r) = 0, \text{ at } r = r_2 .$$

Let $x_-(r)$ be the solution which satisfies the boundary condition at the origin and $x_+(r)$ be the solution which satisfies the right-hand side boundary condition, be it at the wall or at the $q = 2$ surface. Note that $x_-(r)$ and $x_+(r)$ will then be non-zero throughout the plasma, and in particular at the rational surface r_s . Indeed, a zero inside the plasma would indicate instability of the $m = 2$ kink⁴¹, and we have seen in ch. 2 that this cannot occur. We may thus normalize these solutions so that their value on the rational surface is unity:

$$x_-(r_s) = x_+(r_s) = 1 .$$

The solution of the sideband equation can be expressed in terms of these functions as

$$\xi_{r2}^{(1)} = \begin{cases} -(\alpha + r/2)\xi_0 + c_-x_-(r) & , \text{ for } r < r_s \\ c_+x_+(r) & , \text{ for } r > r_s \end{cases} \quad (5.3)$$

The first jump conditions at the rational surface is that ξ_2 be continuous. The second condition is found by integrating the sideband equation across the

rational surface. One must thus require

$$\{\xi_2\} = 0 \quad (5.4)$$

$$\{\xi_2'\} = \left[(\alpha')_s + 3 \frac{\alpha_s}{r_s} - 1 \right] \xi_0, \quad (5.5)$$

where the brackets $\{\cdot\}$ denote the jump in quantities across the singular surface

$$\{\xi\} = \xi(r_s + \epsilon) - \xi(r_s - \epsilon).$$

These conditions constitute a second order linear inhomogeneous system for the unknowns c_- and c_+ .

$$\begin{pmatrix} x_+ & -x_- \\ x'_+ & -x'_- \end{pmatrix} \cdot \begin{pmatrix} c_+ \\ c_- \end{pmatrix} = \begin{pmatrix} -(\alpha_s + r_s/2) \\ 3 \frac{\alpha_s}{r_s} - \frac{3}{2} \end{pmatrix} \xi_0,$$

The determinant of this system is

$$\det X = x_+ x'_- - x_- x'_+.$$

Following Bussac et. al we define the coefficients b and c by

$$b = \frac{r_s}{4} \frac{dx_-}{dr} \Big|_{r=r_s} - \frac{1}{4}, \quad (5.6)$$

$$c = \frac{r_s}{4} \frac{dx_+}{dr} \Big|_{r=r_s} + \frac{3}{4}. \quad (5.7)$$

The determinant is given in terms of these coefficients by

$$\det X = \frac{4}{r_s} (1 + b - c).$$

The solution is then

$$\begin{pmatrix} c_+ \\ c_- \end{pmatrix} = \frac{\xi_0}{\det X} \begin{pmatrix} -x'_- & x_- \\ -x'_+ & x_+ \end{pmatrix} \cdot \begin{pmatrix} -(\alpha_s + r_s/2) \\ 3 \frac{\alpha_s}{r_s} - \frac{3}{2} \end{pmatrix}. \quad (5.8)$$

Explicitly,

$$c_+ = - \left(\frac{(\beta_p + s) + b(\beta_p + s + 3/4)}{1 + b - c} \right) r_s \xi_0 , \quad (5.9)$$

$$c_- = - \left(\frac{3/4 - c(\beta_p + s + 3/4)}{1 + b - c} \right) r_s \xi_0 , \quad (5.10)$$

where s is defined by

$$\begin{aligned} s &= \int_0^{r_s} \frac{dr}{r_s} \left(\frac{r}{r_s} \right)^3 (\mu^2 - 1) \\ &= \frac{1}{2} l_i(r_s) - \frac{1}{4} . \end{aligned}$$

The boundary layer analysis of the singular differential equation for the $m = 1$ mode amplitude now goes as follows. Near marginal stability, or for $\zeta \simeq 3$, and for $n = 1$, Eq. (4.41) takes the form

$$\epsilon^{-2} \frac{d}{dr} \left\{ [(\mu - 1)^2 + 3\hat{\rho}\hat{\gamma}^2] r^3 \frac{d\xi_{r1}^{(0)}}{dr} \right\} = G_T^{(2)}[\xi_{r1}^{(0)}] + C^{(1)}[\xi_{r2}^{(1)}] .$$

It can immediately be integrated once to give

$$[(\mu - 1)^2 + 3\hat{\rho}\hat{\gamma}^2]_{r_s-0} r^3 \frac{d\xi_{r1}^{(0)}}{dr} = \epsilon^2 \int_0^{r_s-0} dr \left\{ G_T^{(2)}[\xi_{r1}^{(0)}] + C^{(1)}[\xi_{r2}^{(1)}] \right\} . \quad (5.11)$$

The right hand side is proportional to the (small) free energy available in the bulk of the plasma for the kink:

$$\delta W_T = \epsilon^2 \int_0^{r_s-0} dr \xi_0 \left\{ G_T^{(2)}[\xi_{r1}^{(0)}] + C^{(1)}[\xi_{r2}^{(1)}] \right\} . \quad (5.12)$$

The two terms on the right hand side are as follows:

$$\begin{aligned} \int_0^{r_s-0} dr \xi_0 G_T^{(2)}[\xi_{r1}^{(0)}] &= \\ \xi_0^2 \int_0^{r_s-0} dr &\left(\mu - \frac{1}{2} \right)^2 r \left[r^2 \left(\alpha' + \frac{1}{2} \right)^2 + 3 \left(\alpha + \frac{r}{2} \right)^2 \right] \\ &+ \xi_0^2 \frac{r_s^4}{4} \left\{ 2s + 3 \left(\beta_p + s + \frac{1}{4} \right)^2 - 3 \left(\beta_p + s + \frac{1}{4} \right) \right\} \end{aligned} \quad (5.13)$$

This integral is clearly continuous at the singular surface. It is not evident at first that this should also be the case for the second term since it involves second derivatives of a function, $\xi_{r2}^{(1)}$, which has a discontinuous first derivative. The second term is evaluated as follows:

$$\begin{aligned}
\int_0^{r_s-0} dr \xi_0 C^{(1)}[\xi_{r2}^{(1)}] &= \langle \xi_{r1}^{(0)}, C^{(1)}[\xi_{r2}^{(1)}] \rangle \\
&= \langle C^{(1)\dagger}[\xi_{r1}^{(0)}], \xi_{r2}^{(1)} \rangle \\
&= \langle L_2[\xi_{r2}^{(1)}], \xi_{r2}^{(1)} \rangle \\
&= - \int_0^{r_s-0} dr r \left(\mu - \frac{1}{2} \right)^2 \left[r^2 \left(\frac{d\xi_{r2}^{(1)}}{dr} \right)^2 + 3(\xi_{r2}^{(1)})^2 \right].
\end{aligned}$$

The unknown solutions x_- and x_+ can be eliminated from this integral in favor of the constants c and b by integration by parts. One finds

$$\begin{aligned}
&\int_0^{r_s-0} dr \xi_0 C^{(1)}[\xi_{r2}^{(1)}] \\
&= -\xi_0^2 \int_0^{r_s-0} dr r \left(\mu - \frac{1}{2} \right)^2 \left[r^2 \left(\alpha' + \frac{1}{2} \right)^2 + 3 \left(\alpha + \frac{r}{2} \right)^2 \right] \\
&\quad - \xi_0^2 \frac{r_s^4}{4} \left\{ \frac{3[(1+b)(\beta_p + s) + \frac{9}{4}b][\beta_p + s - \frac{1}{4}]}{1+b-c} \right. \\
&\quad \left. + \frac{(4b+1)[\frac{3}{4}(1-c) - c(\beta_p + s)][\beta_p + s + \frac{3}{4}]}{1+b-c} \right\}. \tag{5.14}
\end{aligned}$$

The two right hand side terms in Eq. (5.12) may now be replaced by their values given by Eqs. (5.13) and (5.14). One finds

$$\begin{aligned}
&\int_0^{r_s-0} dr \xi_0 \left\{ G_T^{(2)}[\xi_{r1}^{(0)}] + C^{(1)}[\xi_{r2}^{(1)}] \right\} \\
&= \left\{ \frac{8s(1+b-c) + 9b(1-c) - 24bc(\beta_p + s) - 16c(b+1)(\beta_p + s)^2}{16(1+b-c)} \right\} r_s^4 \xi_0^2.
\end{aligned}$$

The width of the singular layer is given by requiring that the inertial term, proportional to $\hat{\gamma}^2$, be comparable to the line bending term and to the driving force:

$$w^{-1}\hat{\gamma}^2 \sim (\mu')^2 w \sim \epsilon^2$$

This condition is satisfied for

$$w \sim (\epsilon/\mu')^2$$

Note that for $\mu' \sim \epsilon$ one has $w \sim 1$ and the boundary layer analysis is no longer appropriate. This case will be considered in the next section. In this section we assume $\mu' \sim 1$, so that the ordering

$$\hat{\gamma}^2 \sim (\mu')^2 w^2 \sim \epsilon^4$$

must apply. In the layer, variations in the right hand side can be neglected and the equation can be integrated once again. Approximating $(\mu - 1)$ by $-r_s q' x$ where $x = (r - r_s)/r_s$, one finds

$$\xi_{r1}^{(0)} = \frac{\delta W_T}{(3\hat{\rho})^{1/2} \hat{\gamma} \xi_0 r_s^3 q'} \arctan \left(\frac{r_s q' x}{(3\hat{\rho})^{1/2} \hat{\gamma}} \right) + C^{st}.$$

Matching this solution to the outer solution yields an expression for the growth rate

$$\begin{aligned} \hat{\gamma} &= \frac{\pi \delta W_T}{(3\hat{\rho})^{1/2} \xi_0^2 r_s^3 q'} \\ &= \frac{\pi \epsilon^2 r_s}{(3\hat{\rho})^{1/2} q'} \left\{ \frac{8s(1+b-c) + 9b(1-c) - 24bc(\beta_p + s) - 16c(b+1)(\beta_p + s)^2}{16(1+b-c)} \right\} \end{aligned}$$

Note that this growth rate scales as the square of the pressure for large pressures. The toroidal kink mode has been studied numerically by Wesson et. al⁶⁰, and Sykes et. al⁶¹.

5.2 Low Shear Solution: The Quasi-Interchange Mode

For the cases of low or very low shear the mode equations can be written

$$\begin{aligned}
& \frac{d}{dr} \left\{ \epsilon^{-2} \left[(\mu - 1)^2 + \left(1 + \frac{2}{n^2} \right) \hat{\gamma}^2 \right] r^3 \frac{d\xi_1}{dr} \right\} \\
& + \left(1 - \frac{1}{n^2} \right) \left\{ (r\beta'_p + 4\beta_p) + (\mu + 3)(\mu - 1) \right\} r^3 \xi_1 \\
& - \frac{4}{n^2} \left\{ \left(\frac{r}{4} \beta'_p + \beta_p \right)^2 + \frac{13}{16} (\mu - 1) \right\} r^3 \xi_1 \\
& = \frac{1}{n} \left(\frac{r}{4} \beta'_p + \beta_p \right) \frac{d}{dr} (r^3 \xi_2)
\end{aligned} \tag{5.15}$$

$$\frac{d}{dr} \left\{ r^3 \frac{d\xi_2}{dr} \right\} - 3r \xi_2 = -\frac{4}{n} r^3 \frac{d}{dr} \left\{ \left(\frac{r}{4} \beta'_p + \beta_p \right) \xi_1 \right\}. \tag{5.16}$$

We first remark that the cylindrical equations are recovered in the limit $n \rightarrow \infty$. Setting $n = 1$ we integrate the second equation, assuming ξ_1 and ξ_2 are bounded at the origin:

$$\xi_2 = r^{-3} \int_0^r \tilde{r}^4 \beta_p(\tilde{r}) \frac{d\xi_1(\tilde{r})}{d\tilde{r}} d\tilde{r} + [e - \beta_p(r) \xi_1(r)] \cdot r, \tag{5.17}$$

where e is an integration constant. Thus (5.15) becomes

$$\frac{d}{dr} \left\{ \epsilon^{-2} \left[(\mu - 1)^2 + 3\hat{\gamma}^2 \right] r^3 \frac{d\xi_1}{dr} \right\} - \frac{13}{4} (\mu - 1) r^3 \xi_1 = \frac{d}{dr} \{ e r^4 \beta_p \}. \tag{5.18}$$

In order to determine e we now specialize to the moderately low shear case for which the current-driving term, proportional to $(\mu - 1)$, can be dropped. Equation (5.18) is then easily integrated:

$$\frac{d\xi_1}{dr} = \frac{\epsilon^2 e r \beta_p}{(\mu - 1)^2 + 3\hat{\gamma}^2}. \tag{5.19}$$

As in the cylindrical case we now consider two possibilities for the boundary conditions. In the first case we assume that the low shear assumptions are satisfied throughout the entire plasma. The appropriate boundary conditions are then $\xi_1(1) = \xi_2(1) = 0$. This leads to

$$1 = - \int_0^1 \frac{r^5 (\epsilon \beta_p)^2}{3\hat{\gamma}^2 + (\mu - 1)^2} dr \quad (5.20)$$

which can only be satisfied by $\hat{\gamma}^2 < 0$. We conclude that in the absence of shear the mode is stable. This is due to the stabilizing influence of the $m = 2$ harmonic which is driven off-resonance by the $m = 1$ mode.

In the second case the low shear central region is separated from the wall by a sheared region. We will solve the mode equations by matching the solution in the inner (low shear) region to the solution in the outer (sheared) region. In practical terms this procedure can be expected to yield good results when the transition is sufficiently abrupt. In the sheared region $(\mu - 1) \sim 1$ but $\xi_1 \sim \epsilon^2$. Retaining terms of order ϵ^2 , we obtain from (4.42) the following outer equation for ξ_2 :

$$L_2 \xi_2 = \frac{d}{dr} \left\{ \left(\mu - \frac{1}{2} \right)^2 r^3 \frac{d\xi_2}{dr} \right\} - 3 \left(\mu - \frac{1}{2} \right)^2 r \xi_2 = 0. \quad (5.21)$$

With the boundary condition $\xi_2(1) = 0$ if $q(1) < 2$ or ξ_2 bounded as $r \rightarrow r_2$ for $q(r_2) = 2$. The asymptotic form of the solution to this equation in the low shear region is

$$\xi_2 \sim \left(\frac{r}{r_2} \right) + \sigma \left(\frac{r}{r_2} \right)^{-3}. \quad (5.22)$$

The constant σ is determined by integrating (5.21) through the outer region. The dispersion relation is now determined by matching this asymptotic solution to the corresponding asymptotic form of the inner region solution in the outer region:

$$\sigma = \left(\frac{r_2}{a} \right)^2 \int_0^a \frac{(\epsilon \beta_p(r))^2}{3\hat{\gamma}^2 + (\mu - 1)^2} \left(\frac{r}{r_2} \right)^5 d \left(\frac{r}{r_2} \right), \quad (5.23)$$

where we have restored the dimensions. Note that the integrand becomes negligible in the sheared region. Equation (5.23), in which σ is implicitly determined by Eqs. (5.22) and (5.21), gives the general dispersion relation for the quasi-interchange instability at low shear.

The qualitative features of the linear growth rate of the quasi interchange as a function of the equilibrium parameters can be deduced from the structure of the dispersion relation. The integral in the right hand side of Eq (5.23) is a positive definite monotone decreasing function of $\hat{\gamma}^2$ for $\hat{\gamma}^2 > 0$. Two possibilities arise:

- If the plasma contains a $q = 1$ rational magnetic surface then the integrand in the dispersion relation is singular at $\hat{\gamma}^2 = 0$. In this case the integral takes values in the entire positive real axis so that an unstable root can be found for any positive value of σ (Fig.12). Note that $\sigma = 0$ is the condition for marginal stability of the uncoupled cylindrical $m = 2$ mode. Thus $\sigma < 0$ corresponds to instability for this mode. We have already demonstrated, however, that this mode is always stable unless the plasma contains a finite region with magnetic pitch resonant with the helicity of this mode, $m/n = 2/1$. This never occurs in practice and σ must therefore always be greater than zero. We conclude that in the presence of a $q = 1$ rational surface a low shear, $\beta_p \sim 1$ plasma is always unstable.
- If $q > 1$ throughout the plasma, however, instability will only occur when the driving pressure gradient, represented by the term β_p , overcomes the stabilizing effect of field line bending contained in $(\mu - 1)$. This is the distinguishing feature of the low-shear interchange instability. Instead of

a fixed, finite threshold for instability the plasma is found to be unstable to arbitrarily low pressure gradients provided the shear is sufficiently low.

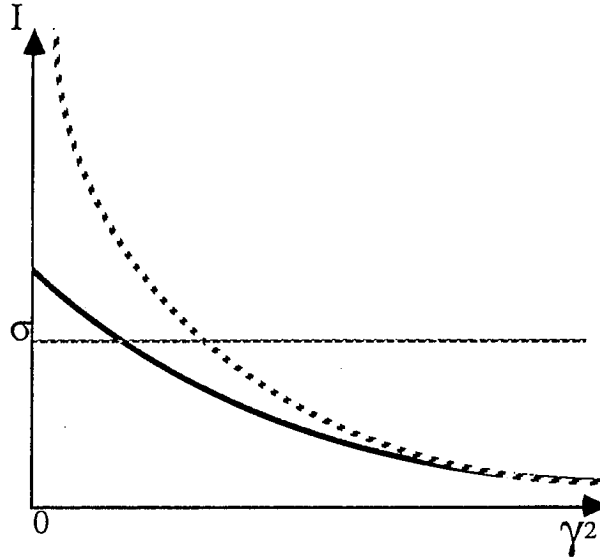


Fig.12: Geometric solution of the dispersion relation

To obtain an explicit dispersion relation, we use the model safety factor profile $\mu = \frac{1}{2} + \left(\mu_0 - \frac{1}{2}\right) \left[1 - (r/r_2)^{2\lambda}\right]$, for which Eq. (5.21) is a hypergeometric equation. To see this let

$$E = \left(\mu - \frac{1}{2}\right)^2 .$$

In terms of this variable the outer mode equation is written

$$(Er^3\xi_2')' - 3Er\xi_2 = 0 .$$

We introduce the operator D defined by

$$D = r \frac{d}{dr} .$$

In terms of this operator the outer mode equation is

$$D^2 \xi_2 + \left(\frac{DE}{E} + 2 \right) D \xi_2 - 3 \xi_2 = 0 .$$

Changing the independent variable to $z = (r/r_2)^{2\lambda}$ is then easily accomplished by using $D_r = 2\lambda D_z$. The equation becomes

$$4\lambda^2 D_z^2 \xi_2 + 2\lambda \left(2 + \frac{4\lambda z}{z-1} \right) D_z \xi_2 - 3 \xi_2 = 0 .$$

It has three singular points with characteristic exponents ν given by:

$$\begin{aligned} z = 0 \quad ; \quad & 4\lambda^2 \nu^2 + 4\lambda \nu - 3 = 0 \quad ; \quad \nu = \begin{cases} 1/2\lambda \\ -3/2\lambda \end{cases} \\ z = 1 \quad ; \quad & \nu^2 + \nu = 0 \quad ; \quad \nu = \begin{cases} 0 \\ -1 \end{cases} , \quad (5.24) \\ z = \infty \quad ; \quad & 4\lambda^2 \nu^2 - (2 + 4\lambda)2\lambda \nu - 3 = 0 \quad ; \quad \nu = \begin{cases} \nu_+ \\ \nu_- \end{cases} \end{aligned}$$

where

$$\nu_{\pm} = \left(1 + \frac{1}{2\lambda} \right) \pm \sqrt{\left(1 + \frac{1}{2\lambda} \right)^2 + \frac{3}{4\lambda^2}} .$$

These are the only singular points of this equation throughout the entire complex plane so that it is, indeed, a hypergeometric equation. Its general solution can be displayed in Riemann's notation as

$$\begin{aligned} \xi_2 &= P \left\{ \begin{matrix} 0 & 1 & \infty \\ 1/(2\lambda) & 0 & \nu_- \\ -3/(2\lambda) & -1 & \nu_+ \end{matrix} ; z \right\} , \\ &= P \left\{ \begin{matrix} 0 & 1 & \infty \\ 0 & 0 & a \\ -1 & -2/\lambda & b \end{matrix} ; 1-z \right\} \cdot z^{\frac{1}{2\lambda}} , \end{aligned}$$

where

$$\left. \begin{matrix} a \\ b \end{matrix} \right\} = 1 + \frac{1}{\lambda} \pm \sqrt{1 + \frac{1}{\lambda} + \frac{1}{\lambda^2}} .$$

Applying the boundary condition at r_2 , assuming the existence of a $q = 2$ surface within the plasma, we must choose the so-called “small” solution at r_2 , or, equivalently, $z = 1$:

$$\xi_2 = z^{\frac{1}{2\lambda}} {}_1F_2(a, b; 2; 1 - z) .$$

Analytic continuation of this solution into the low-shear region is then given by

$$\xi_2 = Az^{\frac{1}{2\lambda}} {}_1F_2\left(a, b; 1 + \frac{1}{2\lambda}; z\right) + Bz^{-\frac{3}{2\lambda}} {}_1F_2\left(2 - a, 2 - b; 1 - \frac{1}{2\lambda}; z\right) ,$$

where

$$\frac{B}{A} = \sigma = \frac{\Gamma(a + b - 2)}{\Gamma(2 - a + b)} \cdot \frac{\Gamma(2 - a)\Gamma(2 - b)}{\Gamma(a)\Gamma(b)} .$$

This expression can be simplified by applying the formula

$$\frac{\Gamma(z)}{\Gamma(-z)} = -\Gamma^2(z + 1)\mathcal{A}(z) ,$$

where \mathcal{A} is the airy function, defined as

$$\mathcal{A}(z) = \frac{\sin \pi z}{\pi z} .$$

One finds

$$\sigma = \frac{B}{A} = -\frac{\mathcal{A}(a + b - 2)}{\mathcal{A}(a - 1)\mathcal{A}(b - 1)} [(a + b - 1)\mathcal{B}(a, b)]^{-2} , \quad (5.25)$$

where $\mathcal{B}(a, b)$ is the Euler beta-function;

$$\mathcal{B}(a, b) = \frac{\Gamma(a)\Gamma(b)}{\Gamma(a + b)}$$

The application of this result to the low shear stability problem is clearly restricted to large values of λ such that the above asymptotic solution applies to a good degree of accuracy away from the magnetic axis. An additional limitation is imposed by the fact that the two characteristic exponents at the origin

become separated by an integer when $\lambda = 2$ so that in this case the solution at the origin involve logarithmic terms and the connection formulas must be modified to account for this fact⁶². It is thus desirable to expand this result for large values of λ in order to have a more readily usable formula. This is given by

$$\sigma = \frac{B}{A} = \frac{1}{3} \left(1 - \frac{2}{\lambda} \right) ,$$

where the error is less than 5% for $\lambda \geq 3$. In order to calculate the integral in Eq. (5.23) we use the pressure profile $p(r) = p_0 [1 - (r/a)^{2\nu}]$. Near marginal stability ($\hat{\gamma}^2 \ll |\mu_0 - 1|^2$), this integral can be evaluated asymptotically for $|\mu_0 - 1| \ll 1$.

$$\sigma = \left(\frac{\epsilon \beta_{p0}}{(\mu_0 - 1)} \right)^2 \left(\frac{r_1}{a} \right)^{4\nu-2} \left(\frac{r_1}{r_2} \right)^6 \cdot \int_0^{a/r_1} \frac{x^{4\nu+1}}{g^2 + (1 + x^{2\lambda})^2} dx ,$$

where

$$g^2 = 3 \frac{\hat{\gamma}^2}{(\mu_0 - 1)^2} .$$

Substituting $y = x^{2\lambda}$ and expanding the integrand near marginal stability, the dispersion relation takes the form

$$\sigma \simeq \frac{1}{4\nu + 2} \left(\frac{r_1}{r_2} \right)^6 \left(\frac{r_2}{a} \right)^2 \left(\frac{\epsilon \beta_{p1}}{\mu_0 - 1} \right)^2 (I_1 - g^2 I_2) ,$$

where

$$I_n = \frac{2\nu + 1}{\lambda} \int_0^\infty \frac{y^{\frac{2\nu+1}{\lambda}-1}}{(1+y)^{2n}} dy .$$

In terms of the parameter ζ , defined by

$$\zeta = \frac{2\nu + 1}{\lambda} ,$$

this integral is given by

$$\begin{aligned} I_n &= \zeta \mathcal{B}(\zeta, 2n - \zeta) \\ &= \zeta \Gamma(\zeta) \Gamma(1 - \zeta) (1 - \zeta) \cdot \begin{cases} 1 & , \text{ for } n = 1 \\ \frac{1}{3!} (3 - \zeta)(2 - \zeta) & , \text{ for } n = 2 \end{cases} . \end{aligned}$$

One finds in this way the explicit dispersion relation

$$\hat{\gamma}^2 = E \left\{ K (\epsilon \beta_{p1})^2 - (\mu_0 - 1)^2 \right\} + O \left[(\mu_0 - 1)^{4-\zeta} \right], \quad (5.26)$$

where

$$K = \frac{1}{2\sigma(2\nu+1)} \left(\frac{r_1}{a} \right)^2 \left(\frac{r_1}{r_2} \right)^4 \frac{(\pi\zeta)(1-\zeta)}{\sin(\pi\zeta)}$$

$$E = [3(1-\zeta/3)(1-\zeta/2)]^{-1}$$

$$\zeta = (2\nu+1)/\lambda$$

$$r_1 = r_2 \left(\frac{1-\mu_0}{\mu_0 - \frac{1}{2}} \right)^{1/2\lambda}$$

$$\beta_{p1} = \beta_p(r_1).$$

Equation (5.26) is in good agreement with numerical results,^{31,56} allowing for corrections related to the current-driving term. An estimate of the error made in neglecting that term can be obtained from the zero pressure, constant q solution⁴²: $\xi_r = \frac{1}{r} J_1(\kappa r)$ with $\kappa^2 = -\frac{13}{4}\epsilon^2(\mu-1)[3\hat{\gamma}^2 + (\mu-1)^2]^{-1}$. Taking $\xi(r_1) = 0$, one finds $\hat{\gamma}^2 = (\mu-1)(\mu_c - \mu)$, where $\mu_c = 1 - \frac{13}{4}\frac{\epsilon^2}{j_{1,1}^2} \left(\frac{r_1}{a} \right)^2$. The current term is thus destabilizing for $q > 1$.

We emphasize that Eq.(5.26) apply only to nearly marginal conditions. However, for the particular case $\mu_0 = 1$, our model profile also allows a calculation of the growth rate far from marginality. By integrating Eq. (5.23) in this case one finds

$$\hat{\gamma}^2 = \frac{1}{12} \left[\frac{2}{\sigma(2\nu+1)} \left(\frac{r_2}{a} \right)^2 (\epsilon \beta_{p2})^2 \frac{\pi}{2} \zeta \csc \left(\frac{\pi}{2} \zeta \right) \right]^{\frac{1}{1-\zeta/2}}, \quad (5.27)$$

where $\beta_{p2} \equiv \beta_p(r_2)$. Thus, in the flat current profile limit ($\lambda \gg \nu$), the growth rate scaling is similar to that near marginal stability ($\tilde{\gamma}^2 \sim (\epsilon \beta_{p2})^2$). However,

for more rounded current profiles ($\zeta \lesssim 1$) we find a different scaling, leading to a reduced growth rate away from marginal stability (e.g., for $\lambda = 3$, $\nu = 1$, $\hat{\gamma} \sim (\epsilon\beta_{p2})^2$).

We conclude this section by looking at the “low-shear” $n \neq 1$ modes. Although these modes remain stable when the $m = n = 1$ mode reaches criticality, they will be important during the nonlinear development of the instability. The mode equations for general m, n are^{57,59}:

$$\begin{aligned} \epsilon^{-2} (L_m + T_m) \xi_m &= \frac{1}{n^2 m^2} \left\{ \frac{1}{2} (r\beta'_p + 4\beta_p)^2 + \left(1 - \frac{n^2}{m^2}\right) (r\beta'_p + 4\beta_p) \right\} r^3 \xi_m \\ &= \frac{1}{2nm^2(1 \pm m)} r^{1 \mp m} (r\beta'_p + 4\beta_p) \frac{d}{dr} (r^{2 \pm m} \xi_{m \pm 1}) \\ L_{m \pm 1} \xi_{m \pm 1} &= \frac{1}{m^2(1 \pm m)^2} \left\{ \frac{d}{dr} \left(r^3 \frac{d\xi_{m \pm 1}}{dr} \right) - [(m \pm 1)^2 - 1] r \xi_{m \pm 1} \right\} \\ &= -\frac{1}{2nm^2(1 \pm m)} r^{2 \pm m} \frac{d}{dr} \left\{ (r\beta'_p + 4\beta_p) r^{1 \mp m} \xi_m \right\}. \end{aligned}$$

The sideband equations may again be integrated:

$$n\xi_{m \pm 1} = -\frac{1}{2}(1 \pm m)r^{-(2 \pm m)} \int_0^r d\hat{r} (\hat{r}\beta'_p + 4\beta_p) \hat{r}^{2 \pm m} \xi_m + e_{\pm} r^{m \pm 1 - 1}, \quad (5.28)$$

leaving a decoupled main-harmonic equation:

$$\begin{aligned} \frac{d}{dr} \left\{ \left[\left(1 + 2\frac{m^2}{n^2}\right) \frac{\hat{\gamma}^2}{m^2} + \left(\mu - \frac{1}{m}\right)^2 \right] r^3 \frac{d\xi_m}{dr} \right\} \\ - (m^2 - 1) \left[\left(1 + 2\frac{m^2}{n^2}\right) \frac{\hat{\gamma}^2}{m^2} + \left(\mu - \frac{1}{m}\right)^2 \right] r \xi_m \\ - \frac{\epsilon^2}{n^2 m^2} \left(1 - \frac{n^2}{m^2}\right) \frac{d}{dr} (r^4 \beta_p) \xi_m = \frac{\epsilon^2}{n^2} \frac{e_+}{m^2} \frac{d}{dr} (r^4 \beta_p) r^{m-1}. \end{aligned}$$

We solve this equation for constant $\mu = \mu_0 \simeq 1$, $m = n$, and $\beta_p = \beta_0 r^{2\nu-2}$. After imposing the boundary condition $\xi_m(r_1) = 0$ at the transition radius r_1 between the low-shear and finite-shear regions, one finds

$$\xi_m(r) = \left(\frac{\epsilon}{n}\right)^2 \frac{\nu+1}{2\nu(\nu+m)} \frac{e_+\beta_0}{3\hat{\gamma}^2 + \left(\frac{1}{q} - 1\right)^2} (r^{2\nu} - r_1^{2\nu}) r^{m-1}. \quad (5.29)$$

The dispersion relation is then obtained by matching the solution for ξ_{m+1} in the low shear region to the low-shear limit of the outer solution equations:

$$\xi_{m+1}(r) \sim \left(\frac{r}{r_2}\right)^m + \sigma_m \left(\frac{r}{r_2}\right)^{-(2+m)}. \quad (5.30)$$

We find

$$\hat{\gamma}^2 = E \left[K_m \left(\frac{\epsilon}{n} \beta_p\right)^2 - \left(\frac{1}{q_0} - 1\right)^2 \right], \quad (5.31)$$

where $E = 1/3$,

$$K_m = \frac{1}{4\sigma_m} \frac{(\nu+1)^2(1+m)}{(\nu+m)^2(2\nu+m)} \left(\frac{r_1}{r_2}\right)^{2m+2} \left(\frac{r_1}{a}\right)^2. \quad (5.32)$$

The value of σ_m calculated for our model q profile is

$$\sigma_m = \frac{m}{m+2} \left[1 - \frac{m+1}{\lambda} + O\left(\frac{1}{\lambda^2}\right) \right]. \quad (5.33)$$

From the large m behavior of K_m ,

$$K_m \sim m^{-2} \exp \left\{ -2m \left| \ln \left(\frac{r_1}{r_2} \right) \right| \right\}$$

we see that the growth rate at resonance ($q_0 = 1$) for toroidal geometry will decrease much faster for large values of m than the corresponding cylindrical result. We note that the presence of the sheared region is also necessary for instability with $n \neq 1$.

Chapter 6

Nonlinear Growth

6.1 Introduction

Ideal magnetohydrodynamic instabilities, such as the quasi-interchange mode investigated here, are often invoked to explain rapid, large-scale instabilities in magnetic confinement experiments. However, in view of the relatively slow evolution of the equilibrium, it is not clear how such instabilities can appear suddenly as fast growing modes. This difficulty is particularly acute for the sawtooth crashes observed in JET because of the extreme slowness of the transport processes in this tokamak. Nonetheless, sensitive diagnostics are in complete agreement regarding the absence of precursors and the rapidity of the onset of growth^{5,63}.

In this chapter nonlinear effects on the growth of the quasi-interchange are investigated. The analysis presented here differs from previous bifurcation calculations^{64,65,20} by the inclusion of toroidal coupling effects. Toroidal curvature, which is important for pressure-driven modes, destroys the helical symmetry which is typical of kink-like instabilities.

The nonlinear corrections are evaluated by expanding the equations of motion for the unstable mode near marginal stability.⁶⁵ This procedure yields the following equation for the mode amplitude ξ :

$$\frac{d^2\xi}{dt^2} = \gamma^2\xi + \Gamma\xi^3 + O(\xi^5), \quad (6.1)$$

where γ is the linear growth rate. The coefficient Γ is the main goal of the analysis. Its sign determines the qualitative behavior of the mode as the linear stability threshold is crossed:

(1) For $\Gamma < 0$, the nonlinear terms are stabilizing and lead to the appearance of secondary, stable equilibria. In this case the plasma will simply shift adiabatically from the initial unstable equilibrium branch to the nearby bifurcated equilibrium branch (Fig. 13).

(2) For $\Gamma > 0$, however, there are no nearby equilibria above marginal stability (Fig. 13). A robust, explosive instability can develop even near the stability threshold. In the absence of higher-order stabilizing terms the mode would grow to infinite amplitude over a finite time. These two cases are referred to as supercritical and subcritical bifurcations, respectively.

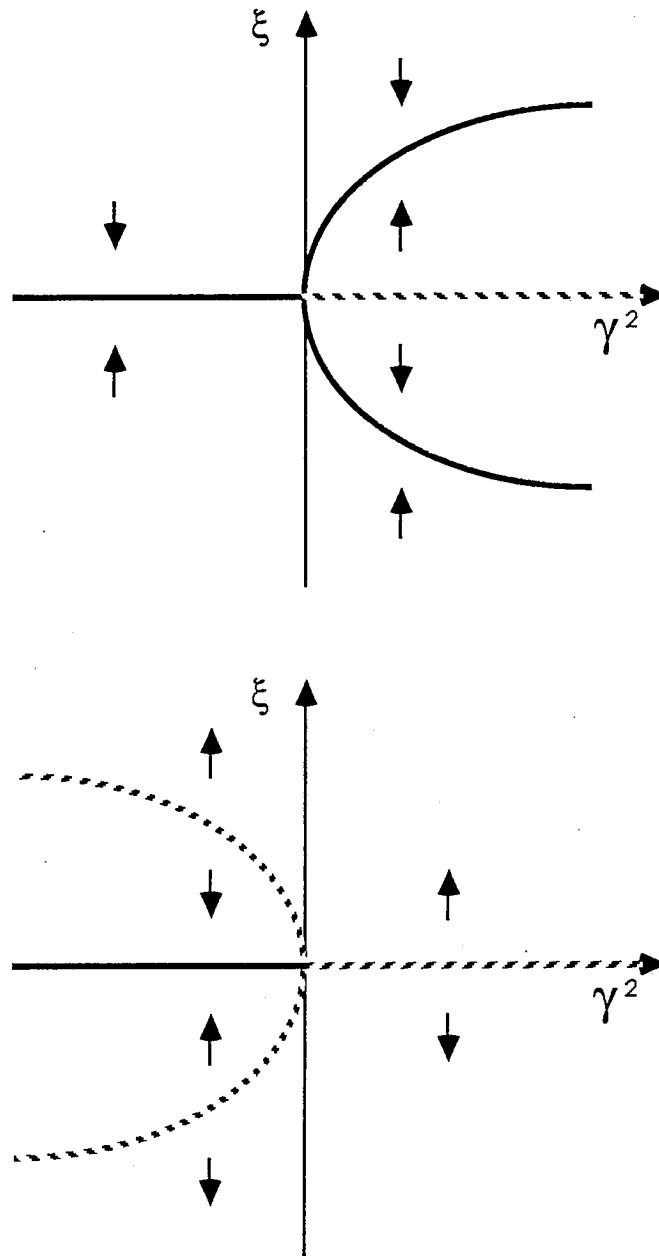


Fig.13: Supercritical (top) and subcritical (bottom) bifurcations of equilibrium. Solid lines indicate stable equilibria, dashed lines unstable equilibria.

The analysis is developed from the high-beta reduced magnetohydrodynamic (RMHD) equations of Strauss.³² These equations describe nonlinear plasma dynamics in large aspect ratio tokamak geometry. They are the result of a systematic ordering of the magnetohydrodynamic (MHD) equations, in which only the lowest order terms in the inverse aspect ratio, $\varepsilon = a/R_0$, are retained (here a is the minor radius and R_0 the major radius of the torus). In particular, RMHD takes $\beta \sim k_{\parallel} \sim \varepsilon$, where $\beta = P/B_0^2$ is the ratio of kinetic pressure to magnetic pressure and $k_{\parallel} = B^{-1}(\mathbf{B} \cdot \nabla)$ is the inverse of the characteristic scale length along the magnetic field.

In order to describe interchange-like instabilities in relatively low-beta plasmas, we introduce the secondary ordering parameter δ and assume $\beta \sim k_{\parallel} \sim \varepsilon\delta$, with $\delta \ll 1$. Note that a global instability with $k_{\parallel} \ll \varepsilon$ can only occur if the plasma contains a low-shear resonant region where the safety factor q is close to a rational number: specifically, $q - q_s \sim \delta$ where $q_s = m/n$. The quasi-interchange model of sawtooth disruptions assumes that this condition holds in a central region of the plasma with $q_s = 1$.

The basic nonlinear interchange equations are then derived by expanding the RMHD equations to lowest significant order in δ . However, consistency with the reduced MHD ordering requires $\varepsilon \ll \delta$. This condition is generally not satisfied, typical values of the inverse aspect ratio being $\varepsilon \sim 1/4$. Nonetheless, one would expect RMHD to remain qualitatively valid, particularly for pressure-driven modes, when $\delta \lesssim \varepsilon$. This hypothesis is supported by an examination of the linearized MHD equation in the low-shear, low-beta approximation.⁵⁷

The exact (non-reduced) energy principle for these equations contains the following terms:

- Cylindrical kink and line-bending terms proportional to $(q - q_s)^2$.
- Interchange terms proportional to $(p')^2$, including the sideband energy.
- A term proportional to $p'(q^2 - 1)$.

The first two terms are clearly included in the RMHD equations, but the last term will be missing. For $q_s = 1$, however, this term should be neglected from the MHD equations as well. This is of course the case relevant to the sawtooth problem, and we thus conclude that the RMHD equations will produce the correct potential energy for the quasi-interchange in this case.

The RMHD kinetic energy, however, neglects the parallel velocity and the effects of compressibility. Compressibility is unimportant near marginal stability, while the neglect of parallel velocity will result in growth rates being overestimated by a factor of $(1 + 2q_s^2)$. This clearly does not affect the nature of the bifurcation.

The RMHD equations are described in Sec. 2. The interchange ordering, $\delta \ll 1$, is used in Sec. 3 to simplify the system further. The resulting, “interchange-reduced” equations involve only the helically resonant components of the fields, but contain numerical constants related to the behavior of the non-resonant components in the sheared outer region of the plasma. The perturbation expansion in the mode amplitude is described in the first section of chapter 8 and the resulting equations will be solved for model profiles in Secs. 8.2 and 8.3.

6.2 Formulation

The RMHD system is derived in detail in the paper by Strauss³² and is presented here mainly for ease of reference.

The coordinate system is defined in terms of cylindrical coordinates (R, ζ, Z) by $x = (R - R_0)/a$, $y = Z/a$ and $z = -\zeta$, where x and y are coordinates in the poloidal plane and z is the toroidal angle. The magnetic field is given in sufficient accuracy by

$$\mathbf{B} = \hat{z} + \varepsilon(-\hat{z}x + \hat{z}B_{\parallel} - \hat{z} \times \nabla_{\perp}\psi) ,$$

where ψ is the poloidal flux and B_{\parallel} represents diamagnetic corrections to the vacuum toroidal field. All operations involving the perpendicular gradient operator

$$\nabla_{\perp} = \hat{x} \frac{\partial}{\partial x} + \hat{y} \frac{\partial}{\partial y} ,$$

are to be carried out using the Euclidean metric. The lowest order force balance equation,

$$\nabla_{\perp}(B_{\parallel} + p/2) = 0 ,$$

allows B_{\parallel} to be eliminated in favor of the pressure p . An important operator for interchange-like modes is the parallel gradient operator,

$$\mathbf{B} \cdot \nabla = \varepsilon \nabla_{\parallel} .$$

This operator is conveniently expressed in terms of the conventional bracket,

$$[f, g] = \hat{z} \cdot (\nabla_{\perp} f \times \nabla_{\perp} g) ,$$

by

$$\nabla_{\parallel} = \frac{\partial}{\partial z} - [\psi, \cdot] . \quad (6.2)$$

Ampere's law is written

$$J = \nabla_{\perp}^2 \psi , \quad (6.3)$$

where J is the negative of the toroidal current density.

The principal dynamical equation is the shear-Alfvén law, given by

$$\frac{\partial U}{\partial \tau} + [\varphi, U] = -\nabla_{\parallel} J - [x, p] , \quad (6.4)$$

where the vorticity U is given in terms of the stream function φ by

$$U = \nabla_{\perp}^2 \varphi . \quad (6.5)$$

The left-hand-side of the shear-Alfvén law contains the convective derivative of the vorticity while the right-hand side consists of the parallel-current driving term and the interchange term. The system is completed by the parallel Ohm's law,

$$\frac{\partial \psi}{\partial \tau} + \nabla_{\parallel} \varphi = 0 , \quad (6.6)$$

and the pressure evolution equation,

$$\frac{\partial p}{\partial \tau} + [\varphi, p] = 0 . \quad (6.7)$$

The analysis of these equations is simplified by making use of such properties of the bracket as antisymmetry and the Jacobi identity:

$$[f, g] = -[g, f] ,$$

$$[f, [g, h]] + [g, [h, f]] + [h, [f, g]] = 0 .$$

It should also be noted that the bracket is a derivation: it satisfies

$$[f, gh] = [f, g] \cdot h + [f, h] \cdot g .$$

The integral invariants of RMHD can also be used to reduce the complexity of the problem. These can be derived from the identities³⁹

$$\int f[g, h]dV = \int g[h, f]dV = \int h[f, g]dV ,$$

which can be seen to hold by writing the bracket as a divergence,

$$[f, g] = \nabla_{\perp} \cdot (g \hat{z} \times \nabla_{\perp} f) ,$$

and integrating by parts, assuming the vanishing of surface terms. The following integral invariants are particularly useful:

$$C = \int F(p) dV , \quad (6.8)$$

$$D = \int G(\nabla_{\parallel} p) dV , \quad (6.9)$$

where F and G are arbitrary functions.

In the following analysis we will consider only conditions such that the pressure is initially a flux function: $\nabla_{\parallel} p = 0$ at $\tau = 0$. Equation (6.9) then implies

$$\nabla_{\parallel} p = 0 \quad (6.10)$$

at all possible times ($\tau > 0$).

To summarize, the RMHD system consists of Eqs. (6.4), (6.6), and (6.7), with the defining relations (6.3) and (6.5). Equation (6.7) will be replaced by Eq. (6.10) under the assumption stated above.

Chapter 7

Interchange-Reduced Equations

7.1 Simplification of the equations

The quasi-interchange ordering allows considerable simplification of the equations of motion. The simplification is largely a consequence of the partial linearization resulting from the small- δ expansion. It is important to note, however, that no assumptions regarding the size of the perturbation from equilibrium are made. In this sense, the interchange-reduced equations remain fully nonlinear.

The analysis in this section follows a similar derivation by Kotschenreuther et al.⁶⁶

In terms of the normalized variables used in RMHD the quasi-interchange ordering is simply $p \sim \nabla_{\parallel} \sim \delta \ll 1$. The equations of motion then imply $\frac{\partial}{\partial \tau} \sim \delta$. To zeroth order the plasma is thus in a force-free, closed-line, cylindrically symmetric equilibrium. Clearly this state is marginally stable to the exchange of flux tubes. Introducing polar coordinates in the poloidal plane by $x = r \cos \theta$ and $y = r \sin \theta$, we obtain the resonance condition on interchange perturbations ξ as

$$\nabla_{\parallel} \xi = \frac{\partial \xi}{\partial \theta} + \frac{\partial \xi}{\partial \zeta} = 0. \quad (7.1)$$

It is satisfied by $\xi = f(r, \theta - \zeta)$, for arbitrary f . Thus, the quasi-interchange ordering describes the evolution of the plasma between states which are, to

lowest order, helically symmetric. This observation motivates the change of coordinates $(r, \theta, \zeta) \rightarrow (r, \alpha, \eta)$, where $\alpha = \theta - \zeta$ and $\eta = \zeta$. α is a field-line label for the zeroth-order magnetic field. The bracket in these new coordinates is simply

$$[f, g] = \frac{1}{r} \left\{ \frac{\partial f}{\partial r} \frac{\partial g}{\partial \alpha} - \frac{\partial f}{\partial \alpha} \frac{\partial g}{\partial r} \right\}.$$

The parallel gradient is then most simply expressed in terms of the helical flux defined by

$$\chi = \psi + r^2/2.$$

We then have

$$\nabla_{\parallel} = \frac{\partial}{\partial \eta} - [\chi, \cdot]. \quad (7.2)$$

Note that $\chi \sim \delta$.

The dynamics of interchange perturbations are of course determined by higher-order terms. For finite δ , the helical symmetry is broken by the toroidal curvature. Nonetheless, the field quantities remain approximately helically symmetric. It is useful to separate them into their η -averaged part,

$$\bar{f} = \frac{1}{2\pi} \oint d\eta f(r, \alpha, \eta), \quad (7.3)$$

and an η -fluctuating remainder,

$$\tilde{f} = f - \bar{f}. \quad (7.4)$$

\bar{f} clearly satisfies the resonance condition, Eq. (7.1). Note that the bracket behaves as a typical quadratic form under helical averaging:

$$\overline{[f, g]} = [\bar{f}, \bar{g}] + \overline{[\tilde{f}, \tilde{g}]}. \quad (7.5)$$

The shear-Alfvén law, Eq. (6.4) and the pressure equation (6.10) are now separated into resonant and non-resonant parts. The helical average of these equations is

$$\frac{\partial \bar{U}}{\partial \tau} + [\bar{\varphi}, \bar{U}] + [\bar{\varphi}, \bar{U}] = [\bar{\chi}, \bar{J}] + [\bar{\chi}, \bar{J}] - \overline{[x, \bar{p}]}, \quad (7.6)$$

$$[\bar{\chi}, \bar{p}] + \overline{[\bar{\chi}, \bar{p}]} = 0. \quad (7.7)$$

The relative magnitude of the resonant terms is as follows:

$$(i) \bar{p} \sim \bar{\chi} \sim \delta, \bar{J} = 2 + O(\delta).$$

$$(ii) \text{ From the } \eta\text{-averaged Ohm's law, Eq. (6.6), one finds } \bar{\varphi} \sim \frac{\partial}{\partial \tau} \sim \delta.$$

The non-resonant quantities are determined by the η -fluctuating part of the equations. For the pressure law, subtracting Eq. (7.7) from Eq. (6.10) yields

$$\frac{\partial \tilde{p}}{\partial \eta} = [\tilde{\chi}, \bar{p}] + [\bar{\chi}, \tilde{p}] + [\tilde{\chi}, \tilde{p}] - \overline{[\tilde{\chi}, \tilde{p}]}.$$

It follows that $\tilde{p} \sim \delta^2$. \tilde{p} is thus determined to leading order by

$$\frac{\partial \tilde{p}}{\partial \eta} = [\tilde{\chi}, \bar{p}]. \quad (7.8)$$

Thus the non-resonant pressure results from advection of the resonant pressure by the non-helical component of the magnetic field.

From the non-resonant part of Ohm's law, one finds $\tilde{\varphi} \sim \frac{\partial \tilde{\chi}}{\partial \tau} \sim \delta^2$. This implies that the kinetic terms can be neglected entirely from the non-resonant shear-Alfvén law. The remaining terms are

$$\begin{aligned} \frac{\partial \tilde{J}}{\partial \eta} &= [\tilde{\chi}, \bar{J}] + [\bar{\chi}, \tilde{J}] + [\tilde{\chi}, \tilde{J}] - \overline{[\tilde{\chi}, \tilde{J}]} \\ &\quad - [x, \bar{p}] - [x, \tilde{p}] + \overline{[x, \tilde{p}]}. \end{aligned} \quad (7.9)$$

The leading order term on the right-hand side is $[x, \bar{p}] \sim \delta$, so that $\tilde{J} \sim \tilde{X} \sim \delta$. The other terms are then of higher order and Eq. (7.9) becomes

$$\frac{\partial \tilde{J}}{\partial \eta} = -[x, \bar{p}] . \quad (7.10)$$

The current \tilde{J} may be interpreted as a Pfirsch-Schlüter current.⁶⁶

The non-resonant equations can be integrated:

$$\tilde{p} = \left[\int d\eta \tilde{X}, \bar{p} \right] , \quad (7.11)$$

$$\tilde{J} = - \left[\int d\eta x, \bar{p} \right] . \quad (7.12)$$

Substituting the result into Eq. (7.6) and neglecting the higher order term $[\bar{\varphi}, \tilde{U}]$, one finds

$$\frac{\partial \bar{U}}{\partial \tau} + [\bar{\varphi}, \bar{U}] - [\bar{X}, \bar{J}] = -\frac{1}{2\pi} \oint \left\{ \left[x, \left[\int d\eta \tilde{X}, \bar{p} \right] \right] + \left[\tilde{X}, \left[\int d\eta x, \bar{p} \right] \right] \right\} d\eta .$$

Integrating the last term by parts and using Jacobi's identity yields the η -averaged shear-Alfvén law

$$\frac{\partial \bar{U}}{\partial \tau} + [\bar{\varphi}, \bar{U}] - [\bar{X}, \bar{J}] - [\bar{p}, h] = 0 , \quad (7.13)$$

where

$$h = \overline{\left[x, \int d\eta \tilde{X} \right]} . \quad (7.14)$$

This term may be interpreted as follows:

The curvature in RMHD is given by $\kappa = -\nabla x$. The function x plays a role analogous to gravitational potential in a gravity-driven interchange. It can be shown that, to required order, h is the average of x along a magnetic field line,

$$h = \oint \frac{d\ell}{B} \cdot x . \quad (7.15)$$

Note that only the non-resonant part of the flux contributes at this order, and that the field lines generated by $\tilde{\chi}$ alone close after one period. ∇h therefore plays the role of an average curvature in Eq. (7.13). Note also that the field line average is carried out on the potential x and not on the curvature itself, so that the geodesic curvature is not eliminated from ∇h .

7.2 Calculation of the average curvature

The average curvature is calculated by integrating Ampere's law,

$$\nabla_{\perp}^2 \tilde{\chi} = \tilde{J} ,$$

for the non-resonant current given in Eq. (7.12) and substituting the result in Eq. (7.14). The solution depends of course on the choice of boundary conditions. We are primarily interested in equilibria consisting of two regions:

(i) A central, low-shear region where the quasi-interchange ordering is satisfied with $q_s = 1$.

(ii) A sheared outer region where $\nabla_{\parallel} \sim 1$, $p \sim \delta$. The appropriate boundary conditions are then obtained by requiring the solutions in the low-shear region to asymptotically match those in the outer, sheared region.

The integrations are most easily accomplished after Fourier decomposition of the fields:

$$\bar{p}(r, \alpha) = \sum_{n=-\infty}^{+\infty} \bar{p}_n(r) e^{in\alpha} , \quad (7.16)$$

$$x = \frac{1}{2} r \left\{ e^{i(\alpha+\eta)} + e^{-i(\alpha+\eta)} \right\} .$$

The reality condition can be written

$$\bar{p}_n^* = \bar{p}_{-n} .$$

Substituting these expressions into Eq. (7.12) one finds

$$\tilde{\chi}(r, \alpha, \eta) = \sum_{\pm} \sum_{n=-\infty}^{+\infty} \tilde{\chi}_{n,\pm}(r) \exp \{i(n \pm 1)\alpha \pm i\eta\} , \quad (7.17)$$

where the $\tilde{\chi}_{n,\pm}(r)$ are determined by

$$\left\{ \frac{1}{r} \frac{d}{dr} \left(r \frac{d}{dr} \right) - \frac{1}{r^2} (n \pm 1)^2 \right\} \tilde{\chi}_{n,\pm}(r) = \frac{1}{2r} \left\{ r \frac{d}{dr} \mp n \right\} \bar{p}_n(r) . \quad (7.18)$$

The general solution regular on axis is

$$\tilde{\chi}_{n,\pm}(r) = \frac{1}{2} r^{-(1 \pm n)} \int_0^r r^{1 \pm n} \bar{p}_n(r) dr + \frac{1}{2} \frac{C_{n,\pm}}{(n \pm 1)} r^{n \pm 1} , \quad (7.19)$$

where the last term is the solution to the homogeneous equation. This term represents the deformation of the field lines caused by non-resonant currents outside of the low-shear interchange region. These currents are themselves induced by the perturbations inside this region. The constants $C_{n,\pm}$ are determined by asymptotically matching the inside solution, Eq. (7.19), to the solution in the outer region.

We now consider the equations in the outer region. Since the shear in the outer region is now finite, $\nabla_{\parallel} \sim 1$, while the pressure remains small, $p \sim \delta$, the equations in this region will reduce to the cylindrical equations to lowest order in δ . The shear-Alfvén law is given to required order by

$$\frac{\partial \tilde{J}}{\partial \eta} = [\tilde{\chi}, \bar{J}] + [\bar{\chi}, \tilde{J}] + [x, \bar{p}] .$$

Of course the η -averaged components of the fields are no longer resonant. The line-bending forces and circular confinement vessel then combine to constrain the fields so that all the η -averaged components except $n = 0$ vanish as the shear becomes large. Thus, for $n \neq 0$ the shear-Alfvén law becomes

$$\frac{\partial \tilde{J}}{\partial \eta} = [\chi_0, \tilde{J}] + [\tilde{\chi}, J_0] , \quad (7.20)$$

where χ_0 and J_0 are the $n = 0$ components of $\bar{\chi}$ and \bar{J} , respectively. As the low-shear region is approached, $\chi_0 \rightarrow O(\delta)$ and the solutions to this equation take the asymptotic form

$$\tilde{\chi}_{n,\pm} \sim A_{n,\pm} r^{-(n\pm 1)} + B_{n,\pm} r^{(n\pm 1)} . \quad (7.21)$$

Note that the shear-alfven law is linear in $\tilde{\chi}$, so that only the ratio $\sigma_{n,\pm} = A_{n,\pm}/B_{n,\pm}$ is relevant. The constants $\sigma_{n,\pm}$ are determined by integrating Eq. (7.20) inwards starting from the vessel wall or from the appropriate mode-rational surface.

Returning to the low-shear solution, one finds that the integrand in Eq. (7.19) will vanish as the shear increases in the matching region. It follows that the asymptotic form of the inner solution in the outer region is

$$\chi_{n,\pm} \sim \left(\frac{1}{2} \int_0^1 r^{1\pm n} \bar{p}_n(r) dr \right) \cdot r^{-(1\pm n)} + \left(\frac{1}{2} \frac{C_{n,\pm}}{(n \pm 1)} \right) \cdot r^{n\pm 1} ,$$

where the upper limit of integration has been taken to be the confinement vessel wall. The matching of the solutions is thus achieved when

$$\sigma_{n,\pm} = \frac{n \pm 1}{C_{n,\pm}} \int_0^1 r^{1\pm n} \bar{p}_n(r) dr , \quad n \neq 0 .$$

The effect of the currents induced in the outer region is thus entirely contained in the constants σ . Note that effects related to the motion of the matching region are of higher order in δ .

The potential function h is now found by substituting Eq. (7.19) into Eq. (7.14). We find

$$h = \frac{1}{2} \bar{p} + \lambda ,$$

where

$$\lambda = \sum_{n=-\infty}^{+\infty} \lambda_n e^{in\alpha},$$

$$\lambda_n = \frac{1}{2} C_{n,+} r^n. \quad (7.22)$$

The terms containing $C_{n,-}$, corresponding to perturbations with pitch $d\theta/d\zeta$ less than one, do not contribute. This is not a local effect: it is a consequence of requiring the perturbation to be regular at the origin.

The result of the curvature calculation may now be substituted in the η -averaged shear-Alfvén law. The resulting, interchange-reduced shear-Alfvén law takes the form

$$\frac{\partial \bar{U}}{\partial \tau} + [\bar{\varphi}, \bar{U}] - [\bar{\chi}, \bar{J}] - [\bar{p}, \lambda] = 0. \quad (7.23)$$

This equation is completed by

$$[\bar{\chi}, \bar{p}] = 0, \quad (7.24)$$

and the matching condition

$$C_n \sigma_n = (n+1) \int_0^1 r^{n+1} \bar{p}_n(r) dr, \quad (7.25)$$

where $\sigma_n = \sigma_{n,+}$. Equation (7.24) is obtained from Eq. (7.7) by neglecting the higher-order term $[\bar{\chi}, \bar{p}]$.

The dimensionality of the problem has thus been reduced to two. It should be emphasized, however, that the plasma does not have helical symmetry. Significantly, the interchange is found to be driven only by the part of the curvature which is caused by the currents induced in the sheared outer region.

We conclude this section by considering the η -averaged Ohm's law:

$$\frac{\partial \bar{\chi}}{\partial \tau} + [\bar{\varphi}, \bar{\chi}] + [\bar{\varphi}, \bar{\chi}] = 0.$$

The last term may be neglected. It follows that, to the order of the calculation, $\bar{\chi}$ is an advected quantity and the quantity

$$T = \int S(\bar{\chi}) r dr d\alpha \quad (7.26)$$

is conserved by the interchange-reduced system for any choice of the function S .

Chapter 8

Solution for Model Profiles

8.1 General Formulation

The equations derived in the preceding section are now applied to the nonlinear evolution of the quasi-interchange mode. This is accomplished through a perturbation expansion in the mode amplitude ξ , where ξ is the displacement of the flux surfaces from their equilibrium position. From Eq. (6.1), the nonlinear regime near marginal stability is found to be characterized by $\gamma \sim \frac{d}{d\tau} \sim \xi \ll 1$.

The following two basic assumptions are made:

(i) The perturbed initial state is taken to be accessible from the equilibrium within the confines of perfect conductivity theory.²⁰ That is, the integral invariants given by Eqs. (6.8) and (7.26) take the same value for the perturbed initial state as for the equilibrium state. A similar restriction on the initial conditions has already been used to replace Eq. (6.7) by Eq. (6.10).

(ii) The mode is assumed to grow coherently. More specifically, the near-marginal eigenvalue is assumed to be simple, with $\gamma \ll \omega$ where ω is the eigenfrequency of the nearest nonlinearly driven mode.

The accessibility constraint requires

$$C = \int F(p_e) dV = \int F(p) dV ,$$

for any choice of F . To order ξ^3 , this condition is equivalent to

$$\bar{p}_0(r) = p_e(r) + \frac{1}{r} \frac{d}{dr} \left(\frac{r}{p'_e} p_1^2 \right), \quad (8.1)$$

where $p'_e = \frac{dp_e}{dr}$. Henceforth, the overbars will be omitted. The flux conservation constraint, Eq. (7.26), requires similarly

$$\chi_0(r) = \chi_e(r) + \frac{1}{r} \frac{d}{dr} \left(\frac{r}{\chi'_e} \chi_1^2 \right). \quad (8.2)$$

Note that

$$\chi'_e(r) = \left(1 - \frac{1}{q(r)} \right) \cdot r, \quad (8.3)$$

where $q(r)$ is the rotational transform, correct to first order, of the flux surface which reduces to a circle of radius r to lowest order in δ .

We now consider the interchange-reduced shear-Alfvén and pressure laws, Eq. (7.23) and (7.24). To first order in ξ they can be written

$$\chi'_e J_1 - J'_e \chi_1 = -p'_e \lambda_1, \quad (8.4)$$

$$\chi'_e p_1 - p'_e \chi_1 = 0. \quad (8.5)$$

The quantities φ and U can be shown from Ohm's law to be of order ξ^2 , so that the term $\frac{\partial U}{\partial \tau}$ appears only in the third-order equations, while $[\varphi, U]$ is of even higher order and is neglected in the following treatment.

In terms of the convenient abbreviation

$$\dot{F} = \frac{F'}{\chi'_e} = \frac{dF_e}{d\chi_e},$$

Eq. (8.4) becomes

$$J_1 - \dot{J}_e \chi_1 = -\dot{p}_e \lambda_1, \quad (8.6)$$

$$p_1 = \dot{p}_e \chi_1. \quad (8.7)$$

The left-hand side of Eq. (8.6) contains a second-order differential operator applied to χ_1 . This operator can be inverted for an arbitrary source function $f(r)$. Let

$$\chi_1(r) = \chi'_e \xi_1(r) . \quad (8.8)$$

$\xi_1(r)$ is the $n = 1$ component of the displacement of the flux surface. Substituting Eq. (8.8) into the left-hand side of Eq. (8.6), and replacing the right-hand side by the arbitrary source $f(r)$, one finds

$$J_1 - j_e \chi_1 = \frac{1}{r \chi'_e} \frac{d}{dr} \left(r (\chi'_e)^2 \frac{d\xi_1}{dr} \right) = f(r) .$$

Integrating twice yields

$$\xi_1(r) = - \int_r^1 \frac{d\hat{\rho}}{\hat{\rho} (\chi'_e(\hat{\rho}))^2} \int_0^{\hat{\rho}} f(\rho) \chi'_e(\rho) \rho d\rho . \quad (8.9)$$

The solution to Eq. (8.6) is now found by replacing f by $-\dot{p}_e \lambda_1$, in Eq. (8.9). p_1 , given by Eq. (8.7) can then be substituted into the matching condition. After integration by parts, this becomes

$$\sigma_1 = \int_0^1 \frac{(\delta \cdot \hat{\beta}_p)^2}{\left(\frac{1}{q} - 1\right)^2} r^5 dr , \quad (8.10)$$

where $\hat{\beta}_p$ is the RMHD normalized poloidal beta,

$$\delta \cdot \hat{\beta}_p = -\frac{1}{r^4} \int_0^r \rho^2 p'_e(\rho) d\rho .$$

Equation (8.10) is of course the linear marginal stability condition for the $n = 1$ mode.

To next order in ξ , the $n = 1$ mode couples into $n = 0$ and $n = 2$. The $n = 0$ components have already been calculated from the conservation laws: they are given by Eqs. (8.2) and (8.1). The $n = 2$ components are determined

by Eqs. (7.23) and (7.24):

$$J_2 - \dot{J}_e \chi_2 = -\dot{p}_e \lambda_2 + \frac{1}{2} \ddot{J}_e \chi_1^2 - \ddot{p}_e \chi_1 \lambda_1, \quad (8.11)$$

$$p_2 = \dot{p}_e \chi_2 + \frac{1}{2} \ddot{p}_e \chi_1^2. \quad (8.12)$$

Equation (8.11) is a second-order inhomogeneous differential equation for χ_2 . Unlike Eq. (8.6) for χ_1 , however, it cannot be integrated by simple quadratures. Assuming nonetheless that a solution has been found, the constant C_2 is then determined by the matching condition:

$$C_2 \sigma_2 = 3 \int_0^1 r^3 p_2(r) dr.$$

The third-order corrections to the $n = 1$ equations can now be calculated. The corrected source term f becomes

$$\begin{aligned} f = & -\dot{p}_e \lambda_1 - \ddot{p}_e ((\chi_2 + \chi_0 - \chi_e) \lambda_1 + \chi_1 \lambda_2) + \ddot{J}_e \chi_1 \chi_2 \\ & - \dot{J}_e \chi_1 \dot{\chi}_0 + \chi_1 \dot{J}_0 - \frac{1}{2} \ddot{J}_e \chi_1^3 - 2 \ddot{J}_e \chi_1^2 \dot{\chi}_1 \\ & + \frac{1}{2} \ddot{p}_e \lambda_1 \chi_1^2 + 2 \ddot{p}_e \chi_1 \dot{\chi}_1 \lambda_1 + 2 \ddot{p}_e \dot{\lambda}_1 \chi_1^2 - \frac{1}{r \chi_e'} \frac{d}{dr} \left(r^3 \frac{d}{dr} \left(\frac{\partial^2 \xi_1}{\partial \tau^2} \right) \right) \end{aligned} \quad (8.13)$$

The corrected pressure fluctuation is

$$p_1 = \dot{p}_e \chi_1 + \ddot{p}_e (\chi_1 \chi_2 + \chi_1 \chi_0) + \frac{1}{2} \ddot{p}_e \chi_1^3.$$

Replacing these quantities in the matching condition yields the bifurcation equation, Eq. (6.1).

It is clear from this analysis that the practical calculation of the nonlinear corrections can only be accomplished for special equilibria such that Eq. (8.11) can be inverted analytically. The solution of the bifurcation equations for model profiles is the subject of the following chapter.

8.2 Constant current case

It is assumed throughout the rest of this chapter that the pressure profile is parabolic in the low-shear region: $p'_e = -2p_0r$.

We consider first a safety-factor profile with constant $q(r) = q_0$ for $r < r_s$ and with q rising abruptly beyond r_s . This requires a thin current-sheet at $r = r_s$ and a constant current profile within $r < r_s$. Such configurations have the property that the equilibrium fields are linearly related in the constant-current, parabolic pressure region: that is, $\dot{p}_e = \text{cst.}$ and $\dot{J}_e = 0$. The only remaining nonlinear coupling arises from the flux and pressure-conservation constraints, which imply coupling to the $n = 0$ component only. This case is thus of a quasilinear nature.

The bifurcation equation is obtained by following the procedure described in the first section of this chapter. The linear eigenmode is given by

$$\chi_1(r) = -\frac{\kappa_0 C_1}{8} r^3 + A \cdot r \quad , \quad r < (r_s - w) \quad ,$$

where

$$\kappa_0 = \frac{p_0}{\left(\frac{1}{q_0} - 1\right)} \quad ,$$

and w is the half-width of the current sheet. For $w \ll 1$, the integration constant A is determined by the condition $\chi_1(r_s) = 0$. The third-order accurate flux perturbation is then

$$\begin{aligned} \chi_1 = & \frac{\kappa_0}{8} r \cdot (r_s^2 - r^2) \left(C_1 - \left(\frac{1}{q_0} - 1 \right)^{-2} \frac{d^2 C_1}{dt^2} \right) \\ & - \left(\frac{\kappa_0 C_1}{4} \right)^3 \cdot \left(\frac{1}{q_0} - 1 \right)^{-2} (r^4 - 3r_s^2 r^2 + 2r_s^4) r \quad . \end{aligned}$$

The matching condition yields the bifurcation equation:

$$\frac{d^2 \hat{\xi}}{d\tau^2} = \left(\frac{r_s^6}{24\sigma_1} p_0^2 - \left(\frac{1}{q_0} - 1 \right)^2 \right) \hat{\xi} - 12 \left(\frac{1}{q_0} - 1 \right)^2 \hat{\xi}^3, \quad (8.14)$$

where $\hat{\xi} = \xi_1(0)/r_s$. This is thus a supercritical bifurcation. Note that this result is independent of the precise form of the current profile in the outer region, since σ_1 does not appear in Γ .

8.3 Gaussian rotational transform

Before drawing conclusions, it is desirable to solve the bifurcation equations for a fully nonlinear case. The following q -profiles satisfy this requirement while remaining analytically tractable. Let

$$\left(\frac{1}{q} - 1 \right) = \left(\frac{1}{q_0} - 1 \right) \exp \left(\frac{r^2}{2s^2} \right), \quad (8.15)$$

with $s^2 = \frac{1}{2}(r_2)^2 |\ell n [2 \cdot (1 - 1/q_0)]|^{-1} < 1$, where r_2 is the radius of the $q = 2$ surface. In terms of the radial variable z defined by $z = r^2/s^2$, the equilibrium quantities are given by

$$\dot{p}_e = 2\kappa_0 e^{-z/2},$$

$$\dot{J}_e = (4 + z)/s^2.$$

The solution of the linear equations is

$$\chi_1 = K_1 z^{1/2} e^{-z/2},$$

where $K_1 = \kappa_0 C_1 s^3 / 8$. The marginal stability condition is

$$\kappa_{0,c}^2 = 4\sigma_1/s^6 + O(\xi^2). \quad (8.16)$$

The equation for the $n = 2$ flux-perturbation χ_2 is

$$\hat{J}_2 - (4 + z)\chi_2 = -s^4 \kappa_0 C_2 z e^{-z/2} - \frac{9K_1^2}{\left(\frac{1}{q_0} - 1\right)} - \frac{z}{s^2} e^{-3z/2},$$

where

$$\hat{J}_2 = 4 \left(z \frac{d^2 \chi_2}{dz^2} + \frac{d\chi_2}{dz} - \frac{1}{z} \chi_2 \right).$$

After substitution of χ_2 by

$$\chi_2 = z e^{-\frac{z}{2}} \cdot u(z),$$

the sideband equation becomes

$$zu'' + (3 - z)u' - \frac{5}{2}u = -\frac{\kappa_0 C_2}{4} - \frac{9}{4} \frac{K_1^2}{(\mu_0 - 1)} e^{-z}.$$

The inhomogeneity can be partly simplified by substituting

$$u = \frac{\kappa_0 C_2}{10} + v(z) e^{-z},$$

resulting in following the equation for v :

$$zv'' + 3(1 - z)v' + \left(2z - \frac{11}{2}\right)v = -\frac{9}{4} \frac{K_1^2}{(\mu_0 - 1)}.$$

The inhomogeneous term has thus been reduced to a constant. It can be removed, at the cost of raising the order of the system, by taking the derivative of the equation. The resulting equation is a generalized confluent hypergeometric equation for which integral representations of the solutions can be found by the method of kernels⁶⁷. We write the linear operator corresponding to the third degree homogeneous equation $L(v)$.

$$L(v) \equiv zv''' + (4 - 3z)v'' + \left(2z - \frac{17}{2}\right)v' + 2v = 0.$$

We look for a solution with a laplace kernel.

$$v(z) = \int_a^b e^{zt} w(t) dt .$$

The operator M_t such that

$$M_t(e^{zt}) = L_z(e^{zt}) ,$$

is given by

$$M_t(f) = t(t^2 - 3t + 2) \frac{df}{dt} + \left(4t^2 - \frac{17}{2}t + 2\right) w .$$

Its adjoint, M_t^\dagger is

$$M_t^\dagger w = -t(t-1)(t-2) \frac{dw}{dt} + \left(t^2 - \frac{5}{2}t\right) w .$$

so that the following identities hold:

$$\begin{aligned} L_z[v(z)] &= \int_a^b L_z[e^{zt}] w(t) dt \\ &= \int_a^b M_t[e^{zt}] w(t) dt \\ &= \int_a^b e^{zt} M_t^\dagger[w(t)] dt \\ &\quad + \left[t(t-2)(t-1) e^{zt} w(t) \right]_a^b \end{aligned}$$

The equation will thus be satisfied if both conditions

$$M_t^\dagger[v(t)] = 0$$

$$\left[t(t-2)(t-1) e^{zt} w(t) \right]_a^b = 0$$

are satisfied. The general solution to this equation is given by

$$w(t) = (t-1)^{3/2} (t-2)^{-1/2}$$

The integration bounds a and b must now be chosen so as to satisfy the boundary conditions. The following three choices provide a complete, linearly independent solution set for $z > 0$:

$$[a, b] = \begin{cases} [-\infty, 0] & (1) \\ [0, 1] & (2) \\ [1, 2] & (3) \end{cases}$$

The first solution is singular at the origin and so must be rejected on physical grounds. The third solution behaves as $\exp(2z)$ for large values of z and so must also be rejected. The second solution has the proper behavior at the origin as well as at infinity. We thus take

$$v(z) = K_2 \int_0^1 e^{zt} (1-t)^{3/2} (2-t)^{-1/2} dt$$

This yields the solution for χ_2 :

$$\chi_2 = \left\{ \frac{\kappa_0 C_2 s^4}{10} + \frac{9\sqrt{2}}{8s^2} \frac{K_1^2}{\left(\frac{1}{q_0} - 1\right)} \int_0^1 e^{-2y} y^{3/2} (1+y)^{-1/2} dy \right\} z e^{-z/2}.$$

The constant C_2 is determined by the matching conditions. One finds

$$C_2 = \frac{21}{20} \frac{\kappa_0 s^2 K_1^2}{\left(\frac{1}{q_0} - 1\right)} \frac{1}{\left(\sigma_2 - \frac{3}{5} s^8 \kappa_0^2\right)}. \quad (8.17)$$

Note that $C_2 \rightarrow \infty$ for $\sigma_2 = \frac{3}{5} s^8 \kappa_0^2$. This is of course the linear marginal stability condition for the $n = 2$ mode. Comparing this to the marginal stability condition for the $n = 1$ mode, $\sigma_1 = \frac{s^6}{4} \kappa_0^2$, one concludes that degeneracy occurs when $\sigma_2/\sigma_1 = 2.4s^2$. Numerical and analytical estimates indicate that typically $\sigma_2/\sigma_1 \gtrsim 4s^2$ so that the non-degeneracy assumption is well satisfied.

Placing these results in the $n = 1$ matching condition yields the bifurcation equation:

$$\frac{d^2 \xi}{d\tau^2} = 8 \left(\frac{s^6}{4\sigma_1} p_0^2 - \left(\frac{1}{q_0} - 1 \right)^2 \right) \xi + \Gamma \xi^3, \quad (8.18)$$

where

$$\Gamma \cong -\frac{5.39}{s^4} \left(\frac{\sigma_2 - 2.95\sigma_1 s^2}{\sigma_2 - 2.4\sigma_1 s^2} \right) \left(\frac{1}{q_0} - 1 \right)^2. \quad (8.19)$$

Thus $\Gamma < 0$ for $\sigma_2/\sigma_1 > 2.95s^2$. It is noteworthy that $|\Gamma|$ decreases as the marginal stability threshold of the $n = 2$ mode approaches that of the $n = 1$ mode. This is also the case for the free-boundary kink bifurcation (Fig. 14).⁶⁵ However, exterior current profiles with $\sigma_2/\sigma_1 < 2.95s^2$ were not found in this investigation. We must therefore conclude that the fully nonlinear gaussian-profile case is also supercritical.

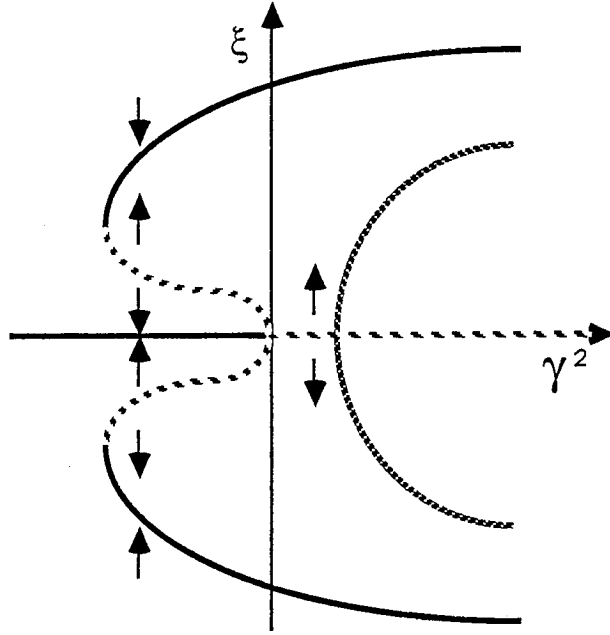


Fig.14: Effect of near-degenerescence on bifurcated equilibria.

Chapter 9

Resistive Interchange

9.1 Introduction

In this chapter the effect of resistivity on the quasi-interchange is considered. The primary effect of resistivity is to allow the quasi interchange to develop in otherwise ideally stable equilibria by relaxing the requirement that the perturbed radial magnetic field of the $m/n = 2/1$ sideband vanish at the $q = 2$ rational magnetic surface. This effect is very similar to that found when resistivity is taken into account for ballooning modes, to which the quasi-interchange is closely related. The stability threshold has been shown numerically to be significantly affected by resistivity⁵⁶. Complete simulations of the entire sawtooth cycle reveal that the quasi-interchange begins growing relatively early during the ramp phase of the sawtooth oscillations, but is not the direct cause the crash⁶⁸. The failure of this instability to cause a disruption shortly after the onset of growth can be attributed to its nonlinear saturation. These conclusions are supported by extending the analytical model introduced previously to include resistivity and nonlinear effects. We will show that the quasi-interchange evolves continuously into a $m/n = 2/1$ tearing mode as resistivity is introduced. The following investigation can thus equally be looked on as a study of the effects of low central shear, and of coupling to the $m/n = 1/1$ mode, on the $2/1$ tearing mode. These effects were considered earlier by Bussac et. al for the case of finite shear. These authors concluded that although the

effect of toroidal coupling is negligible in the finite shear case, that it could become significant for low central shear. Later numerical investigations by Connors et. al confirmed these conclusions.

There have been experimental observations of sawtooth crashes related to the growth of a 2/1 magnetic island, but such islands are not always present. Another motivation for investigating this effect comes from the importance of the growth of 2/1 magnetic islands on the disruptive instability.⁶⁹ Sawtooth activity has been observed in some cases to trigger major disruptions, and the relationship between the quasi-interchange mode and the 2/1 tearing mode could provide new insight into this phenomenon. Recent X-ray tomography results revealing atypical behavior of the perturbation in the vicinity of the magnetic islands may also be due to the presence of a large $m = 1$ component in the tearing eigenmode.

Resistivity is only important in a narrow singular layer at the resonant surface where $k_{\parallel} = 0$. Since tearing mode growth rates are always significantly smaller than the characteristic rates for ideal motion the ideal marginal stability equations are appropriate outside of the tearing layer. The growth rate γ is then determined by a process of matching the ideal MHD outer solutions to the resistive layer solutions. This matching takes the form

$$\Delta' = \Delta(\gamma)$$

where $\Delta(\gamma)$ is calculated analytically for some model of the resonant layer physics. The outer matching parameter can be shown to be a measure of the free energy available to drive the perturbation. It is defined in terms of the ratio of the coefficients of the asymptotically large and the asymptotically small components of the perturbation as the singular layer is approached from the

outside. In the low beta limit and for finite shear Δ' takes the form

$$\Delta' = \lim_{\epsilon \rightarrow 0} \frac{r_s}{\psi} \frac{d\psi}{dr} \bigg|_{r_s-\epsilon}^{r_s+\epsilon},$$

where the solutions on either side of the singular surface are determined so as to satisfy the appropriate boundary conditions at the wall and on the magnetic axis. This separation of the problem into an ideal MHD outer problem and a layer problem allows the consideration of quite complex and realistic models for the processes taking place within the layer. For example diamagnetic effects, finite Larmor radius effects, collisional and semi-collisional electron dynamics can be modeled in this way.

9.2 Stability

The dispersion relation is found by asymptotically matching the solution of the low shear mode equations in the center of the plasma to the solution in the sheared outer region. The $m/n = 1/1$ Fourier component of the mode vanishes outside the low shear central region but the $2/1$ component survives and must obey the cylindrical mode equation in the outer region. The asymptotic form of the outer solution in the low shear region is

$$\xi_2 = \sigma r^{-3} + r, \quad (9.1)$$

where ξ_2 is the $2/1$ component of the radial displacement eigenfunction. The constant σ is found by integrating the mode equation inwards from r_2 , the radius of the $q = 2$ surface. Note that r_2 is a singular point for the $2/1$ mode equation. In the ideal model the appropriate boundary condition at r_2 is $\xi'_2 = 0$. Matching of Eq. (9.1) to the inner solution then yields the ideal dispersion relation

$$\sigma = \int_0^a \frac{(\epsilon\beta_p)^2}{\hat{\gamma}^2 + (1/q_1)^2} r^5 dr. \quad (9.2)$$

For finite resistivity one must generalize this boundary condition to allow for a jump Δ' in the ratio of the coefficients of the small and the large solutions at r_2 . The constant σ is then related to Δ' by a Möbius, or affine transformation:

$$\sigma = \frac{a\Delta' + b}{c\Delta' + d}, \quad (9.3)$$

where a, b, c, d are constants determined by continuation of the fundamental solutions of the mode equations at one singular point (e.g. the $q = 2$ surface) to the neighborhood of the other (the origin). As emphasized by Connor et. al,⁷⁰ this is a very general relation, dependent only on linearity and not limited to the case of low aspect ratio and circular cross-section considered here. Following the procedure described in ref. 70, the dispersion relation is obtained by replacing σ and Δ' by their values in terms of $\hat{\gamma}$. These are given respectively by Eq.(9.2) and by an appropriate tearing layer model at r_2 . Eq.(9.3) is now written in the more perspicuous form

$$\Delta' = \Delta_c \frac{1 - \sigma/\sigma_r}{1 - \sigma/\sigma_i} \quad (9.4)$$

where Δ_c is the cylindrical Δ' which results when $\beta_p = 0$, σ_i corresponds to ideal marginal stability and σ_r to marginal stability of the tearing mode. The roots of the dispersion equation can be visualized as the intersection of the hyperbola given by Eq. (9.4) and of the curve defined parametrically by $\sigma = \sigma(\hat{\gamma})$ and $\Delta' = \Delta(\hat{\gamma})$. Clearly σ is nearly independent of $\hat{\gamma}$ for small growth rates so that this parametric curve is essentially a vertical line until the instability is well into the ideal regime. This implies that there is only one root to the dispersion relation. As β_p rises, a 2/1 tearing mode first appears when σ reaches σ_r . This instability contains a large 1/1 component and is essentially a low- n resistive interchange. As β_p continues to rise it evolves into a large- Δ' tearing mode, and finally into the ideal Quasi-Interchange (Fig.15).

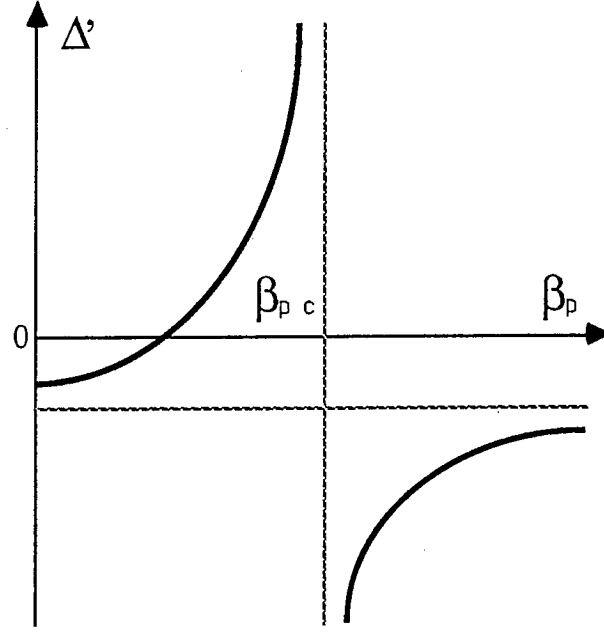


Fig.15: Evolution of Δ' with β_p for a low shear equilibrium⁷¹

The value of the quantities Δ_c , σ_i and σ_r can be estimated for the model safety-factor profiles used earlier as follows. The asymptotic limit of the sideband amplitude in the low shear region is given for these profiles by

$$\xi_2(r) = r {}_2F_1(a, b, 1 + 2/\lambda; r^{2\lambda}) + \sigma r^{-3} {}_2F_1(2 - a, 2 - b; 1 - 2/\lambda; r^{2\lambda})$$

where r has been normalized to r_2 , the radius of the $q = 2$ singular surface, and σ is given by Eq.(9.2) for $\hat{\gamma} = 0$. The solution of the marginal equation between the singular layer and the wall is more difficult to obtain. Note that the solutions on either side of the layer are entirely independent so that Δ' may be decomposed as follows:

$$\Delta' = \Delta'_+ + \Delta'_-$$

where

$$\Delta'_{\pm} = \pm \lim_{\epsilon \rightarrow 0} \frac{r_s}{\psi_{\pm}} \frac{d\psi_{\pm}}{dr} .$$

Evidently ideal marginal stability for the $m = 1$ quasi-interchange is characterised by $\Delta'_- \rightarrow \infty$ so that near ideal marginal stability one has $\Delta' \sim \Delta'_-$. The value of Δ'_c and σ_r , however, depend critically on Δ'_+ , which is itself sensitive to the details of the equilibrium configuration on the outer edge of the plasma. The value of Δ'_+ can only be calculated analytically in two limiting cases: for an infinitely removed wall and for a wall very close to the $q = 2$ singular surface.

The continuation of the inside solution to the $r = 1$ singular point is complicated by the fact that the characteristic roots at this point differ by an integral value, namely unity. This fact expresses itself in the following relations between the parameters of the hypergeometric function:

$$a + b - 1 = 1 + 2/\lambda ,$$

$$(2 - a) + (2 - b) - 1 = 1 - 2/\lambda ,$$

which can easily be verified from the expressions for a and b given previously. This results in the appearance of logarithmic terms in the solution around the rational surface. It is a generic difficulty inevitably encountered in any calculation of the tearing Δ' and does not pose any fundamental problems. The continuation of the hypergeometric function to the $r = 1$ singular point is given by

$$\begin{aligned} \frac{{}_2F_1(a, b; a + b - 1; z)}{\Gamma(a + b - 1)} &= \frac{(1 - z)^{-1}}{\Gamma(a)\Gamma(b)} \\ &+ \frac{1}{\Gamma(a - 1)\Gamma(b - 1)} \sum_{n=0}^{\infty} \frac{(a)_n(b)_n}{(n + 1)!n!} \\ &\times [-h_n + \log(1 - z)](1 - z)^n , \end{aligned}$$

where $z = r^{2\lambda}$ and

$$h_n = \psi(1+n) + \psi(2+n) - \psi(a+n) - \psi(b+n) .$$

The continuation of the solution $\xi(r)$ to the neighborhood of the $q = 2$ singular surface at $r = 1$ is then given by

$$\begin{aligned} \xi(r) &= \left\{ r \frac{\Gamma(a+b-1)}{\Gamma(a)\Gamma(b)} + \sigma r^{-3} \frac{\Gamma(3-a-b)}{\Gamma(2-a)\Gamma(2-b)} \right\} (1-r^{2\lambda})^{-1} \\ &- \frac{r\Gamma(a+b-1)}{\Gamma(a-1)\Gamma(b-1)} \sum_{n=0}^{\infty} \frac{(a)_n(b)_n}{(n+1)!n!} [h_n - \log(1-z)] (1-z)^n \\ &- \frac{\sigma r^{-3}\Gamma(3-a-b)}{\Gamma(1-a)\Gamma(1-b)} \sum_{n=0}^{\infty} \frac{(2-a)_n(2-b)_n}{(n+1)!n!} [\hat{h}_n - \log(1-z)] (1-z)^n \end{aligned}$$

where

$$\hat{h}_n = \psi(1+n) + \psi(2+n) - \psi(2-a+n) - \psi(2-b+n) .$$

Expanding for large λ one finds

$$\begin{aligned} \xi(r) &= -\frac{1}{\lambda^2} \left\{ \frac{\Gamma(\frac{2}{\lambda})}{\Gamma(a)\Gamma(b)} - \sigma \frac{\Gamma(-\frac{2}{\lambda})}{\Gamma(2-a)\Gamma(2-b)} \right\} \frac{1}{x} \\ &+ \frac{1}{2\lambda^2} \left\{ \frac{\Gamma(\frac{2}{\lambda})}{\Gamma(a)\Gamma(b)} [(2\lambda-3) + (4\lambda+1)(h_1 - \log(2\lambda))] \right. \\ &\left. - \sigma \frac{\Gamma(-\frac{2}{\lambda})}{\Gamma(2-a)\Gamma(2-b)} [(2\lambda+5) + 4(\lambda+1)(\hat{h}_1 - \log(2\lambda))] \right\} \end{aligned}$$

The value of Δ'_- can easily be evaluated from this equation for different values of λ . For $\lambda = 3$ we find

$$\Delta'_- = \frac{-5.32}{\sigma - 0.12} - 1.31 \quad (9.5)$$

The value of Δ'_+ can be estimated for an infinitely far away wall in a similar way. We find

$$\Delta'_+ = \frac{3}{2} + (1-2a) + 2(\lambda+1)(\log(2\lambda) - h) .$$

For $\lambda = 3$ this is

$$\Delta'_+ = 11.2 .$$

In the opposite limit the value of Δ'_+ for a nearby wall is

$$\Delta'_+ = -1 + (r_w - 1) , \text{ for } (r_w - 1) \ll 1 ,$$

where r_w is the radius of the wall normalised to the radius of the $q = 2$ surface.

Note that the value of Δ'_+ is independent of σ so that the effect of this term is simply to shift the entire curve of $\Delta'(\sigma)$ vertically. This will of course affect the marginal stability point for the tearing mode but will have no significant effect in the vicinity of the marginal ideal stability point where the $m = 2$ tearing mode transforms itself into a so-called infinite- Δ' tearing mode with a large growth rate, scaling as $\eta^{1/3}$, in contrast to the usual “finite Δ' ” scaling of $\eta^{3/5}$. For yet larger values of β_p this mode simply becomes the ideal quasi-interchange studied previously.

9.3 Nonlinear Growth

Nonlinear effects on the growth of the $m = 2$ tearing mode can thus be deduced from the bifurcation theory developed for the quasi-interchange. An amplitude-dependent value of Δ' can be obtained by replacing σ by its nonlinear value as a function of the amplitude. Note however that to obtain an expression valid away from ideal marginal stability one must refrain from making use of the lowest order marginality condition to simplify the third order equations. The result of the analysis is an amplitude-dependent correction term to the linear value of σ :

$$\sigma = \sigma_l + \Lambda(\beta_p)\xi_1(0)^2 , \tag{9.6}$$

where $\xi_1(0)$ is the amplitude of the 1/1 component of the perturbation at the origin. The values of Λ for the current profiles considered previously are

$$\Lambda = -\frac{\kappa_0^2}{32} \quad (9.7)$$

for the constant current profile and

$$\Lambda = -.17 \left(\frac{\sigma_2 - .74\kappa_0^2}{\sigma_2 - .6\kappa_0^2} \right) \kappa_0^2 \quad (9.8)$$

for the gaussian $1 - 1/q$ profile, where

$$\kappa_0 = \frac{p_0}{1 - 1/q_0} .$$

Chapter 10

Conclusion

We have re-examined the stability of $m = 1$ modes in a low-beta tokamak, allowing for relatively weak magnetic shear. Our formalism is sufficiently general to allow previous results^{27,53–54,56–59} to be recovered in appropriate limits. However, in the weak shear, $|q - 1| \ll 1$ case we obtain a novel growth rate, given in general by Eq. (5.23), and more explicitly, for a model profile, by Eq. (5.26). The new quasi-interchange instability displays no threshold with regard to the poloidal beta. The scaling of its growth rate ($\hat{\gamma} \sim \epsilon\beta_p$ for flat current profiles) and its continuous, cellular-convection type of flow set it sharply apart from the usual kink mode ($\hat{\gamma} \sim (\epsilon\beta_p)^2$). The quasi-interchange mode does, nonetheless, share some features with the kink mode, such as a sensitivity to the location of the $q = 2$ surface. Our analysis differs in this respect from that of Ramos⁷² for noncircular tokamaks in which the sidebands as well as the principal harmonic were assumed to vanish outside the low-shear region. Numerical results for the noncircular case have also been obtained by Turnbull.⁷³ Note that the $m = 1$ kink was shown not to be marginally stable for shaped cross sections by Laval⁷⁴ and Edery et. al.⁷⁵

The nature of the marginal stability condition is, however, the most important characteristic of this model. Indeed, by requiring the pressure gradient to balance the line-bending force at marginal stability, we have taken a significant step away from the traditional emphasis on q profiles to deter-

mine critical stability. This trait distinguishes this model from that of Kleva et al.,⁷⁶ which is also based on a low-shear central region but which relies on the line-bending term in a surrounding island to drive the instability. In Wesson's model,⁸ therefore, the evolution of the pressure profile during the rise phase of the sawtooth becomes as important as the current diffusion. In particular, it is not clear in this model why additional heating fails to shorten the sawtooth period.

After this work was completed we learned of a similar analysis by Hastie and Hender, in which equivalent marginal stability criteria were obtained.⁷⁷

After reaching the conclusion that the linear theory failed to account for the suddenness of the onset of the instability we carried out a bifurcation analysis of the nonlinear equations for a low shear tokamak. We found that the linearized Reduced Magnetohydrodynamics equations are identical to the full Magnetohydrodynamics equations in the ordering of Ware and Haas, except for the neglect of parallel kinetic energy and the effects of compressibility. The growth of the $n = 1$ quasi-interchange was found to saturate for finite values of the perturbation amplitude away from marginal stability, in contrast to the kink mode which is known to saturate at small amplitudes. The saturation of the growth is related to the existence of nearby bifurcated equilibria above ideal linear marginal stability. The eigenmode expansion approach used in this investigation guarantees the stability of these secondary equilibria to low mode-number interchange-like perturbations. However, these equilibria may be unstable to large mode-number ballooning instabilities. Such a two-instability mechanism has been suggested by Bussac et al. for rotational transform profiles with an off-axis minimum.⁷⁸ Note that the lack of symmetry of the bifurcated

equilibria implies the existence of small regions of magnetic stochasticity. It is unlikely, however, that this effect can account for the sudden onset of growth during sawtooth disruptions. Such a stochasticity induced crash may however occur if the safety factor decreases below unity, thereby leading to the growth of an $m = n = 1$ magnetic island. The interaction of this island with a saturated $m/n = 2/1$ magnetic island could then account for rapid internal, or minor disruptions. We have shown that the growth and saturation of such a $2/1$ island should be expected for an initially flat, $q \simeq 1$ profile.

Another possibility is that the quasi-interchange is stabilized by kinetic effects until sufficient free energy has been accumulated to account for the large growth-rates observed. However, no mechanism is known by which the stabilization could disappear sufficiently abruptly to account for the observations. Kinetic effects on linear stability have been considered by Hastie and Hender.⁷⁷

BIBLIOGRAPHY

- [1] S. von Goeler, W. Stodiek and N. Sauthoff, Phys. Rev. Lett. **33**, 1201 (1974).
- [2] V. V. Parail and G.V. Pereverzev, Fiz. Plazmy **6**, 27 (1980) [Sov. J. Plasma Phys. **6**, 14 (1980)].
- [3] J. A. Snipes, PhD. Thesis, University of Texas, Austin, 1985 [Fusion Research Center Report FRCR #275 (1985)].
- [4] D. J. Campbell, R. D. Gill, C. W. Gowers, J. Wesson, D. V. Bartlett, C. H. Best, S. Coda, A. E. Costley, A. W. Edwards, S. E. Kissel, R. M. Niestadt, H. W. Piekaar, R. Prentice, R. T. Ross, B. J. D. Tubbing, Nuclear Fusion Letters **26**, 1085, (1986).
- [5] A. W. Edwards, D. J. Campbell, W. W. Engelhardt, H. V. Fahrbach, R. D. Gill, R. S. Granetz, S. Tsuji, B. J. D. Tubbing, A. Weller, J. Wesson, and D. Zasche, Phys. Rev. Lett. **57**, 210 (1986).
- [6] D. J. Campbell, P. A. Duperrex, A. W. Edwards, R. D. Gill, C. W. Gowers, R. S. Granetz, M. Hugon, P. J. Lomas, N. Lopez-Cardozo, M. Malacarne, M. F. Nave, D. C. Robinson, F. C. Schuller, P. Smeulders, J. A. Snipes, P. E. Stott, G. Tonetti, B. J. Tubbing, A. Weller, J. Wesson **Plasma Physics and Controlled Nuclear Fusion Research 1986**, Kyoto, Japan, 1986 (IAEA, Vienna, 1987), Vol. 1, p. 433.

- [7] B. B. Kadomtsev, *Fiz. Plasmy* **1**, 710 (1975) [*Sov. J. Plasma Phys.* **1**, 389 (1975)].
- [8] J. A. Wesson, *Plasma Physics and Controlled Fusion* **28**, 243 (1986).
- [9] J. A. Wesson, P. Kirby, and M. F. F. Nave, in **Plasma Physics and Controlled Nuclear Fusion Research 1986**, Kyoto, Japan, 1986 (IAEA, Vienna, 1987), Vol. 2, p. 3.
- [10] R. D. Hazeltine and J. D. Meiss, *Phys. Reports* **123** (1985).
- [11] M. N. Rosenbluth and C.L. Longmire, *Annals of Phys.* **1**, 120 (1957).
- [12] J. M. Greene and J. L. Johnson, *Plasma Physics* **10**, 729 (1968).
- [13] B. R. Suydam, **Plasma Physics and Controlled Nuclear Fusion Research**, Geneva, 1958 (IAEA, Vienna, 1959), Vol. 1, p. 157.
- [14] C. Mercier, *Nuclear Fusion* **1**, 47, (1960).
- [15] J. M. Greene and J. L. Johnson, *Phys. Fluids* **5**, 510 (1962).
- [16] L. S. Solov'ev, *Sov. Phys. JETP* **26**, 400 (1968).
- [17] G. O. Spies, *Phys. Fluids* **17**, 400 (1974).
- [18] V. D. Shafranov, *Zh. Tekh. Fiz.* **40**, 241 (1970) [*Sov. Phys. Tech. Phys.* **15**, 175 (1970)].
- [19] H. P. Furth, P. H. Rutherford, and H. Selberg, *Phys. Fluids* **16**, 1054 (1973).
- [20] M. N. Rosenbluth, R. Y. Dagazian, and P. H. Rutherford, *Phys. Fluids* **16**, 1894 (1973).

- [21] H. P. Furth, J. Killeen and M. N. Rosenbluth, *Phys. Fluids* **6**, 459 (1963).
- [22] B. Coppi, R. Galvao, R. Pellat, M. N. Rosenbluth, and P. H. Rutherford, *Sov. J. Plasm Phys.* **2**, 533 (1976).
- [23] P. H. Rutherford, *Phys. Fluids* **16**, 1903 (1973).
- [24] B. V. Waddell, M. N. Rosenbluth, D. A. Monticello, and R. B. White *Nuclear Fusion* **16**, 528 (1976).
- [25] G. L. Jahns, M. Soler, B. V. Waddell, J. D. Callen, H. R. Hicks, *Nuclear Fusion* **18** 609 (1978).
- [26] J. D. Callen and G. L. Jahns, *Phys. Rev. Letters* **38**, 491 (1977).
- [27] M. N. Bussac, R. Pellat, D. Edery, and J. L. Soulé, *Phys. Rev. Lett.* **35**, 1638 (1975).
- [28] M. N. Bussac, D. Edery, R. Pellat, J. L. Soule, *Plasma Physics and Controlled Nuclear Fusion Research*, Berchtesgaden, 1977 (IAEA, Vienna, 1978), Vol. 1, p. 607.
- [29] M. F. F. Nave, J. A. Wesson, *Nuclear Fusion Letters* **28**, 297 (1988).
- [30] P. Kirby, *Nuclear Fusion* **28**, 231 (1988).
- [31] A. Y. A. Aydemir, *Phys. Rev. Lett.* **59**, 649 (1987).
- [32] H.R. Strauss, *Phys. Fluids* **20**, 1354 (1977).
- [33] H. Soltwisch, W. Stodiek, J. Manickam, and J. Schlüter, *Plasma Physics and Controlled Nuclear Fusion Research 1986*, Kyoto, Japan, 1986 (IAEA, Vienna, 1987), Vol. 1, p. 265.

- [34] W. P. West, D. M. Thomas, J. S. deGrassie, and S. B. Zheng, Phys. Rev. Letters **58**, 2758 (1987).
- [35] R. D. Hazeltine, D. D. Holm, J. E. Marsden, and P. J. Morrison, Institute for Fusion Studies Report IFSR #139 (1984).
- [36] D. D. Holm, J. E. Marsden, T. Ratiu, and A. Weinstein, Phys. Reports **123** (1985).
- [37] C. S. Gardner, J. Math. Phys. **12** 1548 (1971).
- [38] P. J. Morrison and J. M. Greene, Phys. Rev. Letters **45**, 790 (1980).
- [39] P.J. Morrison and R.D. Hazeltine, Phys. Fluids **27**, 886 (1984).
- [40] I. B. Bernstein, E. A. Frieman, M. D. Kruskal and R. M. Kulsrud, Proc. Roy. Soc. **A244**, 17 (1966).
- [41] W. A. Newcomb, Ann. Phys. **10**, 232 (1960).
- [42] J. P. Goedbloed and H. J. L. Hagebeuk, Phys. Fluids **15**, 1090 (1972).
- [43] J. M. Greene and J. L. Johnson, K. E. Weimer, Phys. Fluids **14**, 671 (1971).
- [44] V. D. Shafranov and E. I. Yurchenko, Soviet Physics JETP **26**, 682 (1968).
- [45] M. Bineau, Nuclear Fusion **2** 130 (1962).
- [46] H. Grad, Proc. Nat. Acad. Sci. U.S.A. **70**, 3277 (1973).
- [47] J. P. Goedbloed, P. H. Sakanaka, Phys. Fluids **17**, 908 (1974).
- [48] J. P. Goedbloed, Phys. Fluids **18**, 1258 (1975).

- [49] J. W. Connor, R. J. Hastie, J. B. Taylor, Phys. Rev. Letters **40**, 396 (1978).
- [50] J. Van Dam, Kinetic Theory of Ballooning Instabilities, PhD. Thesis, Univ. of California, Los Angeles, 1979.
- [51] A.H. Glasser, in: Proc. Finite Beta Workshop (Varenna Summer School of Plasma Physics, Sept. 1977), eds. Bruno Coppi and W. Sadowski (USDOE OFE Conf-7709167,1979), p.55.
- [52] R. L. Dewar and A. H. Glasser, Phys. Fluids **26**, 3038 (1983).
- [53] L. E. Zakharov, Fiz. Plasmy **4**, 898 (1978) [Sov. J. Plasma Phys. **4**, 503 (1979)].
- [54] G. B. Crew and J. J. Ramos, Phys. Fluids **26**, 2621 (1983).
- [55] G. Laval, C. Mercier, and R. Pellat, Nuclear Fusion **5**,156 (1965).
- [56] R. J. Hastie, T. C. Hender, B. A. Carreras, L. A. Charlton, and J. A. Holmes, Phys. Fluids **30**, 1756 (1987).
- [57] A. A. Ware and F. A. Haas, Phys. Fluids **9**, 956 (1966).
- [58] A. A. Ware, Phys. Rev. Lett. **26**, 1304 (1971).
- [59] E. A. Frieman, J. M. Green, J. L. Johnson, and K. E. Weimer, Phys. Fluids **16**, 1108 (1973).
- [60] J. A. Wesson, A. Sykes, Plasma Physics and Controlled Nuclear Fusion Research , Tokyo, 1974 (IAEA, Vienna, 1975), Vol. 1, p. 449.
- [61] A. Sykes, J. A. Wesson, Nucl. Fusion **14**, 645 (1974).

- [62] M. S. Abramowitz and I. A. Stegun, **Handbook of Mathematical Functions**, (Dover, New York, 1972).
- [63] P. A. Duperrex, R. Keller, M. Malacarne, and A. Pochelon, Proc. of the 12th EPS conf. , Budapest, **1**, 126 (1985).
- [64] K. O. Friedrichs, Reviews of Modern Phys. **32**, 889 (1960).
- [65] P.H. Rutherford, H.P. Furth, M.N. Rosenbluth, in *Plasma Physics and Controlled Nuclear Fusion Research* (International Atomic Energy Agency, Vienna, 1971), Vol. 1, p. 533.
- [66] M. Kotschenreuther, R.D. Hazeltine and P.J. Morrison, Phys. Fluids **28**, 294 (1985).
- [67] E.L. Ince, *Ordinary Differential Equations*, Dover, New York (1956).
- [68] A. Y. Aydemir, private communication.
- [69] B. Carreras, H. R. Hicks, J. A. Holmes, and B. V. Waddell, Phys. Fluids **23**, 1811, (1980).
- [70] J. W. Connor, S. C. Cowley, R. J. Hastie, T. C. Hender, A. Hood, and T. J. Martin, Phys. Fluids **31**, 577 (1988).
- [71] R. J. Hastie, "Theory of Resistive Modes in Tokamaks". Presented at the International Theory Workshop, Varenna, Aug. 1987.
- [72] J. J. Ramos, Bull. Am. Phys. Soc. **32**, 1738 (1987).
- [73] A. D. Turnbull, Bull. Am. Phys. Soc. **32**, 1738 (1987).
- [74] G. Laval, Phys. Rev. Letters **26**, 1316, (1975).

- [75] D. Edery, G. Laval, R. Pellat, and J. L. Soule, Phys. Fluids **19**, 260, (1976).
- [76] R. G. Kleva, J. F. Drake, and R. E. Denton, Phys. Fluids **30**, 2119 (1987).
- [77] R.J. Hastie, T.C. Hender, Nucl. Fusion **28**, 585 (1988).
- [78] M.N. Bussac and R. Pellat, private communication.

VITA

Francois Waelbroeck was born in Paris, France, on September 20, 1959, the son of Jean Louis Waelbroeck and Isabelle Waelbroeck. After completing his work at Walt Whitman High School, Bethesda, Maryland, in 1976, he entered the Free University of Brussels in Belgium. He received the degree of Bachelor of Science from the Free University of Brussels in June, 1982, and completed his military service at the Ecole Royale Militaire in Brussels. In September, 1983, he entered The Graduate School of The University of Texas.

Permanent address: 805 E. 32 and 1/2 Street
Austin, Texas 78705

This dissertation was typeset with \LaTeX by Suzy Crumley, Laura Patterson and the author.